NMR STUDIES OF THE KINETICS OF THE EXCHANGE REACTIONS OF THE LITHIUM, SODIUM, AND THALLIUM IONS WITH 18-CROWN-6, 15-CROWN-5 AND PENTAGLYME IN SOME NONAQUEOUS SOLUTIONS

By

Yongsheng Hou

A DISSERTATION

Submitted to

Michigan State University

in partial fulfillment of the requirements

for the degree of

DOCTOR OF PHILOSOPHY

Department of Chemistry

1988

ABSTRACT

NMR STUDIES OF THE KINETICS OF THE EXCHANGE REACTIONS OF THE LITHIUM, SODIUM, AND THALLIUM IONS WITH 18-CROWN-6, 15-CROWN-5 AND PENTAGLYME IN SOME NONAQUEOUS SOLUTIONS

By

Yongsheng Hou

Kinetic studies of the exchange reactions of the metal ions between their uncomplexed and complexed sites by the crown ethers and the linear pentaglyme were carried out by dynamic NMR spectroscopy.

For sodium tetraphenylborate($NaBPh_4$) with the 18-Crown-6, the investigations have been performed in 1,2-dimethoxyethane(DME) solutions, as well as in binary mixtures of DME and THF(tetrahydrofuran). The exchange mechanisms in all cases followed the so-called associative-dissociative process. The nearly linear dependence of the kinetic parameters on the composition of solvent mixtures was found. In pure DME solutions at 298° K, for the associative-dissociative exchange reactions, the

decomplexation reaction rate constant k_{-2} = 8000±2000 s^{-1}, the activation energy E_a = 4.5±0.2 kcal·mol^{-1}, the activation enthalpy $\Delta H^{\ddagger}$ = 3.7±0.2 kcal·mol^{-1}, the activation entropy $\Delta S^{\ddagger}$ = -28.2±0.8 cal·mol^{-1}·K^{-1}, and the activation free energy $\Delta G^{\ddagger}$ = 12.1±0.1 kcal·mol^{-1}. In 3:1 DME:THF mixtures(molar), the results are: k_{-2} = 3500±800 s^{-1}, E_a = 6.8±0.2 kcal·mol^{-1}, $\Delta H^{\ddagger}$ = 6.2±0.2 kcal·mol^{-1}, $\Delta S^{\ddagger}$ = -21.3±0.7 cal·mol^{-1}·K^{-1}, and $\Delta G^{\ddagger}$ = 12.6±0.1 kcal·mol^{-1}. In 1:1 DME:THF mixtures(molar), the results are: k_{-2} = 1800±300 s^{-1}, E_a = 7.7±0.8 kcal·mol^{-1}, $\Delta H^{\ddagger}$ = 7.1±0.8 kcal·mol^{-1}, $\Delta S^{\ddagger}$ = -20±1 cal·mol^{-1}·K^{-1}, and $\Delta G^{\ddagger}$ = 13.0±0.1 kcal·mol^{-1}.

Thermodynamic studies of the complexation reactions of $NaBPh_4$ and NaSCN(sodium thiocyanate) with the 18C6 in DME solutions show that the formation constants for the complexes of these two salts are log K_f = 3.95±0.06 and 2.8±0.2 respectively.

Kinetic parameters of the exchange reactions were also measured for the systems of lithium perchlorate with 15-Crown-5 in acetonitrile and nitromethane solutions. It was found that the exchange reaction for the lithium ion proceeds by the associative-dissociative mechanism in acetonitrile(AN) solutions while in nitromethane(NM) solutions the exchange goes by the bimolecular pathway. In AN solutions, k_{-2} = 2500±400 s^{-1}, E_a = 4.83±0.01 kcal·mol^{-1}, $\Delta H^{\ddagger}$ = 4.24±0.01 kcal·mol^{-1}, $\Delta S^{\ddagger}$ = -24.3±0.3 cal·mol^{-1}·K^{-1}, and $\Delta G^{\ddagger}$ = 11.45±0.09 kcal·mol^{-1}; for the bimolecular exchange in

NM, k_1 = 150000±40000 $s^{-1} \cdot M^{-1}$, E_a = 4.98±0.09 kcal·mol^{-1}, $\Delta H^{\ddagger}$ = 4.39±0.09 kcal·mol^{-1}, $\Delta S^{\ddagger}$ = -20.1±0.2 cal·$mol^{-1} \cdot K^{-1}$, and $\Delta G^{\ddagger}$ = 10.4±0.2 kcal·mol^{-1}.

In AN solutions, the Tl^{+} ion exchange in the $TlClO_4$ + 18C6 system proceeds by the bimolecular pathway; the associative-dissociative and the bimolecular processes both exist for the $TlClO_4$ + pentaglyme(PG) system. In the first case, k_1 = (4.1±0.2)x10^7 $s^{-1} \cdot M^{-1}$, E_a = ~2 kcal·mol^{-1}, $\Delta H^{\ddagger}$ = ~1.4 kcal·mol^{-1}, $\Delta S^{\ddagger}$ = ~-19 cal·$mol^{-1} \cdot K^{-1}$, and $\Delta G^{\ddagger}$ = 7.06±0.03 kcal·mol^{-1} at 298° K. In the second case, for the bimolecular mechanism the results are: k_1 = (3.1±0.1)x10^8 $s^{-1} \cdot M^{-1}$, E_a = 3.00±0.05 kcal·mol^{-1}, $\Delta H^{\ddagger}$ = 2.41±0.05 kcal·mol^{-1}, $\Delta S^{\ddagger}$ = -11.6±0.2 cal·$mol^{-1} \cdot K^{-1}$, and $\Delta G^{\ddagger}$ = 5.88±0.02 kcal·mol^{-1}; for the associative-dissociative mechanism, the results are: k_{-2} = (2.2±0.4)x10^5 s^{-1}, E_a = ~5 kcal·mol^{-1}, $\Delta H^{\ddagger}$ = ~4 kcal·mol^{-1}, $\Delta S^{\ddagger}$ = ~-19 cal·$mol^{-1} \cdot K^{-1}$, and $\Delta G^{\ddagger}$ = 10.2±0.1 kcal·mol^{-1}.

To My Mother

ACKNOWLEDGEMENT

The author wishes to thank Dr. Alexander I. Popov for his patient guidance and warm encouragement, without which the completion of my study at Michigan State University would not be possible.

The author is also indebted to the NMR group for their technical help and their enthusiastic maintenance of NMR facilities. Sincere gratitude is extended to Dr. T.V. Atkinson for his work to ease problems concerning computer applications involved in this work.

Last, but not the least, the author would like to express his greatest appreciations that no words can describe to his mother and brother, and to all his relatives and friends for their loving, caring, and supporting throughout the whole course while he was pursuing his degree.

Table of Contents

Chapter Page

Chapter Page

List of Tables

Table Page

List of Figures

Chapter 1

HISTORICAL REVIEW

1.1 INTRODUCTION

The discovery and successful synthesis of macrocyclic polyether compounds, generally referred to as crown ethers, by Pedersen and coworkers,[1-3] followed by that of macrobicyclic polyether cryptands, by Lehn and coworkers[4-5] in 1960's, sparked tremendous research interest and activities around the world about complexing abilities of these compounds towards metal ions, especially the alkali metal ions.

These compounds are also biologically important for that they resemble their naturally-occurring counterparts which selectively complex and transport alkali metal ions in biological systems. They thus provide very useful models to study the nature and mechanisms of the reactions between metal ions and the naturally occurring ionophores in biological systems. Thermodynamic and kinetic studies of the complexation reactions of metal ions with these synthetic macrocyclic polyether ligands can provide extremely important information about mechanisms of complexation reactions.[6-7]

Immediately following the synthesis of crown ethers, their abilities to complex alkali cations have been extensively investigated.[8-9] The effect of macrocyclic compounds on the ionic permeability of artificial and natural membranes, and the selective transport of alkali

metal ions have been studied.[10-15] Crown ethers have also been recognized for their roles in utilizing alkali metal ions for a variety of uses in catalysis, analysis, preparative chemistry, and drug research.[16-17]

The structures of some typical macrocyclic compounds as well as of some linear polyether ligands are shown in Figure 1. The following nomenclature proposed by Pedersen[1] and Lehn[4] for cryptands and crown ethers will be used throughout this thesis. For typical cryptands, three bridge chains between the two nitrogen atoms are composed of $-CH_2CH_2O-$ units(Figure 1). The nomenclature for cryptands is as follows: C<u>l</u><u>m</u><u>n</u>, where <u>l</u>, <u>m</u>, and <u>n</u> are the numbers of oxygen atoms in three corresponding chains. For example, C221 means that it is a cryptand which has two oxygen atoms on two of the chains, and one oxygen atom on the third one. For crown ethers, the "plane ring" structures are made up by the same unit as in cryptands. Usually, they are named as m-Crown-n, where m and n refer respectively to the total number of atoms in the chain and the number of oxygen atoms it contains. For example, 18-Crown-6(or 18C6 for short) means that this crown ether has eighteen atoms in the ring, and six of them are oxygen atoms. There are also crown ethers which contain other functional groups and atoms such as cyclohexane or benzene on the CH_2CH_2-O unit, as well as sulfur and nitrogen atoms occasionally replacing some oxygen atoms in the ring. The nomenclature of this group of compounds(See Figure 1) is similar to those given above.

In this chapter, some recent studies on thermodynamics and kinetics of complexation reactions between the macrocyclic and linear compounds as ligands and metal ions will be reviewed. The major emphasis in this review will be on kinetics of complexation reactions which is the primary interest of the author.

1.2 THERMODYNAMIC AND KINETIC STUDIES

Although the main objective of this study is the kinetics of the complexations of macrocyclic ligands and linear ligands with metal ions, an introduction to some background knowledge in the thermodynamics of complexations is necessary, since kinetics and thermodynamics are in many ways inseparable.

The complexation reactions between the donor atoms of crown ethers and metal ions are results of ion-dipole interactions.[1] Most importantly, the complexing selectivities of crown ethers for certain metal ions are due to the consonance between the sizes of macrocyclic cavities with those of metal ions(see Table 1 for the sizes). In general, the better their sizes match, the more stable is the complex. The same considerations also hold true for cryptands. Very early studies of macrocyclic complexes, however, have shown that many other factors, such as the nature of the solvents(the solvating ability and the dielectric constant) as well as the nature of anions and the

cationic charge density also have a strong influence in stabilities of these complexes.[1]

Comparisons of stabilities of complexes formed by the polyoxa- and polyaza macrocyclic ligands with those of their linear analogues(Table 2) clearly show that closure of the macrocyclic ring increases stabilities of complexes by several orders of magnitude(the macrocyclic effect!). However, whether the enhanced stabilities of the macrocyclic ligand complexes over the linear ligand complexes is entropic or enthalpic in origin is still not clear.

One should not be surprised to see how little kinetic information is available relative to abundant amount of thermodynamic information. Most of the kinetic data has been obtained by ultrasonic relaxation and NMR measurements, since the complexation rate constants are much too high to be measured by the fast-mixing methods.[18] It should be noted that the complexation reactions are also often accompanied by other simultaneous reactions, such as ion-pair formations, dimerization of the ion pairs of metal salts in solutions of low dielectric constants, as well as conformational change of ligands.

When polyether ligands are added to solutions containing metal ions, complexation reactions between the ligands and cations occur. In order to explain the very high formation rates frequently observed, the concept of the stepwise replacement of coordinated solvent molecules,

together with appropriate changes in the conformation of the ligands has been proposed.[19] Direct evidence of conformational changes in ligands[7,20] prior to complex formation, has come from ultrasonic relaxation studies. The proposed and the observed mechanisms for the complexation reactions of metal ions with macrocyclic ligands can be summarized in the following general scheme using monovalent cations as examples:

$$C_1 \underset{k'_{-1}}{\overset{k'_1}{\rightleftharpoons}} C_2 \qquad (1a)$$

$$M^+\cdot A^- \underset{k_{-1}}{\overset{k_1}{\rightleftharpoons}} M^+ + A^- \qquad (1b)$$

$$M^+ + C_2 \underset{k_{-2}}{\overset{k_2}{\rightleftharpoons}} M^+\cdots C_2 \underset{k_{-3}}{\overset{k_3}{\rightleftharpoons}} M^+\cdot C_2 \underset{k_{-4}}{\overset{k_4}{\rightleftharpoons}} (MC_2)^+ \qquad (1c)$$

where $M^+\cdot A^-$ and M^+ are the ion pair and the free metal ion respectively, C_1 and C_2 are the two conformations of the ligands, while $M^+\cdots C_2$, $M^+\cdot C_2$ and $(MC)^+$ are the three forms the complex representing the initial interaction between the metal ion and the ligand, the intermediate stage of the complex and the final wrapped form of the complex respectively. This reaction scheme postulates the existence of several equilibria prior to the final rate-determining steps of the complexation, which involves an initial

conformational change of a ligand and/or desolvation of both the cation and the ligand, before the final form of the complex is formed.

The following two mechanisms are called Eigen-Winkler[19,26] and Chock's[21] complexation mechanisms and have been observed operative in different situations. They are related to the mechanism given in Equation 1, from which they can be derived:

Eigen-Winkler

$$M^+ + C \underset{k_{-1}}{\overset{k_1}{\rightleftharpoons}} M^+\cdots C \underset{k_{-2}}{\overset{k_2}{\rightleftharpoons}} M^+\cdot C \underset{k_{-3}}{\overset{k_3}{\rightleftharpoons}} (MC)^+ \quad (2)$$

and Chock's

$$C_1 \underset{k_{-1}}{\overset{k_1}{\rightleftharpoons}} C_2 \quad (3a)$$

$$M^+ + C_2 \underset{k_{-2}}{\overset{k_2}{\rightleftharpoons}} (MC_2)^+ \quad (3b).$$

In Eigen-Winkler mechanism, the third step, which is the rearrangement of the ligand around the cation is considered to be the rate-determining step. This mechanism is equivalent to the previous mechanism but omits the step for the conformational change of the ligand. In Chock's

mechanism the complexation step(the second step) is considered to be the rate-determining one and it can be obtained by neglecting the rearrangement steps of the ligand around the cation in the previous mechanism. These mechanisms have been investigated and discussed in several publications.[20,22-26]

Usually, the complexation rates are high(reaching the diffusion controlled range)[32] and can be explained by the assumption that the formation of a complex is a step-wise process so that the desolvation of the metal ions is largely compensated for by interaction with the ligand in the transition state and the activation energy reaches a minimum.[32] It is clear that at this stage there is still no specific interaction between the ligands and the cations which would strongly differentiate between the various cations. Molecular models show that the oxygen atoms in the bridges can rotate outward from the cavity of a macrocyclic ligand, and these may form the basis of the initial interaction between the cations and the ligands. The subsequent steps in which the metal ion enters the cavity of the ligand, where the more specific size-dependent interactions occur, must then proceed rapidly from this stage. This mechanism strongly suggests that the transition state for the complexation reaction lies very close to the reactants.

If, at equilibrium, the amount of a metal ion is in excess of that of the ligand, the cation will undergo an exchange between the free and the complexed sites. The exchange can proceed by one of two mechanisms, the bimolecular (I) and associative-dissociative (II) pathways proposed by Lehn et al.[27] and developed by Shchori et al.[51]:

$$\text{(I)} \qquad {}^{*}M^{+} + ML^{+} \underset{k_1}{\overset{k_1}{\rightleftharpoons}} {}^{*}ML^{+} + M^{+} \tag{4a}$$

or

$$ {}^{*}M^{+} + ML^{+} \underset{k_{12}}{\overset{k_{11}}{\rightleftharpoons}} {}^{*}M^{+}\cdots L\cdots M^{+} \underset{k_{11}}{\overset{k_{12}}{\rightleftharpoons}} {}^{*}ML^{+} + M^{+} \tag{4b}$$

$$\text{(II)} \qquad M^{+} + L \underset{k_{-2}}{\overset{k_2}{\rightleftharpoons}} ML^{+} \tag{5a}$$

or

$$ M^{+} + L \underset{k_{-21}}{\overset{k_{21}}{\rightleftharpoons}} M^{+}\cdots L \underset{k_{-22}}{\overset{k_{22}}{\rightleftharpoons}} ML^{+} \tag{5b}$$

In the bimolecular exchange mechanism, the uncomplexed and the complexed metal ions exchange between their sites in such a way that in the transition state both cations are simultaneously involved with the ligand. In associative-dissociative exchange mechanism, the same metal ion

exchanges between its complexed and uncomplexed sites and only one metal ion is present at the transition state.

As in the thermodynamics of complexation reactions, ligands, cations, solvents, and anions all play important roles in influencing the complexation reaction kinetics. In general, dissociation rates have been shown to be much more sensitive than the formation rates to the variation in the ligand, cation and solvent.[28-32,58]

1.2.1 The influence of ligand properties on the complexation kinetics

Ligands, as one of the two immediate participants of the complexation reactions, have direct influence on thermodynamics and kinetics of these reactions in many ways. The most striking influence of ligand structure on the kinetic behavior may be seen in the dissociation rates while formation rates do not correlate in any simple way with ligand structure(see Table 3).[34,49,58] For instance, the selectivity for a given cation vis-à-vis ligands is primarily determined by the dissociation rates(see Table 3).[32] The type(see Figure 1) of ligands, linear or cyclic, bicyclic(cryptands) or monocyclic(crown ethers), functional groups introduced into the ligands, and charged or ionizable ligands, all have influences on the complexation reactions.

For a given cation , the complexation rate should depend upon the ability of the ligand to substitute, in a

stepwise manner, all or some solvent molecules of the inner coordination sphere of the cation by its coordinating sites.[49] This ability should depend primarily on the flexibility of the ligands, but may also be influenced by the solvation of the ligands. From this point of view, more flexible ligands can interact more readily with the incoming cation, leading to more effective compensation for the loss of solvation energy. Usually, the more flexible crown ethers show faster complexation rates than the less flexible cryptands.[20,32,58]

The more flexible ligands also show faster dissociation rates for the complexes so that overall exchange rates are rapid. Cox et al.[33] investigated complexation kinetics of dibenzo-18-Crown-6 with the strontium ion in methanol solutions at -15 °C by stopped flow technique and found that, as compared to cryptands, the more flexible crown ether ligand shows faster dissociation rate. The dissociation rate of $Sr(Crown)^{2+}$($(2.7\pm0.3)\times10$ s^{-1})is about 10^8 times faster than that of $Sr(C222)^{2+}$(6.8×10^{-9} s^{-1}), while the formation rate constants for the two complexes are very similar(($(9.6\pm0.5)\times10^4$ and 5 ± 1 $M^{-1}s^{-1}$ for $Sr(Crown)^{2+}$ and $Sr(C222)^{2+}$ respectively). The stability constant for the complex $Sr(C222)^{2+}$($K_f=7.9\times10^{12}$ M^{-1}) is correspondingly higher than that of $Sr(Crown)^{2+}$($K_f=3.6\times10^3$ M^{-1}). Thus, although the particular bicyclic structure of C222 does not appear in this case to strongly influence the formation rates, it has

a dramatic effect on the dissociation rates and on the stability constants.

Introduction of functional groups on the skeletons of macrocyclic rings can change the flexibility and consequently influence the complexation kinetics. Cox and et al.[34] studied the stabilities, formation and dissociation rate constants of alkali metal complexes with $C2_B22$ and $C2_B2_B2$ cryptands in propylene carbonate solutions. The authors found that the substitution of the central $-CH_2CH_2-$ group in C222 by a benzene ring makes the ligand less flexible, and reduces the cavity size. The benzene structure also decreases the electron density on the oxygen atoms of the ligand, and increases the "organic" character of the ligand. The combined effect of these changes is the reduction in the stability constants of $C2_B22$ and $C2_B2_B2$ cryptates, relative to those of the unsubstituted cryptates and on the increase of the dissociation rates of the complexes. For example, the formation constants of $Rb(C222)^+$, $Rb(C2_B22)^+$ and $Rb(C2_B2_B2)^+$ are $(1.047\pm0.002)\times10^9$, $(3.890\pm0.003)\times10^7$, and $(4.266\pm0.003)\times10^6$ M^{-1} respectively, while the dissociation rate constants of the same complexes are $(1.7\pm0.1)\times10^{-1}$, 3.3 ± 0.2, and $(1.88\pm0.09)\times10$ s^{-1}.

Open chain polyethers and macrocyclic polyether ligands form complexes with metal ions with substantial differences in the stabilities of the resulting complexes, i.e. the "macrocyclic effect" discussed previously(page 5).

Stabilities of complexes(measured by complex formation constants K_F's) are directly related to the free energy change of the complexation reactions such that:

$$RT \ln K_F = -\Delta G^\circ$$

and ΔG° in turn is related to both the entropy change and enthalpy change of the reactions, i.e.

$$\Delta G^\circ = \Delta H^\circ - T\Delta S^\circ.$$

A negative change in ΔH° and a positive change in ΔS° both contribute to the stabilities of complexes.

Kodama and et al.[35-37] studied equilibria and kinetics of complex formation between copper(II), zinc(II), lead(II), and cadmium(II) ions, and 12-, 13-, 14-, and 15-membered macrocyclic tetraamines(see Figure 1). In their studies, the authors have attempted to interpret the macrocyclic effect in terms of both thermodynamics and kinetics. These complexes show apparent macrocyclic effects and the formation constants of the macrocyclic complexes are several orders of magnitude larger than those for their linear analogues. The elevated stabilities of the macrocyclic complexes are the results of the favorable change of the entropy, with the enthalpy change having a slightly negative contribution(ΔH° is less negative for the cyclic ligands than the linear ligands). The authors argued that the

favorable entropy term is due to the favorable orientation of the macrocyclic ligands prior to chelation, and also due to the decreased macrocyclic complex solvation, as compared to that of linear complexes, in the inner coordination sphere as well as in the outer sphere because of the distorted geometry and the hydrophobic exterior of the ligands. The lower heat of formation of the cyclic complex may be attributed to several factors such as: the higher rigidity, and less coordinate bond energy in the change from two primary and two secondary to four secondary nitrogen atoms,(both with positive ΔH^{o} terms), and less ligand solvation (a negative ΔH^{o} term). The comparison of the calculated dissociation rate constants indicates that the macrocyclic effect occurs most notably in the dissociation step. It was concluded in their study that the thermodynamic macrocyclic effect reflects more the dissociation rather than the formation process. It should be mentioned that protonation of the ligands dramatically retards the dissociation as well as the formation rate of the cyclic complexes. The authors also proposed that for the reaction of non-cyclic polyamine ligands, the kinetics are well explained by a dissociative mechanism which involves the desolvation of metal ions followed by the rate-determining step of the complexation-the first coordination bond formation; for a macrocyclic ligand, the reaction is likely to proceed by a concerted process of the desolvation and

metal-ligand bond formation because of the restricted geometry and the proximity of the N donors.

In contrast to the macrocyclic effect observed in Kodama and coworkers study are those which seem to arise entirely or partially from the enthalpy term. Hinz and Margerum,[38-39] assume that a 10^6-fold increase in the stability constant of Ni(cyclam)$^{2+}$, as compared to Ni(2,3,2-tet)$^{2+}$, is due to a more favorable change in enthalpy which overcomes a less favorable change in entropy(cyclam: 1,4,8,11-tetraazacyclotetradecane; 2,3,2-tet: N,N'-bis(2-aminoethyl)-1,3-prrpanediamine, also see Figure 1 for structures). They reasoned that the free macrocycle is less solvated than their linear counterparts due to steric hindrance and hence less enthalpic energy need be expended for desolvation before complexation. The cyclization of the ligands also contributes to the enhanced strength of the metal-nitrogen bond and leads to the favorable enthalpy change.

The difference in ligands can also cause differences in the mechanism of the interactions of ligands with metal ions. Degani[40] studied kinetics of monensin(see Figure 1) complexation with sodium ions by ^{23}Na NMR spectroscopy and the results were compared to those of valinomycin(see Figure 1) and dicyclo-18-crown-6(DCC). In going from MonNa to ValNa$^+$ the association rate constants for all three complexes differ by about one order of magnitude, while the

dissociation rate constants differ by several orders of magnitude. The specificity of monensin for the sodium ion is thus mainly reflected in the slow dissociation rate of this complex. In observing the change in the entropies of activations, it can be seen that a very small decrease in entropy occurs when the activated sodium-monensin complex is formed from the free species. In contrast, the formation of the DCC-Na^+ complex is accompanied by an appreciable negative activation entropy. This difference in the association activation entropies of the two complexes indicates that the crown ether conformation is most likely altered before the association with the sodium ion occurs, while the monensin anion does not undergo a conformational change prior to interaction with the sodium ion. The increase in entropy which occurs while going from the activated state to the complex is similar for both complexes, suggesting that a conformational change occurs after the sodium ion has interacted with the ionophore as has been shown to occur in Val-sodium complexation process.[41] The conformational change of a crown ether prior to the association with a metal ion has also been observed for dicyclo-30-crown-10 by Chock and coworkers.[21]

Ionizable crown ethers(See Figure 1) represent another group of macrocyclic compounds, consisting of a polyether cavity and a proton ionizable group, which are capable of complexing cations with varying degrees of stability. Kinetically, complexations of alkali metal cations by

neutral crown ethers are very fast, approaching the diffusion-controlled limit of 10^8-10^9 M^{-1} s^{-1}.[42] Again, a stepwise substitution of solvent molecules surrounding the ions, rather than a concerted process, has to be proposed to account for the high rates obtained.[43] It is expected that a negatively charged crown ether has a complexation rate as high as, or possibly even higher, than that for a neutral crown ether ligand. Actually, diffusion-controlled rates of formation for complexations of Na^+ by the negatively charged antibiotics nigericin($2x10^{10}$ $M^{-1}.s^{-1}$) and monensin($1.1x10^9$ $M^{-1}.s^{-1}$) have been found.[7,44] The formation rate constant of one order of magnitude faster for the Na^+ + nigericin reaction than that for the Na^+ + monensin reaction indicates that there exists a direct interaction between the metal ion and the carboxylate group in nigericin but not between the metal ion and monensin in which the complex has a "zwitterionic" structure.[45-46] Eyring et al.[47-48] studied sodium ion complexation by ionizable crown ethers in methanol-water solvent mixtures, and thermodynamics and kinetics of side-arm interaction were investigated. The authors found that the overall formation rate constants are in the range of diffusion-controlled reaction rates($\sim 10^{10}$ $M^{-1}.s^{-1}$). This formation rate is one order of magnitude greater than that for the Na^+ + monensin reaction and similar to that of the Na^+ + nigericin reaction. These results probably suggest

that the charged carboxylate side-arm interact with the cation to lower the energy barrier for the complexation.

1.2.2 The role of cations in complexation kinetics

Cations, the other immediate participants of the complexation reactions, influence the reactions in very straight forward ways. The size-match of cations and ligands primarily determines the stabilities of the complexes and the selectivities of the complexations as discussed on page 4. As shown in the previous section(page 10), the selectivities are basically reflected in the dissociation rates of the complexes. Another one of the most important characters of cations that should be considered in these reactions are charge densities, which determine the abilities to be solvated by solvents and tendencies to form ion pairs.

Most of such studies have dealt with the investigations of the complexations of alkali and alkaline earth ions. As the alkali and alkaline earth cations all have "noble gas" electronic configurations, the complexing properties of the ions depend primarily on their charge densities. The alkaline earth-metal complexes show much wider variations in stability reflected in the change of K_f and both the formation(k_f) and dissociation rates(k_d) are smaller than those of the corresponding complexes of alkali metal cations of similar size.[49]

For example, the formation rates of alkaline earth-metal cryptates are 10^2-10^5 times lower than those of the corresponding complexes of alkali metal ions of similar size(see Table 3).[49] It has been shown that the characteristic solvent substitution rate constants of the alkaline earth cations (except for Mg^{2+}) are extremely high (ca. 10^8-10^9 s^{-1} in water) and are not very different from those of the alkali metal ions.[49] In terms of the Eigen-Winkler mechanisms, this means that during complexation ligands may not be able to substitute the solvent molecules in the alkaline earth ion solvation shell in a stepwise manner, and the energy required to achieve complexation is increased because there is no immediate compensation for the loss of solvation of the cation by the formation of cation-ligand bonds. As the result, any desolvation or partial desolvation required to reach the transition state in the complexation reaction should demand more energy if the cation is a strongly solvated M^{2+} than if it is a less solvated M^{+}. For the dissociation rate constants of the alkaline earth-metal complexes and the alkali-metal complexes, a difference of the order 10^2-10^5 s^{-1} is observed when comparing $k_d(MCry^{2+})$ with $k_d(MCry^{+})$.[49]

For the ligands studied, it has been found that in the alkaline earth family the formation rate constants of the complexes are in the order $Ba^{2+}>Sr^{2+}>Ca^{2+}$ (see Table 3).[49] This is the opposite order to that of the free energies of solvation of the cations. Thus, the energy barrier required

is lowest in the complexation process involving Ba^{2+}, larger for Sr^{2+}, and largest for Ca^{2+} which is the most strongly solvated of these three cations. A similar trend for the formation rate constants has also been observed for the alkali metal ions, but the differences in the values of k_f from cation to cation, for a given ligand, are larger in the case of alkaline earth ions than in that of alkali ions.[49] The values of k_f for Na^+ and K^+ complexes vary only by a factor of 2 or 3, whereas k_f values for Ba^{2+} cryptates are normally around 100 times higher than those for the Ca^{2+} cryptates. If the argument of solvation is used again, this difference is not unexpected, as the difference in free energy of solvation between Ba^{2+} and Ca^{2+} is much larger than that between K^+ and Na^+.[49]

The nature of the cations influences both the reaction rates and the exchange mechanisms. It seems that there is a trend of the change of the preference between the associative-dissociative and the bimolecular exchange mechanisms in the alkali metal family, from Na^+, K^+ to Cs^+.[50] The predominant exchange mechanism varies from that of either the associative-dissociative or bimolecular process for the Na^+ ion to primarily the bimolecular process for the Cs^+ ion.

Strasser et al.[50] discussed their results of the exchange kinetics of the cesium ion with dibenzo-21-crown-7 and dibenzo-24-crown-8 in acetone and methanol solutions. In

all systems studied, the mechanisms of the exchange between the solvated and complexed Cs^+ sites are predominantly the bimolecular process. A tendency to form more ion pairing or the decrease in charge density as one goes to the larger cation has been considered as the explanation of this trend, because ion pairing, or the decrease in charge density, actually minimizes the charge-charge repulsion in the bimolecular exchange mechanism and allows the bimolecular exchange mechanism to predominate.

Shporer and et al.[51] noticed the effect of the ionic strength of the solution on the rates of the reactions involving ionic species. Comparison of the results of experiments of DB18C6 with the same sodium concentrations but with and without LiSCN present shows that in N,N-dimethylformamide the addition of the second salt slows down the rate of exchange. Since it has been shown that lithium ions do not compete effectively with sodium ions for the ligand, this observation were attributed to changes in activity and/or ion pairing. Conductivity measurements indicate that ion pair formation of metal salts in this solvent is not very large, and the effect of ionic strength on the rate constants, at least in this case, is due to changes of activities rather than to ion pairing. In terms of the transition-state theory, the observed rate constant is given by:

$$k_f = K^{\ddagger}(kT/h)(y^n_{DMF}y_{NaDBC}/y^{\ddagger})$$

where $K^{\ddagger}$ is the equilibrium constant for the formation of the activated complex, the y's are molar activity coefficients of the corresponding species and n is the number of solvent molecules involved in solvation of the cation. As can be seen, the change in solvent activity is one of the factors responsible for the decrease of k_f with increasing electrolyte concentration. Replacement of the very bulky tetraphenylborate anion by the relatively small SCN^- anion also leads to a considerable increase in the rate of the exchange. The very bulky tetraphenylborate anion may hinder the reorganization of solvent molecules in the vicinity of the sodium complex more effectively than the small SCN^- ion, thus decreasing the activity of the solvent.

It is clear that in some other cases ion pair formation does influence the complexation reaction kinetics to an important extent.[52-53] $NaBPh_4$ + 18C6 system shows slow exchange in THF at room temperature and 42.27 kG, while under the same condition the exchange reactions are fast with other sodium salts such as NaSCN, NaI and $NaClO_4$. This observation most likely is due to the differences in the types of ion pairs formed in the solutions. It is believed that in tetrahydrofuran solutions $NaBPh_4$ forms solvent-separated ion pairs[54-55] whereas the other three sodium salts tend to form contact ion pairs.[56] In the latter case the anions can compete with the ligand for the cation more effectively, which lowers the stability of the sodium complex and increases the exchange rates.

Further investigations of the kinetics of the exchange reactions showed that the ion pair formation can also explain the difference in exchange mechanisms for $NaBPh_4$ + 18C6 and NaSCN + 18C6 systems in THF solutions.[53] The associative-dissociative exchange mechanism prevails for $NaBPh_4$ + 18C6 while for NaSCN + 18C6 the bimolecular exchange mechanism dominates. It seems that the difference in the exchange kinetics in these two systems is due to the difference in the types of ion-pair formed. Contact ion pairs $Na^+ \cdot SCN^-$ in THF solutions effectively reduce the cation-cation repulsion at the transition state of the bimolecular exchange mechanism and lower the energy level of the transition state, $NaBPh_4$ only forms solvent-separated ion pairs and the exchange occurs by the associative-dissociative mechanism.

1.2.3 The influences of solvent properties on the kinetics of the complexation and the exchange reactions

Thermodynamics and kinetics of complexation reactions are influenced by the solvating abilities of solvents since the complexation process involves partial or complete desolvation of the cations and of the ligands. Moreover, as shown above, complexation process is influenced by interionic association and, therefore by the dielectric constant of the medium.

The solvating abilities can be measured by the donor numbers of the solvents defined by Gutmann[57] as the negative change of the enthalpy in kcal $mole^{-1}$ upon the complexation of the solvents with $SbCl_5$ in dilute 1,2-dichloroethane solutions:

$$\text{Solvent} + SbCl_5 \xrightarrow{\text{1,2-DCE}} \text{Solvent}\cdot SbCl_5, \quad DN = -\Delta H$$

Higher DN's correspond to more negative $-\Delta H$ and better solvating abilities.

Influences of solvents on the complexation reaction kinetics, like the influences of cations and ligands, are reflected much more in the dissociation rates than in the formation rates of the complexation reaction(see Table 4).[58] For example, the dissociation rates increase sharply with increasing donor number of the solvent, covering a range of more than 9 orders of magnitude for the alkali ion cryptates, whereas the formation rates decrease but are much less sensitive to solvent variation.

The significance of the solvent dependence of the formation and the dissociation rate constants of the complexation reactions is due to the fact that the properties of the transition state most closely resemble those of the reactants, therefore the transition state is closer to the reactants. The structures of the transition states can be identified from the differences of the

activation parameters of the complexation reactions. Shamsipur et al.[67] studied the kinetics of the complexation reaction of Cs^+ + C221 and Cs^+ + C222 systems in dimethylformamide solutions. The activation enthalpy, the activation free energy, and especially the activation entropy are quite different for the two different ligands. These differences arise mainly from the difference in the transition-state structure. Based on the positive entropy change for the release of Cs^+ from the complex with C222 in DMF, it has been suggested[59] that the transition state for the release of the cation resembles the final state of the solvated Cs^+ ion and cryptand. Although the change in activation energy with solvents for the Cs^+·C221 complex also requires the resemblance of the transition state to the final states of the solvated cation and the cryptand, negative activation entropy value for the decomplexation step implies the more rigid transition state for C221 than for C222.

Differences in solvations of both cations and ligands in different solvents can readily explain the variation of the stabilities as well as the formation and the dissociation rate constants with solvents. As mentioned before, the complexation rates depend on solvations of cations in the inner coordination sphere and solvations of the ligands.[49] The stability constants and the rates of formation and dissociation of complexes of the alkaline earth-metal cations Ca^{2+}, Sr^{2+}, and Ba^{2+} with cryptands C211,

C221, C222, $C2_B22$, and $C2_B2_B2$ have been measured in methanol solutions by Cox et al..[49] The authors examined the solvent's influence on the complexation kinetics by comparing the results to those obtained in aqueous solutions. The change of reaction environment from water to methanol has the effect of increasing the formation rates of the complexes and reducing their dissociation rates, the both being related to the higher stabilities of the complexes in methanol compared to in water. Higher complexation rates in methanol are very probably due to weaker solvation of the free cation, and in cases like C222, also to weaker solvation of the ligand. However, the authors stated that ligands such as $C2_B22$ and $C2_B2_B2$ are more strongly solvated in methanol than in water because of the more organic nature of these two cryptands than that of C222. This stronger solvation of the monobenzo and dibenzo ligands in methanol should contribute to lowering the values of formation rate constants k_f, and in the case of $Ca(C2_B2_B2)^{2+}$ k_f is extremely low(5×10^2 $M^{-1}s^{-1}$). For the alkali cryptates, the stronger solvation of ligands in water than in methanol was also proposed to explain the faster formation and the slower dissociation rates of cryptates in methanol solutions.[32] The large increase in the stability of the cryptates on transfer from water to methanol supports assumption that the free cryptands are considerably more

strongly solvated in aqueous solution than in nonaqueous solvents.

However, certain specific interactions between ligands and solvents and between ligands and cations can make exceptions to the generally observed solvent dependence of the complexation and the decomplexation reaction rate constants in terms of the solvating power of solvents.[60] For example, the formation rates in water are much lower, and the dissociation rates much higher than expected because of the H-bonded interactions between water and the electronegative atoms, such as O and N, of the ligands. This specific interactions of water with the ligand is the explanation for the unusual kinetic behavior for the cryptate $K(C222)^+$ in acetonitrile + water mixtures at 25 °C.[60] Both k_d and k_f have similar contributions to the increase of the stability constant of the complex with increasing mole fraction of acetonitrile due to the specific interactions of water with both the free cryptand and the resulting cryptate(see Table 5). In mixtures of acetonitrile + water the properties of the transition state cannot be closely related to those of either the reactants or the product. In the case of the cryptate $Ag(C222)^+$ in acetonitrile + water mixtures at 25 °C, the dissociation rate constant, k_d, of the complex shows a quite different dependence on solvent composition(see Table 5).[60] The decomplexation rate constant is almost independent of solvent composition and the rapid decrease of the stability

constant with X_{AN} near X_{AN} = 0 is determined entirely by the variation in the formation rate constant due to the preferential solvation of the Ag^+ ion by acetonitrile. The independence of k_d for the $Ag(C222)^+$ complex in the mixtures indicates that in the transition state the silver ion is strongly bonded to the C222 nitrogen lone pairs in a way typical of the partially covalent interaction of monovalent d^{10} ions with nitrogen donors, therefore the strong preferential solvation by acetonitrile of the free silver is lost in the transition state and its properties resemble those of the fully complexed silver in the product state.

Not only can the solvating power towards cations largely influence formation and especially decomplexation rates of complexation reactions, but it also affects the number of steps involved in complexation reactions.[61] For Na^+ + 18C6 and Li^+ + 18C6 systems, it appears that the Eigen-Winkler multistep mechanism is operative, the number of steps during the complexation between the cation and 18C6 depends on the nature of the cation and the solvent. In ethanol, the Na^+ ion reacts with 18C6 in a single step but in DMF the reaction involves two steps. It may be that the desolvation step in DMF has a larger energy barrier so that it shows itself as a separate relaxation process while in ethanol solution the desolvation and the complexation are probably of equal rates within the resolution of the time scale of the experimental method. For the Li^+ + 18C6 system, the cation reacts with the ligand by a two-step process in

ethanol but only by a one-step process in DMF, an opposite situation of the Na^+ + 18C6 case. It is likely that the greater desolvation energy and ligand rearrangement involved in complexing Li^+ with respect to Na^+ force the appearance of a two-step process in ethanol. The first step is an encounter process with a partial desolvation and ligand rearrangement and the second step is the complete encapsulation of the small Li^+ ion in the oversized 18C6 cavity, forcing the ligand to wrap around cation. In DMF, the last process involving the elimination of the coordinating solvent around Li^+ by 18C6, cannot occur to a significant extent due to the greater solvation of Li^+ than that of Na^+ in this solution. The above results demonstrate the importance of the solvent in determining the number of steps in the complexation process.

The solvation of cations can also make the complexation reaction kinetics of crown ether-complexes different from those of cryptates, especially in the formation rate constants. The formation rate constants are much slower for cryptates than for the crown ether-complexes.[63] One of the explanations for this behavior is the incomplete compensation for the loss of solvation of cations, because of the difficulties that cryptands have in adopting optimal conformations at various stages of complexation. The other explanation for the slower formation rates of cryptates than the crown ether-complexes is that in the multistep process of cryptate formation, there is a rate-determining step in

which two or more remaining solvent molecules of a partially complexed cation have to be removed prior to entry of the cation into the ligand cavity.[62] To summarize, lower rates should occur for higher charge density cations and for solvents in which cation-solvent interactions are particularly strong, as well as for more rigid ligands which cannot effectively compensate for the loss of the solvation of cations by complexation.[63]

Solvents also play an important role in determining the exchange reaction mechanism. Shamsipur et al.[64] studied the exchange reaction kinetics of Cs^+ ion with DB30C10 in nitromethane, acetonitrile, propylene carbonate, and methanol solutions by ^{133}Cs NMR. It was seen that in nitromethane solutions the dissociative exchange mechanism is predominant at all temperature studied, while in the other three solvents, the exchange is bimolecular below -10 °C; in propylene carbonate and methanol solutions above -10 °C the exchange follows the dissociative pathway. In the bimolecular exchange mechanism, the conformational rearrangement of the ligand must favor in the transition state a simultaneous departure of the complexed cation and an arrival of the new cation. Apparently, solvents with strong solvating ability help reduce the cation-cation repulsion in the transition state in the bimolecular exchange mechanism, while in solvents of poor solvating power the associative-dissociative mechanism is favored. At higher temperature, even in the good solvating solvents, the

associative-dissociative mechanism becomes predominant since the solvation ability of a solvent decreases with increasing temperature.

The influences of solvents on the complexation reaction kinetics are also reflected in the activation parameters, such as activation energies, activation entropies and activation free energies, of the transition states of the reactions. The positive entropy of activation indicates solvent participation in the transition state.[68] Usually, the high activation enthalpies correspond to weak solvation in the transition state and the net energy required to transfer M^+ cation from the complexed state to the solvent(uncomplexed M^+) decreases with increasing solvent donicity which is a good measure of the solvation energy. For example, in the complexation kinetic study of K^+ + 18C6 in dioxolane and in a acetone-dioxolane mixture(80:20,v/v), the activation enthalpy values for the exchange reactions are 16.2±0.3 and 13.2±0.5 kcal mol^{-1} respectively, while in acetone solutions it is 8.6±0.5 kcal mol^{-1}.[65] Bhattacharyya et al.[56] have shown that the large alkali cations remain practically unsolvated in tetrahydrofuran solutions. It is expected that the same lack of solvation would be observed in 1,2-dioxolane. Cahen et al.[66] showed that the activation energies for the release of the Li^+ ion from Li^+-C211 complexes in pyridine, water, dimethyl sulfoxide, dimethylformamide, and formamide increase with the increasing donicity of the solvents. The fact that the

activation energy for the release of the lithium ion from the cryptate complex increases with solvent donicity, opposite to the overall energy change between the initial and the final states for the decomplexation, indicates that the transition state must involve substantial ionic solvation. Shamsipur et al.[67] also reported a similar trend of the change of the dissociation rates as well as activation energy and free activation energy with the change of the donicity of solvents.

In other studies, the influence of solvent donicity on complexation kinetics was not observed. Ceraso et al.[68] found that in THF, H_2O, pyridine solutions the activation energy for the release of both sodium and lithium ions are not related to solvent donicity. Shchori et al.[51,69] showed that the activation energies of the decomplexation of some $Na(Crown)^+$ complexes are independent of solvents, although the three solvents that they chosen in their study (methanol, dimethylformamide, and dimethoxyethane) coincidently have similar donicities--DN_{MeOH}=25.7, DN_{DMF}=26.6, and DN_{DME}=24.

It should also be noted that in complexation kinetic studies of metal ions with macrocyclic ligands, it is not uncommon that activation entropy(ΔS°) and enthalpy(ΔH°) of the decomplexation reactions compensate each other($\Delta G^\circ = \Delta H^\circ - T\Delta S^\circ$) , so that the free activation energy somewhat

insensitive to solvents, and exchange rates vary by only a small factor.[66,65,70]

1.3 PURPOSES OF THIS STUDY

As described previously, kinetic data are relatively meager as compared to widely investigated thermodynamics of complexation,[8,15,71-73] even though they are equally important for the understanding of the selective transport process of cations by crown ethers or catalysis in reactions involving ionic species.[74] More studies about kinetics of the complexation in terms of the influences of solvents, ligands, cations and their counter ions on complexation kinetics are necessary to enlarge our present understandings of this field.

Recent studies have reveal some interesting aspects of the kinetics of the complexation and the exchange reactions. The dependence of the exchange mechanism on temperature and on concentration was observed in studies by Popov et al.[64,75] and by Detellier et al.[76], respectively. The exchange reaction takes different pathways between the associative-dissociative and bimolecular processes at different temperatures in the same solutions or changes with the concentration of cations. The change of the activation energy with temperature was also observed. These observations are still not fully understood and further investigations are necessary.

The multistep complexation reaction mechanism proposed by Petrucci and Winkler[19-20,22-26] emphasizes, in the complexation reactions, the influence of solvation of ligands and cations, of conformation change of ligands, and of the ion pair formation. The ion pair formations of electrolytes and aggregations of the ion pairs are determined by the dielectric constants of solvents. Dimethoxyethane and tetrahydrofuran have almost the same dielectric constants(7.20 and 7.39 at 25 °C respectively) but different solvating abilities towards cations.[54] Since in these two solvents the extent of ion pair formations should be approximately the same, they provide a fine opportunity to isolate the effects of the ion pair formation from that of solvation on the complexation kinetics.

It has been postulated that in THF solutions there is a relationship between the types of the ion pairs formed and the exchange reaction kinetics.[53] In the case of $NaBPh_4$ ion pairs are solvent-separated, while for NaSCN, NaI and $NaClO_4$ the contact ion pairs are formed. At room temperature on the NMR time scale of a spectrometer operating at 42.27 kG, the exchange reaction is slow for $NaBPh_4$ and fast for the other sodium salts between their uncomplexed sites and complexed sites by 18C6 ligand. For NaSCN, the charge-charge repulsion at the transition state of the bimolecular exchange mechanism is supposedly reduced by the contact ion pairs formed and the bimolecular exchange mechanism therefore prevails and the exchange reaction is fast. In the THF

solutions of $NaBPh_4$, since the majority of the electrolyte forms solvent-separated ion pairs, the exchange reaction has to proceed by the associative-dissociative pathway and the reaction rates are relatively slow. Since DME has almost the same dielectric constant as that of THF, any differences in the exchange kinetics will reveal the difference of the two solvents in terms of the solvations. In addition, the kinetic investigation of the exchange reactions in DME solutions can serve as a probe to test the postulate of the influence of the ion pair formations on the exchange reaction kinetics.

As pointed out by Strasser,[50] kinetic studies of the exchange reactions involving lithium ions and crown ethers are essential to the full understanding of the influence of cations on the exchange reaction kinetics. Two mechanisms(the associative-dissociative and the bimolecular, Equations 4 and 5 on page 9) for the exchange of metal ions between their uncomplexed and the complexed sites. But which mechanism prevails depends on the factors such as ion pair formations, solvent donicities, and etc. Previous studies have shown that for the alkali metal ions with crown ethers there is a trend for the preference of the exchange pathways going from Na^+ to K^+, and Cs^+. The predominant exchange mechanism for the Na^+ ion is either the associative-dissociative or bimolecular process while the bimolecular process is primarily preferred for the Cs^+ ion. Increased tendency to form ion pair due to the decreased charge

density as one goes to the larger cation has been considered as the explanation of this trend,[50] because the charge-charge repulsion in the bimolecular exchange mechanism can be minimized by the ion paring and thus the bimolecular mechanism predominates. However, this conclusion has been based only on the kinetic studies of three of the five alkali cations and therefore is incomplete. The contribution of the of other alkali metal ions to the kinetic information is important for the complete explanation of the influence of cations on the exchange kinetics in the future.

Thallium is a transition metal; the size of the Tl(I) ion(r=1.40Å) is very close to that of the potassium(I) ion(r=1.33Å, r's are the Pauling ionic radii). It provides an opportunity to compare the influence of alkali metal and non-alkali metal cation, on the kinetics of the exchange reactions. The thallium nucleus has the spin of I=1/2, a desirable property for the NMR measurement because of the narrow line-width and good sensitivity of the ^{205}Tl resonance. Because of the similarity of the potassium and thallium ions in their sizes, and because of the good sensitivity of ^{205}Tl NMR, in studies of the influences of charge densities of cations on the exchange reaction kinetics, thallium(I) can also serve as a substitute for potassium, which has a low sensitivity and makes the accurate NMR measurements difficult.

Thermodynamic studies are still unable to elucidate unambiguously the nature of the macrocyclic effect. Kinetic studies, generating the reaction rate constants and information of the reaction mechanism, can offer insights into the detailed reaction pathways, and can possibly help to clear the problem of the role of entropy or enthalpy in providing extra stabilities of the cyclic complexes. In addition, there have been very few kinetic studies that deal with the linear polyether ligand complexing metal ions, and any contribution to the kinetic studies of linear ligand complexations would be significant for the further development in this field.

In this study, dynamic NMR spectroscopy will be employed to investigate the kinetics of the exchange reactions between the uncomplexed and the complexed metal ions, with a variety of cations(Li^+, Na^+ and Tl^+), ligands(18C6, 15C5, and pentaglyme), and solvents(THF, DME, AN, and NM) for the objectives given above.

Table 1. Ionic diameters of cations and diameters of cavities of crown ether molecules(Å)

Alkali metal	Ionic diameter	Crown ether	Cavity size
Li^+	1.36	14-Crown-4	1.2-1.5
Na^+	1.94	15-Crown-5	1.7-2.2
K^+	2.66	18-Crown-6	2.6-3.2
Rb^+	2.94	21-Crown-7	3.4-4.3
Cs^+	3.34		
Tl^+	2.80		

Reference 8.

Table 2. The stability constants of 18C6- and pentaglyme-metal complexes

Ligand	Cation	Solvent	Log K_f	Reference
Pentaglyme	Na^+	Methanol	1.5	8
18-Crown-6	Na^+	Methanol	4.32	8
Pentaglyme	K^+	Methanol	2.2	8
18-Crown-6	K^+	Methanol	6.1	8
Pentaglyme	Ag^+	Methanol	1.80	77
18-Crown-6	Ag^+	Methanol	4.58	77
Pentaglyme	Tl^+	DMF	0.50	78
18-Crown-6	Tl^+	DMF	3.73	78

Table 3. The complexation and decomplexation rate constants of some alkali and alkaline earth cation cryptates in methanol

Cations		Ligands C211	C221	C222
Li^+	k_f	4.8×10^5	1.8×10^7	----
	k_d	4.4×10^{-3}	7.5×10	$>3 \times 10^2$
Na+	k_f	3.1×10^6	1.7×10^8	2.7×10^8
	k_d	2.50	2.35×10^{-2}	2.87
Ca^{2+}	k_f	9.0×10^3	1.9×10^4	3.6×10^4
	k_d	3.6×10^{-2}	2.3×10^{-6}	2.2×10^{-4}
K^+	k_f		3.8×10^8	4.7×10^8
	k_d		1.09	1.8×10^{-2}
Sr^{2+}	k_f		9.2×10^4	3.1×10^5
	k_d		8.2×10^{-7}	5.5×10^{-7}
Rb^+	k_f		4.1×10^8	7.6×10^8
	k_d		7.5×10	8.0×10^{-1}
Ba^{2+}	k_f		1.9×10^6	5×10^6
	k_d		4.6×10^{-5}	6.3×10^{-7}
Cs^+	k_f		5×10^8	9×10^8
	k_d		2.3×10^4	4×10^4

Reference 32,49;
k_f : M^{-1} s^{-1} ; k_d : s^{-1}.

Table 4. Complexation and decomplexation rate constants of lithium and cesium cryptates in various solvents

Solvent	Cryptate			
	$Li(C211)^+$		$Cs(C222)^+$	
	k_f	k_d	k_f	k_d
H_2O	8.3×10^3	2.5×10^{-2}		
MeOH	4.8×10^5	4.4×10^{-4}	9×10^8	4×10^4
EtOH	1.8×10^5	6.0×10^{-4}		
Me_2SO	1.5×10^4	2.1×10^{-2}		
DMF	1.4×10^5	1.4×10^{-2}		
NMP	1.3×10^4	4.8×10^{-3}		
PC	$<3 \times 10^7$	$<10^{-5}$	5×10^6	3×10^2

Reference 58;
k_f : M^{-1} s^{-1} ; k_d : s^{-1}.

Table 5. Rate constants of dissociation (k_d), formation (k_f), and formation constants (K_F) for the cryptates $Ag(C222)^+$ and $K(C222)^+$ in acetonitrile + water mixtures at 25 °C

	$Ag(C222)^+$			$K(C222)^+$		
X_{AN}	k_d s^{-1}	$k_f x10^{-8}$ $M^{-1}s^{-1}$	$K_F x10^{-8}$ M^{-1}	k_d s^{-1}	$k_f x10^{-8}$ $M^{-1}s^{-1}$	$K_F x10^{-6}$ M^{-1}
0.00	0.46±0.01	15.6	34	7.5±0.8	0.03	0.4
0.05	0.7±0.1	2.5	3.5			
0.1	0.8±0.1	1.3	1.6	3.7±0.4	0.12	3.2
0.2	1.0±0.2	1.1	1.1	1.7±0.2	0.22	13
0.3	1.0±0.2	1.1	1.1	0.87±0.09	0.44	51
0.4				0.66±0.07	0.83	126
0.5	1.0±0.2	1.5	1.5	0.44±0.04	1.75	398
0.6				0.31±0.03	2.46	794
0.7	1.2±0.2	2.4	2.0			
0.9	0.8±0.1	4.3	5.4	0.057±0.006	11.4	20000
1.0	0.5±0.1	4.2	8.4	0.0046±0.0005	11.6	252174

Reference 60.

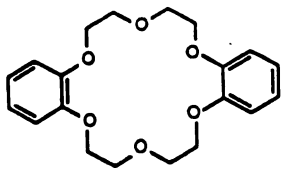

Dibenzo-18-Crown-6
DB18C6

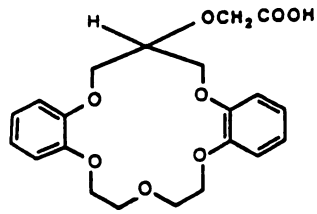

Sym-Dibenzo-16-Crown-5
Oxyacetic acid

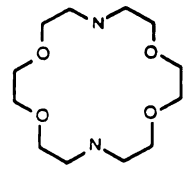

Diaza-18-Crown-6
DA18C6

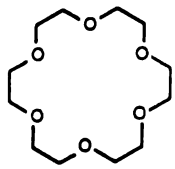

18-Crown-6
18C6

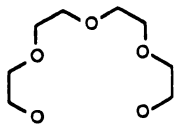

Tetraglyme

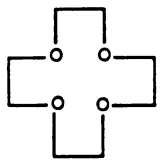

12-Crown-4
12C4

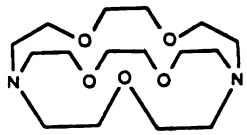

Cryptand
C221

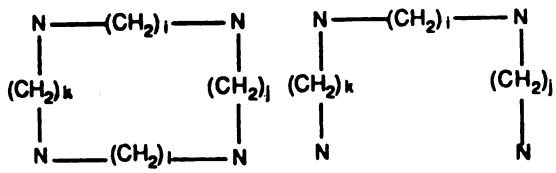

Macrocyclic and linear tetraamines

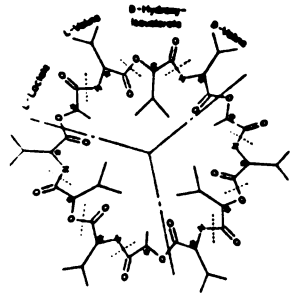

Valinomycin

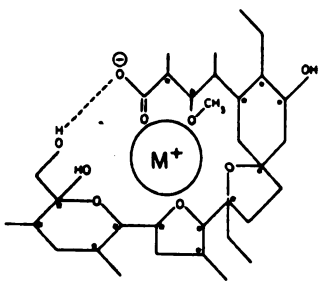

Monensin Complex

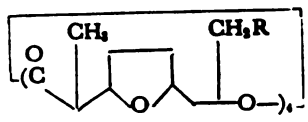

Nonactin
Monactin
Dinactin
Trinactin

Figure 1. Structures of some synthetic and naturally occurring macrocyclic and linear ligands

Chapter 2

EXPERIMENTAL SECTION

2.1 Purifications of solvents and salts

Molecular sieves(3 Å or 4 Å) were washed with deionized water to eliminate soluble impurities followed by being dried in an oven at 130 °C for a few days and then in another oven at ~750 °C for additional few days under nitrogen. These freshly activated molecular sieves were stored in brown bottles in a dry box under helium atmosphere for the future use.

Tetrahydrofuran(THF, Mallinckrodt) and 1,2-dimethoxyethane(DME, J.T.Baker) were refluxed over potassium metal with benzophenone until the color of benzophenone changed to blue and then fractionally distilled. Nitromethane(NM, Specto purity, EM Science) was dried over calcium hydride under nitrogen atmosphere for 48 hours before distilled. Acetonitril(AN, Specto purity, J.T.Baker) was of spectral grade and contained less than 0.0001% water; it was not further purified except for being stored with the freshly prepared molecular sieves before use. All the purified solvents were stored in brown bottles in a dry box under helium atmosphere. In addition, all the purified solvents were tested by a GC test method described in literatures[73a,79] for water contents in order to assure that the solvents contain less than 100 ppm water. All the

purified solvents were again treated with the freshly prepared molecular sieves prior to use.

Sodium tetraphenylborate($NaBPh_4$, Gold label, Aldrich) was dried under vacuum at room temperature for 48 hours. Sodium perchlorate($NaClO_4$, reagent grade, Matheson Coleman Bell) was dried at 110 °C for several days. NaSCN(Reagent grade, Mallinckrodt) was recrystalized from acetonitrile and dried under vacuum at 60 °C for two days. $LiClO_4$(Fisher Scientific) was dried at 190 °C for one week. $TlClO_4$(K&K Chemical Company) was recrystalized from deionized water and then dried at 120 °C for three days.

18-Crown-6(18C6)(Aldrich) was recrystalized twice from acetonitrile and dried in a vacuum oven at room temperature for 48 hours. 12-Crwon-4(12C4, Aldrich) was refluxed at reduced pressure under helium atmosphere and then vacuum dried at room temperature for two days. 15-Crown-5(15C5) was synthesized and purified by a method described by Okoroafor.[80]

2.2 Dynamic NMR spectroscopy

2.2.1 Concepts of dynamic NMR spectroscopy

Sparse information available on the kinetics of the complexation of alkali metal ions by macrocyclic crown ethers may be attributed to experimental difficulties in obtaining such data because of the high reaction rates when

crown ethers are involved, as well as the lack of color of the complexes which makes spectrometric measurements nearly impossible. The formation of stable ion pairs and of higher aggregates in nonaqueous solvents with low dielectric constants can also lend difficulties to the electrochemical measurements and limit the use of them to high dielectric medium in which there is very little or no ionic association.

Dynamic NMR spectroscopy, as compared to the other techniques used for the kinetic measurements, can measure the reaction rates in the middle range.[73b] In the numerical terms, the dynamic range of this technique is from 10^{-1} to 10^{-6} seconds.[73] Generally, the processes of ligand conformational changes, ion pair formations and higher aggregations of ion pairs have faster reaction rates than this limit and cannot be detected by the NMR technique. What are measured by dynamic NMR, however, are the rates of the overall processes (or the rates for the slowest steps) of a series of sequential equilibria.

It was discussed previously in Chapter 1 that when metal ions are encountered by neutral macrocyclic or linear polyether ligands, complexation reactions occur. Complexation reactions may be accompanied by conformational changes of the ligands, the dissociation of the ion paris, the desolvations of both the cations and the ligands, and the conformational change of the complexes before the final

configuration of the complex is formed. The influence of the ionic aggregations is very important especially in nonaqueous solutions of low dielectric constants. When concentrations of metal ions are greater than that of ligands, exchange reactions for the metal ions between the uncomplexed and the complexed sites exist and proceed by the two mechanisms: the associative-dissociative and the bimolecular mechanisms(Equations 4 and 5, Chapter 1).

If one of the steps in the exchange mechanisms has a rate measurable by dynamic NMR, the kinetic information of the exchange reactions can be obtained. This slow step is usually the decomplexation of the exchange reaction while the formation rate reaches the diffusion-controlled range. Thus, by NMR studies, a series of very complicated reactions, which are often times the case in solvents of low dielectric constants, can be "simplified" as an overall one-step exchange reaction, and the important kinetic information such as the reaction rate constants and the activation parameters of the overall reactions can be obtained.

An advantage of the dynamic NMR method is that it studies the overall complexation and the exchange reaction kinetics without being interfered by the other side-reactions. The disadvantage is that dynamic NMR is only capable of kinetically studying the chemical reactions at equilibrium--the exchange reactions. Under the circumstance

which will be described below, this method is unable to deduce the desired kinetic information from the chemical reaction systems. When the exchange reactions proceed through the associative-dissociative mechanism and the exchange rates are in the dynamic range of NMR spectroscopy(10^{-1} to 10^{-6} seconds), the overall rate constants of the decomplexation step k_d can be measured and the overall rate constants of the complex formation k_f can be calculated through the relation: $K_F = k_f/k_d$, if the complexation constant K_F is known. For the exchange reactions by the bimolecular mechanism, the forward and the backward reactions are identical and so are the rate constants associated with each step. The overall rate constants measured by dynamic NMR are the exchange rate constants and the overall complexation and decomplexation rate constants cannot be obtained.

Whether a exchange reaction proceeds by the associative-dissociative or the bimolecular mechanism can be determined by performing dynamic NMR measurement. First, the mean life times of the free and bound metal ions undergoing the exchange reactions at equilibrium are obtained. Through the analysis of the dependence of the mean life times on the metal concentrations, the two exchange mechanisms can be differentiated. Plotting $1/(\tau[M^{n+}]_T)$ against $1/[M^{n+}]$, according to the following equation(Equation 6),

$$\frac{1}{\tau[M^{n+}]_T} = k_1 + \frac{k_{-2}}{[M^{n+}]} \qquad (6)$$

a straight line should be obtained, either with a zero slope and an intercept of k_1, or with a zero intercept and a slope of k_{-2}, depending on which one of the two mechanisms predominates. In the above equation, τ is the mean life time of a metal ion, $[M^{n+}]_T$ and $[M^{n+}]$ are the total and the uncomplexed concentrations of the metal ion respectively, k_1 and k_{-2} are the rate constants of the corresponding exchange reaction mechanisms discussed in Chapter 1. If both the slope and intercept are not zero, it is likely that the two exchange mechanisms coexist.

Measuring the mean life time τ of species at different temperatures generates the rate constants as a function of temperature through Equation 6. Arrhenius plots, ln k vs. 1/T(K) or ln $(1/\tau)$ vs. 1/T, yield activation energies E_a of the reactions. From the following Eyring equations, the other activation kinetic parameters can be obtained:

$$\Delta H^{\ddagger} = E_a - RT \quad (7)$$

$$k_T = \frac{k_B T}{h} \exp\left(\frac{-\Delta G^{\ddagger}}{RT}\right) \quad (8)$$

$$\Delta G^{\ddagger} = \Delta H^{\ddagger} - T\Delta S^{\ddagger} \quad (9)$$

where k_T is the rate constant at temperature T; $\Delta H^{\ddagger}$, $\Delta G^{\ddagger}$ and $\Delta S^{\ddagger}$ are the activation enthalpy, activation free energy, and the activation entropy respectively; k_B, h and R are the Boltzman's constant, the Plank's constant, and the gas constant respectively.

2.2.2 Theoretical Aspects of Dynamic NMR Spectroscopy

2.2.2.1 In the absence of the exchange reactions

For nuclei not undergoing the exchange reactions between different sites, Block equations in a rotating coordinate at the Larmor frequency v_o along z axis have the following forms:[81]

$$\frac{du}{dt} = (W_o - W) - u/T_2 \tag{10}$$

$$\frac{dv}{dt} = -(W_o - W) + irM_zB_1 - W/T_2 \tag{11}$$

$$\frac{dM_z}{dt} = -rW_oB_1 - (M_z - M_o)/T_1 \tag{12}$$

$$\text{and } W_o = rB_o/2\pi \tag{13}$$

where u and v are the components of the magnetization of the nuclei in the x and y directions in the rotating frame respectively; M_z is the z-component of the magnetization; r is the magnetogyric ratio; B_o is the strength of a static magnetic field in which the nuclei are subject to; B_1 is the secondary magnetic field perpendicular to B_o and is used to perturb the magnetization of the nuclei at equilibrium; T_1 and T_2 are the spin-lattice and spin-spin relaxation times characterizing the regaining of the equilibria of the magnetizations in xy plane and in z-axis respectively after the magnetizations are perturbed by an impulse of the

secondary field B_1. Taking the Fourier transform of the solution of the above differential equations yields:

$$R(W) = M_{y'}^{+}\, T_2 \left[\frac{1 - 2\pi i(W_o - W)}{1 + 4\pi^2 T_2^2 (W_o - W)^2}\right] \qquad (14)$$

where $M_{y'}^{+}$ is the magnetization projected on to the y-axis in the rotating frame immediately following the impulse of B_1. It can be seen that the real part of this equation describes a Lorentzian line in character centered at W_o and the line-width at half-height $\Delta W_{1/2}$ can be related to the spin-spin relaxation time T_2 by the following relationship:

$$\Delta W_{1/2}(hz) = 1/\pi T_2 \ .$$

To describe the relaxations of magnetization of nuclei of metal ions by quadrupolar relaxation mechanism, the relaxation rate $(1/T_2)$ can be related to the spin quantum number I of the nucleus, the asymmetry factor Ç of the electric field around the nucleus, the quadrupolar moment Q of the nucleus, the Z component of the electric field gradient d^2V/dZ^2 at the nucleus, and the correlation time τ_c of the nuclei by the following equation:[82]

$$\frac{1}{T_2} = \frac{1}{T_1} = \frac{3(2I+3)}{40I^2(2I-1)} \left(1 + \frac{\zeta^2}{3}\right)\left(\frac{eQ}{h}\frac{d^2V}{dZ^2}\right)^2 \tau_c \qquad (16)$$

and

$$\tau_c = A \cdot \mathrm{EXP}\left[\frac{Er}{RT}\right] \qquad (17)$$

if T_2 equals T_1 under narrowing conditions such as in solutions.

To relate the relaxation rate to temperature, by assuming ζ^2 and d^2V/dZ^2 as constants over the range of temperature, we come to:

$$\frac{1}{T_2} = A' \cdot \mathrm{EXP}\left[\frac{Er}{RT}\right] \quad \text{and} \qquad (18)$$

$$\frac{1}{T_2} = \left(\frac{1}{T_2}_{298.15}\right) \mathrm{EXP}\left[\frac{Er}{R}\left(\frac{1}{T} - \frac{1}{298.15}\right)\right] \qquad (19)$$

where $(1/T_2)_{298.15}$ is the relaxation rate measured at 298.15 K, T is the absolute temperature and R is the gas constant, Er is the activation energy for solvent reorientation.[83]

Usually, relaxation times T_2^* measured experimentally are shorter than actual relaxation times T_2 due to the magnetic field inhomogeneity caused by the instrumental imperfections such that:

$$\frac{1}{T_2^*} = \frac{1}{T_2} + \frac{1}{T_{inhomo}} \qquad (20)$$

2.2.2.2 In the presence of the exchange reactions

When nuclei undergo chemical exchange reactions between two nonequivalent sites(without spin-spin coupling), the effect of the exchange reactions on line shapes(or relaxation times) of the two NMR signals corresponding to the two nonequivalent sites depends on the rates of the exchange reactions.[84] Qualitatively, at a <u>very slow</u> exchange reaction rate, two distinct signals are observed, corresponding to the two sites centered at W_{oA} and W_{oB} with line widths determined by: $1/\pi T_{2A}$ and $1/\pi T_{2B}$ of Lorentzian line shapes respectively, where W_i and T_{2i} are the frequencies and the relaxation times corresponding to site i(i=A or B). In the case of a <u>slow</u> exchange reaction, the similar lines are observed but the line widths $1/\pi T'_{2A}$ and $1/\pi T'_{2B}$ are broadened by the exchange reactions, i.e.:

$$1/\pi T'_{2A} = 1/\pi T_{2A} + 1/\pi \tau_A \qquad (21)$$

and

$$1/\pi T'_{2B} = 1/\pi T_{2B} + 1/\pi \tau_B \qquad (22)$$

respectively, where τ_A and τ_B are the life times of nuclei at sites A and B. When a exchange reaction is very fast, the two signals coalesce to give a population-averaged signal whose line width $1/T_{obs}$ is determined by:

$$1/T_{obs} = P_A/T_{2A} + P_B/T_{2B} \qquad (23)$$

where P_A and P_B are the relative concentrations of the exchanging species at sites A and B respectively. In the case of a fast exchange reaction, again only one signal is observed but it contains a linebroadening factor due to the exchange reaction:

$$1/T_{obs} = P_A/T_{2A} + P_B/T_{2B} + P_A^2 P_B^2(|W_{oA} - W_{oB}|)^2(\tau_A + \tau_B) \qquad (24).$$

Kinetic studies by NMR spectroscopy is done through the line shape analysis of the signals of species undergoing the exchange. As has been shown, very fast and very slow reactions do not have observable influence on the lineshapes, and the reaction rates can not be obtained through the NMR method. Only those of the reactions with rates in a certain limits, as will be demonstrated below, can be investigated by this NMR method. For slow reactions, according to Equations 21 and 22, it can be obtained that:

$$1/\pi\tau_A = 1/\pi T'_{2A} - 1/\pi T_{2A} \qquad (21')$$

and

$$1/\pi\tau_B = 1/\pi T'_{2B} - 1/\pi T_{2B} \qquad (22')$$

where $1/\pi T'_{2i}$ and $1/\pi T_{2i}$ are equal to the line widths $\Delta W'_{(i)1/2}$ and $\Delta W_{(i)1/2}$ respectively. Usually, the precision of the measurements of the line widths is in the neighborhood of 1 to 10 hz, and thus the measurements of τ can be accurate as 1 to 10_1 second. For <u>fast</u> reactions, rearrangement of Equation 24 gives:

$$1/T_{obs} - (P_A/T_{2A} + P_B/T_{2B}) = P_A^2\, P_B^2(|W_{oA} - W_{oB}|)^2(\tau_A + \tau_B) \qquad (24').$$

where the right-hand side is the line-broadening due to the exchange reactions and it has to be greater than 0 in theory, but because of the precision of the measurements, at least greater than 1 hz in practice. It can be realized in the following equation:

$$(\tau_A + \tau_B) > \frac{1}{P_A^2\, P_B^2(|W_{oA} - W_{oB}|)^2} \qquad (24'')$$

$\frac{1}{1}$

P_A and P_B complement each other and can be any numbers in the practical range of 0.1 to 0.9. For P_AP_B, it reaches its maximum at 0.25 and its minimum at 0.09. In turn, $(P_AP_B)^2$ is in the range 0.0081 - 0.0625 and the average is 0.0353.

Substituting this average number into Equation 24", we obtain:

$$(\tau_A + \tau_B) > \frac{28}{(|W_{oA} - W_{oB}|)^2} \qquad (24"')$$

where $(|W_{oA} - W_{oB}|)^2$ can be as high as 10^8(See Chapter 4), thus

$$(\tau_A + \tau_B) > 3 \times 10^{-7} \text{ s.}$$

indicating that the life times can not be smaller than 10^{-7} second if the reaction rates are to be measured by the dynamic NMR method.

As can be seen from the above equations, in order to derive the life times of τ_A and τ_B, T_{2A} and T_{2B}, W_A and W_B, as well as P_A and P_B need to be known beforehand. This same requirement also holds for the method of the full-line-shape-analysis to obtain the life times as will be discussed later in this chapter. The NMR lineshape analysis of the kinetic studies of two-site(A and B) exchange reactions can be done by iteratively fitting a theoretical equation, which contains the relaxation times, resonance frequencies of site A and B, and the mean life times of the metal ions, to experimental spectra. This method is called full-line-shape-analysis and is usually assisted by computers.

To obtain the theoretical equations of spectra of nuclei undergoing exchange reactions, Block equations describing the motions of xy components of magnetizations of un-coupled sites A and B in the rotating frame as modified to include the effect of the chemical exchange on them are:[85]

$$\frac{dM_A}{dt} + \alpha_A M_A = irB_1 M_{OA} + \tau_B^{-1} M_B - \tau_A^{-1} M_A \qquad (25)$$

$$\frac{dM_B}{dt} + \alpha_B M_B = irB_1 M_{OB} + \tau_A^{-1} M_A - \tau_B^{-1} M_B \qquad (26)$$

where

$$\alpha_A = \tau_{2A}^{-1} - i(W_A - W_{rf}) ,$$
$$\alpha_B = \tau_{2B}^{-1} - i(W_B - W_{rf}) ;$$
$$M_A = u_A + iW_A ,$$
$$M_B = u_B + iW_B ;$$

τ_A and τ_B are lifetimes in states A and B respectively; W_{rf} is the variable frequency; the other symbols have their usual meanings. For pulsed sequence experiments, the signal in time domain is obtained by solving the Block differential equations while $B_1 = 0$:

$$\frac{dM_A}{dt} + (\alpha_A + \tau_A^{-1})M_A - \tau_B^{-1} M_B = 0 \qquad (27)$$

$$\frac{dM_B}{dt} + (\alpha_B + \tau_B^{-1})M_B - \tau_A^{-1} M_A = 0 \qquad (28)$$

The solution of the above differential equations is:

$$M(t) = M_A + M_B = C_1 e^{\Gamma_1 t} + C_2 e^{\Gamma_2 t} \qquad (29)$$

where C_1 and C_2 are constants and

$$\Gamma_1 , \Gamma_2 = [-(\alpha_A + \alpha_B + \tau_A^{-1} + \tau_B^{-1} \pm (\alpha_A + \tau_A^{-1} - \alpha_B - \tau_B^{-1})^2 + 4\tau_A^{-1} \tau_B^{-1}\}^{1/2}]/2.$$

By using the initial conditions immediately after a $\pi/2$ pulse:

$$M_x = 0, \; M_y = M_{zo}$$

C_1 and C_2 can be obtained:

$$C_1 = -iM_{zo} (\Gamma_2 + P_A\alpha_A + P_B\alpha_B)/(\Gamma_1 - \Gamma_2)$$

$$C_2 = -iM_{zo} (\Gamma_1 + P_A\alpha_A + P_B\alpha_B)/(\Gamma_1 - \Gamma_2)$$

To obtain the signal in frequency domain, the Fourier transformation is applied to the free induction decay(FID) in time domain(Equation 29):

$$M(W) = \int_0^{\infty} M(t) e^{-i(W-W_{rf})} \, tdt$$

$$= - \frac{C_1}{\Gamma_1 - i(W-W_{rf})} - \frac{C_2}{\Gamma_2 - i(W-e_{rf})}$$

$$= \frac{iM_{zo} [\tau_A + \tau_B + \tau_A\tau_B(\alpha_A P_B + \alpha_B P_A)]}{[(1 + \alpha_A\tau_A)(1 + \alpha_B\tau_B) - 1]} \qquad (30)$$

where α_A and α_B have been redefined as following:

$$\alpha_A = T_{2A}^{-1} + i(W_A - W_{rf}),$$
$$\alpha_B = T_{2B}^{-1} + i(W_B - W_{rf}).$$

To accommodate some instrumental corrections, such as an artificial linebroadening and a delay time in order to improve the quality of a signal, and some phase corrections associated with spectra, these equations need to be modified. Strasser,[72a] Ceraso and Dye[68] have discussed at length the influence of chemical exchange reactions on NMR signal line shape in this aspect. The equation(26) has the form after including all the modifications:

$$M(W) = K\{I\cos[\theta_o - (W_A + \Delta - W)DE] - R\sin(\theta_o - (W_A + \Delta - W)DE]\} + C \quad (31)$$

where

$$I = AIMAM(XS) \; ; \; R = REAL(XS)$$

$$XS = -\frac{C_1 \, Exp[(\Gamma_1 - LB)DE]}{\Gamma_1 - LB} - \frac{C_2 \, Exp[(\Gamma_2 - LB)DE]}{\Gamma_2 - LB} \quad (32)$$

$$C_1 = -iM_{zo} \, (\Gamma_2 + P_A\alpha_A + P_B\alpha_B)/(\Gamma_1 - \Gamma_2)$$

$$C_2 = -iM_{zo} \, (\Gamma_1 + P_A\alpha_A + P_B\alpha_B)/(\Gamma_1 - \Gamma_2)$$

$$\Gamma_1 \, , \Gamma_2 = [-(\alpha_A + \alpha_B + \tau_A^{-1} + \tau_B^{-1} \pm \{(\alpha_A + \tau_A^{-1} - \alpha_B - \tau_B^{-1})^2 + 4\tau_A^{-1} \, \tau_B^{-1} \}^{1/2}]/2.$$

$$\alpha_A = T_{2A}^{-1} + i(W_A - W_{rf}),$$

$$\alpha_B = T_{2B}^{-1} + i(W_B - W_{rf}).$$

$$\tau = \frac{\tau_A \tau_B}{\tau_A + \tau_B} \tag{33}$$

$$P_A = \frac{\tau_A}{\tau_A + \tau_B} \; ; \qquad P_B = \frac{\tau_B}{\tau_A + \tau_B} \tag{34}$$

DE and LB are the delay time and line-broadening respectively; AIMAG(XS) and REAL(XS) are the imaginary and real parts of XS respectively.

The above equations(31-34) contain information such as the intensity K, baseline C, the zero order phase correction θ_o, the frequency shift Δ, and the lifetime τ, the frequencies and relaxation times W_A and W_B, T_{2A} and T_{2B}, of the species in sites A and B respectively without the exchange reaction, the relative concentrations P_A and P_B of the species in forms A and B. The frequencies(W_A and W_B) and the relaxation times(T_{2A} and T_{2B}) can obtained by measuring the resonance signals of the nuclei at A and B in the absence of exchange reactions; P_A and P_B can also be calculated if the equilibrium constant of the reaction is known, or can be directly obtained if the equilibrium constant of is very large. These parameters will be used as known constants in the curve fitting program. The rest of the parameters(K, C, θ_o, Δ, and τ), referred to as the unknown information, can be obtained by the curve-fitting process. After the lifetime, τ, is obtained, the reaction

rate constants can then be obtained in turn because τ is related to the reaction rate constants as has been discussed earlier in this chapter.

2.3 Procedures of dynamic multi-NMR measurement

2.3.1 Multi-NMR measurement

All NMR spectra of ^{1}H, ^{7}Li, ^{23}Na, and ^{205}Tl were taken on a Bruker WH-180 spectrometer with Fourier Transform function and equipped with a temperature control unit for variable temperature operations. The spectrometer was operating at a field of 42.27 KG and frequencies of 180, 69.96, 47.61 and 103.88 Mhz respectively for ^{1}H, ^{7}Li, ^{23}Na, and ^{205}Tl NMR. Chemical shifts of ^{23}Na, ^{7}Li and ^{205}Tl in various nonaqueous solutions were referenced to 0.01M NaCl, 1% $LiClO_4$ and 0.1M $TlClO_4$ in D_2O respectively, with the corrections for the differences in bulk magnetic susceptibilities of sample solutions and D_2O in which the references were contained.[86]

For Na-23 measurement, the configuration of an insert containing a lock solvent such as D_2O or acetone-d_6 inside a 10mm NMR tube was implemented for external locking. This geometry was described by Szczygiel.[73c] The advantage of using this configuration is that the magnetic field of the magnet can be kept from shifting with time and its homogeneity can be conveniently checked and maintained during measurements. However, the insert itself can cause an appreciable amount of inhomogeneity for signals with

extremely narrow linewidths and distort the Lorentzian line shape. In order to avoid such a field inhomogeneity, this configuration was abandoned in the measurements of ^{7}Li and ^{205}Tl which have very narrow linewidths--1-4 hz without exchange reactions present. The optimum homogeneity of the field was achieved by shimming the magnetic field carefully every time prior to data acquisition. During the period of data accumulation, the locking circuit was unplugged, and amplitude, level and the sweep width of lock signals were maintained at the minimum level to prevent the field from shifting.

2.3.2 Temperature calibration of the probe for variable temperature studies

In order to perform variable temperature kinetic studies, accurate temperatures inside probes need to be known. Usually, temperatures inside probes deviate from temperatures set by a temperature control unit on the spectrometer and deviations are different for each probe. Therefore, a temperature calibration is required for each probe. This was done by measuring the difference of the chemical shifts of the two proton signals of methanol contained in an NMR tube inside a probe at different temperatures. The dependence of the difference of the chemical shifts on temperature was known and measuring the difference of the chemical shifts at a experimentally

controlled temperature gives the actual temperature in the probe and the sample tube.[87-89]

On the WH-180 spectrometer, a Bruker B-ST 100/700 temperature control unit was used to control temperature and a calibrated Doric digital thermocouple was placed 1 cm below the sample tube to measure the temperature. A flow of nitrogen gas maintained the equilibrium of temperature.

2.3.3 Data treatment

Since VAX 11/750 system was introduced into chemistry department, the tedium associated with the KINFIT curve-fitting process[90] has been greatly reduced as has been the time required for kinetic studies. Strasser[72] and the other workers[73] have thoroughly described the concepts and the steps of computer-aided kinetic studies, and their work is highly recommended for references. Nevertheless, their work had been performed on a different computer system-CDC/750 and, by that time, the punch cards were still used to input data instead of interactively doing so like on VAX-760. Inevitably, the difference of doing the same type of the kinetic studies on the different computers appears to be significant. It is intended in this thesis to ease these differences by stressing how the work is done on the new computer system--VAX 11/750. The following is to show how the kinetic studies by dynamic NMR is done with the help of computers.

After a spectrum of the frequency domain is obtained, for the purpose of the line shape analysis, a portion of the spectrum of the interest is chosen by the zoom-function built in the software on the NMR spectrometer.

For nuclei in the absence of exchange reactions(either completely complexed or totally free), chemical shifts and relaxation times can be measured by a built-in program called NTCCAP on the WH-180 spectrometer. These information can also be obtained by a method described in Appendix I. The relaxation times and chemical shifts will be used as known constants in the equation of the two-site exchange for the curve-fitting process to get the best fit of the life times τ.

In the case when exchange reactions exist, spectra are taken and treated in the same way as are without exchange reactions. After a range of the spectrum of the species undergoing exchange reactions is chosen, this portion of the spectrum is transferred to a file called, for example, TEST.DAT on VAX miniframe computer for the full-line-shape-analysis to derive the lifetime τ.

Two programs involved in the data transfer routine, NTCDTL on the Bruker-180 spectrometer and GETNMR(Appendix B) on VAX, are coordinated in a way described in Appendix A so that the data can be transferred from the spectrometer to the VAX miniframe and stored in a data file. An example of this file(TEST.DAT) is shown in Appendix E. At this point,

the TEST.DAT file is still not in the correct format for KINFIT program and it needs to be transformed by running NIC180. A copy of this program is shown in Appendix D. The details of the data transformation is presented in Appendix C.

After the data transformation, the name of the file is changed automatically to TEST.KIN by NIC180 program. An example of this file is shown in Appendix E. In order to run KINFIT curve-fitting program, additional information needs to be added to the file. A series of the control parameters are at the top of the file, indicating the number of points in the data file to be fitted, the number of iterations to be permitted if convergence is not obtained, the number of constants to be read with each data set and the maximum value of Δparameter/parameter for convergence to be assumed. Δparameter is the change in the parameter from one iteration to the next which should be small to assume convergence. Next line is the title of the file, an identity of the file. Below the title of the file is a roll of constants, given as the known information. The last line before the actual data contains the initial estimates of the parameters to be fitted. A typical example of a file of this kind is shown in Appendix E(TESTK.DAT). The name of the data file for KINFIT program must not be TEST.KIN because the program only reads files with extensions of ".DAT". Thus, the file was named as TESTK.DAT to differentiate it from TEST.DAT and TEST.KIN.

Before the data can be fitted to a specific equation by KINFIT, a subroutine that contains the equation needs to be constructed, and to be built into the executable program by running KINBLD.COM(Appendix F).

At this point, it is ready to execute the curve-fitting for the data file. The steps of how this is done is given in Appendix H.

KINRUN(Appendix G) is a command file that directs how the curve-fitting process to be done on VAX computer. NMR2SITEB(Appendix H) is an executable file that provides the curve-fitting process with the equation that the data in a data are to be fitted. The actual curve-fitting process is carried out by a program called KINFIT. When the fitting is finished, the computer will prompt with the message: Job TEST is completed. If some messages other than this come back, the curve-fitting is failed by some errors. If there is an error associated with the data file, the message will be very indicative and the error can be found and corrected easily. One error frequently encountered is not the error due to the flaw of the data file itself, but the kind intrinsic with the curve fitting process. Simply speaking, in curve fitting processes, initial estimates of the parameters of the interest are provided to the program to start looking for the best unbiased estimate of these parameters. During the "searching" processes, numerous matrices are evaluated by computers. If the initial

estimates of the parameters are too distant from the true(or the best unbiased) values, the results of these computations may be over the limit of the capacity of the computers, causing the problem so-called floating overflow. Poor selections of coupled parameters can also cause the floating overflow problem because the values of the matrices are equal to zero and the inverse of zero is indefinite. When the fitting is successful, summaries of the fitting process and statistic analysis are stored in a file with the extension ".REP".(For example, TESTK.REP, which contains the results and the analysis of the KINFIT fitting of the data in data file TESTK.DAT.)

Chapter 3

KINETIC STUDIES OF THE COMPLEXATION OF THE SODIUM ION BY 18C6 IN 1,2-DIMETHOXYETHANE AND MIXTURES OF 1,2-DIMETHOXYETHANE AND TETRAHYDRAFURAN

3.1 INTRODUCTION

As was mentioned in Chapter 1, 1,2-dimethoxyethane(1,2-DME) and tetrahydrofuran(THF) have certain remarkably similar properties in terms of density, viscosity, dipole moment, and especially dielectric constant(see Table 6). Both THF and 1,2-DME are etheral solvents, the former having the ring structure with one oxygen donor atom(monodentate) while the latter being a linear molecule with two oxygen donor atoms(bidentate). Usually, metal ions are solvated through ion-dipole interactions, while the donor atoms of the solvents are partially negatively charged. In DME and THF, the sodium ion has a coordination number of four, so that $Na(DME)_2^+$ and $Na(THF)_4^+$ can be formed in DME and THF solutions respectively.[54]

Since the ion pair formations of electrolytes in these two solvents should be approximately the same due to the fact that DME and THF have remarkably similar dielectric constants, the differences in the exchange kinetics should provide information about the differences of the solvents in terms of the solvating powers and their influences on the exchange kinetics.

In this chapter, we will present the results of the thermodynamic and kinetic studies on the complexation and the exchange reactions in DME solution, as well as in DME:THF solvent mixtures. Sodium tetraphenylborate and

sodium thiocyanate salts and 18C6 ligand were chosen for these studies, because these two salts show totally different kinetic behaviors of the exchange reactions with 18C6 ligand in THF solutions as discussed in Chapter 1; $NaClO_4$ was also used to compare the influence of anions on the exchange kinetics.

3.2 Results and Discussion

3.2.1 Solvation and ion pair formation in DME and THF solutions

The Gutmann donor number for DME was reported to be 24, a little higher than that of THF(22).[72] It has been known that in solvents of low dielectric constants electrolytes tend to form ionic aggregates(pairs, triplets etc.). Both THF and DME have relatively low dielectric constants(7.20 for DME and 7.39 for THF at 25 °C), and it has been shown that in these two solvents an appreciable fraction of ions are associated.[91]

Strasser[72] and Szczygiel[73] have measured the equivalent conductances of $NaBPh_4$ and its 18C6 complex in THF solutions. The data are listed in Table 7 together with those obtained in this study for the $NaBPh_4$ and its 18C6 complex in DME solutions. Equivalent conductance for the free $NaBPh_4$ is about the same in both solvents but it is higher for the Na^+·18C6 complex in DME than in THF. The above results indicate that the amounts of the ion pairs of

the solvated $NaBPh_4$ formed in THF and DME solutions are approximately the same, yet the complexed $NaBPh_4$ by 18C6 forms appreciably less ion pairs in DME than in THF solutions. The results also show that conductance for the free sodium salt is higher than that of the complexed salt in both solutions. Strasser has attributed this phenomenon to the bigger size and, therefore, the lower mobility of the complexed ions. The possibility of an increased amount of ion pairs formed for the complexed salt should also be taken into account because the complexed ion should has a lower charge density than the free ion and it is easier to form contact ion pairs for ions with lower charge densities.

A reason for the about same amount of the ion pair formed for the free salt in both solutions is because the solvating abilities for the uncomplexed sodium ion and the dielectric constants of the two solvents are very similar. More ion pairs for the complexed salt in THF than in DME may be due to the fact that more oxygen donor atoms in a DME molecule(2) than that in a THF molecule(1) could result in a higher solvation of the complexed sodium ion in DME than in THF.

The higher conductance of the complexed sodium salt in DME than in THF could also be due to the size difference of the complexed ion in these two solutions. As mentioned above, DME has a higher oxygen concentration per molecules than THF. More THF than DME molecules are needed to reach a

certain stage of the solvation of the complexed ion. Consequently, the solvated $Na^{+}\cdot 18C6$ complex is bigger in THF than in DME and the conductance is higher in DME than in THF solutions.

3.2.2 Thermodynamic studies of sodium salt complexes in 1,2-dimethoxyethane

Tables 8 and 9 show Na-23 chemical shifts of $NaBPh_4$ and NaSCN in 1,2-DME, as functions of the 18C6 mole ratio. The plots of these data are found in Figures 2 and 3. By performing the non-linear least-square curve fitting of these data through KINFIT program,[73] the stability constants of the $NaBPh_4$ and NaSCN complexes with 18C6 in 1,2-DME solution were obtained: log K_F is 3.95(±0.06) for $NaBPh_4\cdot 18C6$ and 2.8(±0.2) for $NaSCN\cdot 18C6$.

The stability constant of $NaBPh_4\cdot 18C6$ complex in THF solution at room temperature is greater than the upper detection limit of the NMR titration method.[92] In other words, log K_F is greater than 4. In DME solutions, Sodium tetraphenylborate forms less stable complex with 18C6 than in THF solution at room temperature. The weaker complex in DME solutions is probably the reflection of a slightly better solvating power of DME than THF, because usually better solvents can more effectively compete for the cations with ligands and consequently reduce the stabilities of complexes. $NaBPh_4$ also forms stronger complexes with 18C6 in

DME than NaSCN, which is in parallel to the results in THF solutions due to the greater contact ion pair formation of NaSCN than $NaBPh_4$ as observed in THF solution. In the case of the contact ion pair formations, anions compete with ligands for cations and weaken the strength of the complexes.

3.2.3 Molecular dynamic studies of the free sodium salts and their complexes by 18C6

In Tables 10 to 14 are listed the chemical shifts and the relaxation times of Na-23 of the free and the complexed sodium salts in DME solution and DME:THF solvent mixtures as functions of temperature. The chemical shifts are plotted in Figures 4 to 8, and the relaxation rates are plotted in Figures 9 to 13 as functions of temperature.

For the uncomplexed sodium salts in all solutions and solvent mixtures except for NaSCN in DME, the Na-23 chemical shifts show downfield shifts with the decrease of temperature, while NaSCN in DME practically maintains a constant value for Na-23 chemical shift in the temperature range studied. Generally, both ion pair formations and solvations of the cations increase the electron density around the nuclei of the ions and would contribute to the shielding of the nuclei. At lower temperatures, ions are more solvated and less amounts of ion pairs are formed due to stronger solvating powers and higher dielectric

constants(see Table 6) of solvents respectively. The down field shifts of the chemical shifts of the uncomplexed sodium salts with the decrease of temperature reveal that at competition the increase of the shielding effect due to the increase of the solvating power can not compensate for the decrease of the shielding effect due to the decrease of the amount of the ion pairs and the decrease of anions in the immediate vicinity of the cations. As the result, the net electron density around the sodium nucleus is decreased with the decrease of temperature, causing the chemical shifts of the uncomplexed sodium salts shift down field with the decrease of temperature. In the exceptional case of the uncomplexed NaSCN in DME solution, this salt has a very strong tendency to form contact ion pairs ($Na^+ \cdot SCN^-$), as has been observed in THF solution.[72] The increase of the solvating power with the decrease of temperature can easily compensate for the slight loss of the shielding effect from a slight dissociation of the contact ion pairs. Therefore, Na-23 chemical shift of NaSCN is independent of temperature in DME solution.

On the other hand, the Na-23 chemical shifts of the complexed sodium salts show upfield shifts with the decrease of temperature with the exception of $NaClO_4 \cdot 18C6$ complex in DME solutions, which shows no change in Na-23 chemical shift with temperature. Usually, for the complexed sodium ion with 18C6, the cation is seated in the center of the cavity of the ligand and is separated or partially separated by the

ligand from solvent molecules and anions. The most influential effect on the shielding of the complexed metal nuclei would be certainly from that of the ligands which are in direct contact and interact the most strongly with the complexed nuclei. The interactions between the Na^+ ion and O-atom of the 18C6 ligand are stronger at lower temperatures, increasing the shielding of the nuclei so that the chemical shifts move to the upperfield(upfield shift). In addition, the higher solvating power of the solvents at lower temperatures would favor the upfield shift too, if the solvent molecules are not completely separated from the complexed cations. For the complexed $NaClO_4$ by 18C6, the independence of the Na-23 chemical shift on temperature is probably due to the very weak complexation and the decrease of temperature does not enhance the complexation significantly.

The dependence of the relaxation rates of nuclei with quadrupolar moment like sodium on temperature is described by Equations 16 to 19 in Chapter 2. The relaxation rate ln $(1/T_2)$ can usually be linearly related to 1/T(K) if A' is a constant over the temperature range under an assumption that d^2V/dZ^2 and Ç do not change with temperature. Both $NaClO_4$ and NaSCN in their uncomplexed and complexed forms in DME solutions follow this linear pattern. This behavior was also observed for the uncomplexed and complexed $NaBPh_4$ in DME:THF (3:1,molar) mixture, and the uncomplexed $NaBPh_4$ in DME:THF (1:1, molar) mixture. For both the uncomplexed and complexed

$NaBPh_4$ in the pure DME, and the complexed $NaBPh_4$ in DME:THF (1:1, molar) mixture, the linear dependence of the relaxation rates on the reciprocal of the absolute temperature does not exist. This observation is probably due to the fact that A' does not remain constant over a range of temperatures, because both d^2V/dZ^2 and Ç may change with temperature.

Another unique feature observed for the $NaBPh_4$ salt in 1,2-DME is that the relaxation rate of the uncomplexed salt is greater than that of the complexed salt by 18C6 at temperatures above 266 K, contrary to all the other cases studied in which the relaxation rates of the free salts are always smaller than those of the complexed salts by crown ethers(Table 23). For example, the relaxation rate of the free $NaBPh_4$ in THF is substantially smaller than that of the complexed $NaBPh_4$ by 18C6(81 vs. 597 s^{-1}). Referring again to Equations 16 to 19 in Chapter 2, the relaxation rate($1/T_2$) of a nucleus with a quadrupolar moment is inversely proportional to the symmetry of the electric magnetic field around it. Faster relaxation rates correspond to lower symmetries. To summarize, the addition of the 18C6 ligand to $NaBPh_4$ decreases the symmetry of the electric magnetic field around sodium ions in THF while it increases the symmetry of sodium ions in 1,2-DME; the free sodium ion has a less symmetric electric magnetic field than that of the complexed sodium ion in 1,2-DME while it the opposite in THF(Table 23).

3.2.4 Kinetic studies of the complexations of sodium salts and 18C6

When the concentration of a ligand is smaller than that of a metal ion, at equilibrium, the metal ion undergoes the exchange reaction by one of the two exchange mechanisms as described in Chapter 1(Equations 4 and 5). For $NaBPh_4$ + 18C6, the mean life times for the sodium ions under the exchange reactions were measured by the method described in Chapter 2 at different temperatures in pure DME solutions, and in DME:THF solvent mixtures(1:1, and 3:1). Table 15, Table 16, and Table 17 list the mean life times of $NaBPh_4$ with various concentrations of 18C6 ligand in the above solutions respectively. By either exchange mechanisms, plotting ln $(1/\tau)$ against 1/T(Temperature) generates slopes proportional to the activation energies of the exchange reactions. These plots are shown in Figures 14 to 16.

Since the mean life times of NaSCN and $NaClO_4$ are shorter than 10^{-5} s, stretching the measurement to the limit of the NMR method for the kinetic studies, the exchange rates for the NaSCN + and $NaClO_4$ + 18C6 systems in DME solutions cannot be measured.

Figure 17 shows the plots of $1/\tau[Na]_T$ vs. $1/[Na^+]_f$ for the system $NaBPh_4$ with 18C6 in 1,2-DME at several temperatures. They are characteristic of the associative-dissociative(or uni-molecular exchange reaction mechanism(mechanism II(Equation 5) in Chapter 1). Figures 18

and 19 show the same plots in 1,2-DME/THF mixtures. Although there are fewer points in the last two plots, the pattern of the associative-dissociative exchange mechanism can still be readily recognized. The exchange mechanism in the mixtures of DME and THF should be the same as that observed in DME and THF, which is the associative-dissociative mechanism.

Tables 18 to 20 show the results of the decomplexation reaction rate constants, k_d(or k_{-2}) in consistence with Equation 5 in Chapter 1), of $NaBPh_4$·18C6 complex obtained by the method described in Chapter 2(Equation 6) at several temperatures for the $NaBPh_4$ + 18C6 system in pure DEM, and in 3:1(molar) and 1:1(molar) mixtures of 1,2-DME and THF respectively. The Arrhenius plots, ln k_d vs. 1/T(K), for each of the systems listed in the above tables can be found in Figures 20 to 22.

Table 21 lists the activation energies, E_a, obtained from the Arrhenius plots for the decomplexation reaction of $NaBPh_4$·18C6 complex in pure 1,2-DME, pure THF, and in 1,2-DME and THF mixtures. The other kinetic parameters(see the same table), $\Delta H^{\ddagger}$, $\Delta S^{\ddagger}$, $\Delta G^{\ddagger}$, were calculated according Equations 7 to 9 in Chapter 2. .

The above results have shown quite different kinetic behaviors for the system of $NaBPh_4$ + 18C6 in 1,2-DME from in THF. As can be seen, the difference in the decomplexation rates is more than 2 orders in magnitude: k_d = 8600±200 s^{-1} in DME solutions and k_d = 58±9 s^{-1} in THF solutions.[72] Since

the two solvents have almost the same dielectric constants, the ion pair formation of the salt and its complex in 1,2-DME and THF are expected to be about the same and the difference in the exchange reaction rates of the same reaction in these two solvents must reveal some differences in solvation of the sodium ion. Faster decomplexation reaction rates in DME than in THF are also reflected in the weaker stability of the $NaBPh_4 \cdot 18C6$ complex in the former solvent(log K_f = 3.95(±0.06)) than in THF(log K_f>4). Since $K_f = k_f/k_d$, where k_f and k_d are the formation and decomplexation reaction rate constants, and k_f usually reaches the diffusion-controlled range, it is k_d that determines the stabilities of complexes.

Activation energies for the decomplexations of the $NaBPh_4 \cdot 18C6$ complex are 4.5 ± 0.2 kcal.mol^{-1} in pure 1,2-DME, and 12.2 ± 0.5 kcal.mol^{-1} in pure THF.[53] In the binary solvent mixtures, they increase with increasing amount of THF(Table 21). The other kinetic parameters, $\Delta H^{\ddagger}$, $\Delta S^{\ddagger}$, $\Delta G^{\ddagger}$, show similar trends(either monotonically increase or monotonically decrease with increasing THF)(Table 21). This trend of change of the kinetic parameters with the composition of the solvent mixture is definite and is graphically shown in Figure 23.

Assuming the additivity of the kinetic parameters for the decomplexation reaction of the $NaBPh_4 \cdot 18C6$ complex, we can write:

$$Y = Y_{THF}X_{THF} + Y_{DME}X_{DME}$$

where Y is the value of a kinetic parameter in a binary mixture, Y_i the corresponding parameter in pure solvent i, and X_i the mole fraction of the solvent i in the mixture. The values for each of the kinetic parameters in solvent mixtures can be calculated according to this equation, and compared to those determined experimentally(Table 22). The experimentally determined values do not agree perfectly with the calculated values, but the trend of the change may be roughly predicted by the above equation. Thus, the influence of the solvents on the kinetics of the exchange of sodium ions between the solvated form and the complexed form by 18C6 ligand can be roughly estimated by the relative compositions of the binary mixture.

While the kinetic parameters of the exchange reactions are functions of the composition of the binary mixture, the exchange mechanism remains unchanged from THF to 1,2-DME. On the ground of the proposed influence of ion-pair formation of both the free salts and the complexed salts on the exchange mechanism,[53] the exchange mechanism would be expected to be the same in DME and THF solutions since the extent of ion-pair formation is approximately the same in these two solvents. That is to say, the associative-dissociative mechanism prevails in both the pure DME and THF solutions as well as in the binary mixtures of these two

solvents, simply because the ion pair formations in DME is similar to that in THF solutions.

After comparing the NMR study results in pure THF, 1,2-DME and THF:DME mixtures, the question remains why the exchange rates are so much faster in 1,2-DME than in THF, and change gradually with the composition of mixtures in between the two extremes of the composition of solvents whereas the solvating powers and the dielectric constants of the two solvents are very similar.

Before answering this question, let us briefly review some of the results about the formation of ion pairs and the dimerization of the ion pairs in DME and THF solutions. Petrucci and co-workers have shown that a competitive reaction mechanism between dimerization of $NaBPh_4$ = M to form the dimmers(M_2) and its complexation with the

macrocycle 18C6 = C to form MC by the following scheme is operative for the $NaBPh_4$ + 18C6 system in 1,2-DME and THF:

$$M_2 \underset{k_2}{\overset{k_{-2}}{\rightleftharpoons}} M\cdots M$$

$$M\cdots M \underset{k_1}{\overset{k_{-1}}{\rightleftharpoons}} 2M$$

$$2M + 2C \underset{k_{-3}}{\overset{k_3}{\rightleftharpoons}} 2MC$$

with overall equation:

$$M_2 + 2C \underset{k_d}{\overset{k_f}{\rightleftharpoons}} 2MC$$

Under this mechanism, different forms of the overall rate constant k_d can be derived for two different situations: a) the decomplexation of MC k_{-3} is the rate determining step of the reverse process; b) the rate (k_2) of formation of the contact dimmer (M_2) is the rate determining step of the dissociation of MC.[91]

The latter explanation, however, suffers a draw back, for that k_d would show a concentration dependence on the ligand, which is demonstrated otherwise by our NMR results. This assumption also requires the overall decomplexation

rates to be independent of the type of ligands, which cannot be justified by our results in conjunction with that obtained by Shporer and coworkers.[69] It was found that the exchange reaction of $NaBPh_4$ between its uncomplexed and complexed site by dibenzo-18-Crown-6(DB18C) in 1,2-DME proceeds by the associative-dissociative mechanism and the decomplexation rate constant of the $NaBPh_4 \cdot DB18C6$ complex at -12 °C is 540 s^{-1}, slower that of the $NaBPh_4 \cdot 18C6$ complex(2800 s^{-1}) in DME solutions. The activation energy for the decomplexation reaction of the $NaBPh_4 \cdot DB18C6$ complex, 13.3 $kcal \cdot mol^{-1}$, is also higher than that of $NaBPh_4 \cdot DB18C6$ complex, 4.5 ± 0.2 $kcal.mol^{-1}$, in 1,2-DME. The other kinetic parameters of the decomplexation reaction, $\Delta G^{\ddagger}$, $\Delta H^{\ddagger}$ and $\Delta S^{\ddagger}$, calculated from the data given in Shporer's paper, are 11.74 $kcal \cdot mol^{-1}$, 12.71 $kcal \cdot mol^{-1}$, and 3.25 $cal \cdot mol^{-1} \cdot K^{-1}$ respectively. The one other major difference in the decomplexation reactions between the systems $NaBPh_4$ + DB18C6 and $NaBPh_4$ + 18C6 in 1,2-DME is that the entropy change is positive when the ligand is DB18C6 while it is negative in the case of 18C6. If the dimerization step of the free salt ion-pairs determined the overall decomplexation reaction, the above results would not be obtained since the overall reaction rate constant under such conditions should be independent of the type of the ligand.

Thus, it seems that explanation a) is more reasonable and, that the decomplexation step of the complex determines the overall k_d. Usually, the properties of the transition

state of a reaction, such as the activation energy and the other activation parameters, are indicative of the easiness of the reaction and reflect the roles of solvents in the reaction. When a multi-step scheme is operative, the apparent activation parameters should closely resemble that of the slowest step. After examining the kinetic results of the overall decomplexations of the $NaBPh_4$ complex by 18C6 ligand, it can be seen that the activation energy E_a, activation enthalpy $\Delta H^{\ddagger}$, and activation entropy $\Delta S^{\ddagger}$ are very sensitive to solvents as shown in Table 21. But $\Delta H^{\ddagger}$ and $\Delta S^{\ddagger}$ change in the same direction and they offset each other so that the activation free energy $\Delta G^{\ddagger}$ is relatively insensitive to the medium(Table 21).

The lower activation energy and enthalpy in DME solutions suggest that at the transition state very probably 1,2-DME molecules participate more effectively than THF molecules, lowering the energy level for the transition state of the decomplexation step. The total entropy change from the ground state to the transition state of the decomplexation is composed of two terms: a solvation term describing the involvement of solvents and a ligand term involving the nature of ligands, such as configuration changes of ligands during complexations. The solvation term of the entropy change is determined by two factors: the strength of the solvent-ion interactions(degrees of freedom associated with this interaction) and the number of the solvent molecules involved in the transition state. The

stronger the solvent-cation interactions in the transition state, the more strongly the solvent molecules are bonded and more degrees of freedom are lost from the ground state to the transition state of the complex(the more negative $\Delta S^{\ddagger}$). The more solvent molecules are needed in the transition state, the more negative is the entropy change. DME molecules are more strongly involved in the transition state but fewer of solvent molecules are needed to complete the solvation of the cations in the transition state than for THF. These two factors are opposing each other and the first one(the solvent-cation interactions) must dominate the overall entropy change so that a more negative $\Delta S^{\ddagger}$ in DME than in THF results. This favored solvation of the sodium ion at the transition state of the decomplexation by DME molecules probably has the origin of the favored steric effect due to the easier access to the complexed sodium ion at transition state for 1,2-DME molecules because the "concentration" of the oxygen atoms per molecule is higher in DME than in THF.

It is well known that the rate of a chemical reaction is determined by the activation energy--the energy difference between the initial and the activated state of the reactant. For the decomplexation of the $NaBPh_4 \cdot 18C6$ complex, the initial complexed form of the sodium ion is at a lower energy level in THF than in DME solutions because of the slightly stronger complexation in THF than in DME. In DME solutions, the energy level of the transition

state(activated state) is substantially lower than that in THF solutions due to the better solvating ability of DME at this stage. The net result is that the activation energy for the decomplexation reaction in DME solutions is substantially smaller than in THF solutions.

As the composition of 1,2-DME increases, 1,2-DME molecules are available for the solvation of the sodium ion. As a result, the activation energy for the decomplexation is lowered and the decomplexation rate becomes faster.

The concept of the involvement of the solvent molecules in transition states of reactions can also be used to explain the faster dimerization reactions of $NaBPh_4$ in DME than in THF as determined by Petrucci and coworkers by ultrasonic relaxation method.

The results of $NaBPh_4$ + DB18C6 in DME obtained by Shchori et. al[69] also indicate that not only solvents but also ligands play important roles in the decomplexation kinetics. As stated earlier, a total entropy change from a ground state to a transition state of a decomplexation step results from entropy changes of solvents and ligands. DB18C6 is a more rigid ligand than 18C6, and consequently the solvents participation in the transition state of the decomplexation reaction is lessened in the former case; therefore,the entropy change of the solvent in the decomplexation path is less negative. As for the entropy change of DB18C6 in the decomplexation, it is positive

because the ligand is more free and it gains degrees of freedom from the complexed state to the transition state of the complex for the decomplexation. The net effect of these two terms is the slightly positive entropy change for the decomplexation reaction. It is worth noticing that the free energy change of the activation remain almost the same as in the $NaBPh_4$ + 18C6 system.

At this point, it is still not clear how slow the rate of the dimerization of the ion-pairs is for $NaBPh_4$ in THF. It is possible that this step is so slow that it could couple with the decomplexation rate of the complex and limits the overall decomplexation rate together with the decomplexation step. It is also not clear whether the differences of ion-pair formation of the complexed salts by different ligands would dramatically change the kinetic behavior of the decomplexation, in the cases of $NaBPh_4$ with 18C6 and DB18C6 in 1,2-DME.

3.3 CONCLUSION

The complexation reaction of the sodium ion with 18-Crown-6 in DME and THF solutions occurs by a multi-step process, which involves ion-pair formation and ion-pair dimerization. Although it was not investigated in this study, it would be only appropriate to include the ligand conformational change in this scheme since it had been reported by other researchers.[41,21] It was found that

dimerization rates are faster in DME solutions than in THF solutions and the decomplexation rates of the overall reaction were shown much faster in DME solutions than in THF solutions, but slower than the dimerization reaction rates in the both solvents. The probability that the dimerization steps in these two solvents are the rate-determining steps is therefore ruled out. Most probably, the decomplexation step of the $Na^{+}18C6$ complex limits the overall reaction rates.

The difference in the reaction rates in DME and THF solutions suggests that in the transition state DME molecules have a better solvating ability than THF molecules even though the two have similar solvating powers towards the sodium ion in the ground state.

Table 6. Physical Properties of 1,2-dimethoxyethane and Tetrahydrofuran as Function of Temperature

Temp. °C	Density gram·cm^{-3}		Viscosity ηx10^3 poises		Dielectric Constant(ϵ)	
	THF	DME	THF	DME	THF	DME
25	0.880	0.859	4.61	4.55	7.39	7.20
10	0.894	0.874	5.42	5.30	7.88	7.60
0	0.904	0.883	6.08	6.10	8.23	8.00
-10	0.914	0.893	6.90	6.70	8.60	8.45
-20	0.924	0.903	7.91	7.80	9.00	8.85
-30	0.934	0.913	9.16	9.30	9.43	9.30
-40	0.945	0.923	10.75	11.30	9.91	9.85
-50	0.955	0.932	12.8	13.8	10.4	10.5
-60	0.966	0.942	15.5	16.9	11.0	11.1
-70	0.978	0.952	19.1	21.0	11.6	11.8

Reference 54.

Table 7. The equivalence conductances of $NaBPh_4$ Salt and its complex with 18C6 in THF and DME at 28°C

Frequency	Equivalence conductance, $\Omega^{-1}\cdot eqv^{-1}\cdot cm^2$					
	in DME		in THF			
(Hz)	0.01M		A		B	
	$NaBPh_4$	$NaBPh_4$ Complex	$NaBPh_4$	$NaBPh_4$ Complex	$NaBPh_4$	$NaBPh_4$ Complex
398 ± 2	19.8	18.0	21.2	16.8	20.98	15.04
629 ± 2	20.2	18.5	21.0	16.7	20.86	15.00
971 ± 1	20.1	18.4	20.8	16.6	20.75	14.92
1942 ± 11	19.9	18.3	20.7	16.4	20.64	14.83
3876 ± 18	19.7	18.2	20.5	16.3	20.44	14.68

A. Determined by B.Strasser.[72]
B. Determined by P.F.Szczygiel.[73]

Table 8. Sodium-23 Chemical Shifts of DME Solutions Containing Sodium Tetraphenylborate[b] and 18C6 at Various Mole Ratios at Room Temperature

Mole Ratio	Chemical Shift (ppm)[a]	Mole Ratio	Chemical Shift (ppm)[a]
0.	-4.47 ± 0.1	1.0490	-14.79 ± 0.08
0.1299	-5.61 ± 0.2	1.0749	-14.89 ± 0.08
0.1998	-6.38 ± 0.2	1.0989	-14.99 ± 0.08
0.2997	-7.40 ± 0.2	1.1249	-15.09 ± 0.08
0.3996	-8.48 ± 0.2	1.1489	-15.15 ± 0.08
0.4995	-9.66 ± 0.2	1.1748	-15.15 ± 0.08
0.5994	-10.58 ± 0.2	1.1988	-15.15 ± 0.08
0.6993	-11.66 ± 0.1	1.2987	-15.20 ± 0.08
0.7992	-12.69 ± 0.1	1.3986	-15.20 ± 0.08
0.8492	-13.40 ± 0.1	1.4985	-15.25 ± 0.08
0.8991	-13.71 ± 0.09	1.5984	-15.25 ± 0.08
0.9251	-13.97 ± 0.09	1.6983	-15.20 ± 0.08
0.9491	-14.12 ± 0.09	1.8981	-15.25 ± 0.08
0.9750	-14.33 ± 0.09	1.9981	-15.20 ± 0.08
0.9990	-14.53 ± 0.09	2.1978	-15.25 ± 0.08
1.0250	-14.63 ± 0.08	2.1978	-15.20 ± 0.08

a. Chemical shifts are relative to that of NaCl(0.1M) in D_2O at 25.0°C.
b. The total concentration of $NaBPh_4$ is 0.025M.

Table 9. Sodium-23 chemical shifts of DME solutions containing sodium thiocyanate[a] and 18C6 at Various Mole Ratios at Room Temperature

Mole Ratio	Chemical Shift(ppm)[b]
0.0000	-2.5 ± 0.2
0.1363	-4.0 ± 0.2
0.2982	-4.8 ± 0.3
0.5326	-6.9 ± 0.2
0.6007	-8.0 ± 0.4
0.7925	-9.1 ± 0.4
0.8947	-9.5 ± 0.3
0.9459	-9.7 ± 0.3
1.040	-10.2 ± 0.3
1.091	-10.5 ± 0.3
1.376	-11.2 ± 0.3
1.542	-11.2 ± 0.3
1.901	-11.3 ± 0.3

a. NaSCN in 0.0444 M.
b. Chemical shifts are relative to that of NaCl(0.1M) in D_2O at 25.0°C.

Table 10. Sodium-23 relaxation rates and chemical shifts of the free $NaBPh_4$ and complexed $NaBPh_4$ by 18C6 in DME solution

Temp. K	Free salt[a] $T_{2A}x10^3$(S)	Free salt[a] δ(ppm)[c]	Complexed salt[b] $T_{2B}x10^3$(S)	Complexed salt[b] δ(ppm)[c]
298.1	7.20±0.07	-4.47±0.09	8.16±0.07	-15.19±0.08
290.2	6.86±0.07	-4.3±0.1	7.83±0.06	-15.20±0.09
282.3	6.39±0.07	-4.1±0.1	7.66±0.05	-15.23±0.09
274.4	6.35±0.07	-4.0±0.1	7.18±0.04	-15.24±0.09
266.5	5.79±0.07	-3.8±0.1	6.16±0.03	-15.3±0.1
258.6	5.49±0.07	-3.6±0.1	4.17±0.01	-15.4±0.2
250.7	4.25±0.07	-3.2±0.2	2.98±0.01	-15.5±0.2
243.0	3.70±0.07	-2.8±0.2	2.92±0.01	-16.0±0.2

a. 0.0514M $NaBPh_4$ in DME solution.
b. 0.0519M $NaBPh_4$ with 0.0600M 18C6 in DME solution.
c. Chemical shifts are relative to that of NaCl(0.1M) in D_2O at 25.0°C.

Table 11. Relaxation times and chemical shifts of ^{23}Na of the free $NaBPh_4$ and complexed $NaBPh_4$ by 18C6 in the mixture of DME:THF (3:1, mole fraction)

Temp. K	Free salt[a] $T_{2A}x10^3$(S)	Free salt[a] δ(ppm)[c]	Complexed salt[b] $T_{2B}x10^3$(S)	Complexed salt[b] δ(ppm)[c]
298.1	7.91±0.04	-4.82±0.08	4.22±0.02	-15.5±0.2
290.2	7.80±0.04	-4.76±0.09	3.54±0.01	-15.5±0.2
282.3	7.27±0.03	-4.69±0.09	3.09±0.01	-15.6±0.2
274.4	6.46±0.05	-4.7±0.1	2.73±0.02	-15.6±0.2
266.5	6.61±0.03	-4.3±0.1	2.40±0.01	-15.6±0.3
258.6	6.16±0.02	-4.2±0.1	2.00±0.01	-15.7±0.3
250.7	5.60±0.02	-3.7±0.1	1.63±0.01	-15.7±0.4
243.0	4.97±0.02	-3.7±0.1	1.35±0.01	-15.7±0.5

a.0.0522 M $NaBPh_4$.
b. 0.0481 M $NaBPh_4$ with 0.0651 M 18C6.
c. Chemical shifts are relative to that of NaCl(0.1M) in D_2O at 25.0°C.

Table 12. Relaxation times and chemical shifts of ^{23}Na of the free $NaBPh_4$ and complexed $NaBPh_4$ by 18C6 in the mixture of DME:THF (1:1, mole fraction)

Temp. K	Free salt[a] $T_{2A}x10^3$(S)	Free salt[a] δ(ppm)[c]	Complexed salt[b] $T_{2B}x10^3$(S)	Complexed salt[b] δ(ppm)[c]
274.4	6.98±0.04	-6.0±0.1	2.10±0.01	-16.1±0.3
282.3	7.25±0.05	-6.07±0.09	2.26±0.01	-16.0±0.3
290.2	7.60±0.05	-6.16±0.09	2.48±0.01	-16.0±0.3
298.1	7.91±0.05	-6.23±0.08	2.84±0.01	-15.9±0.2
306.0	8.54±0.07	-6.36±0.08	3.65±0.01	-15.7±0.2
313.9	9.33±0.07	-6.52±0.07	5.27±0.01	-15.5±0.1

a. 0.0517 M $NaBPh_4$.
b. 0.0484 M $NaBPh_4$ with 0.0607 M 18C6.
c. Chemical shifts are relative to that of NaCl(0.1M) in D_2O at 25.0°C.

Table 13. Sodium-23 relaxation times and chemical shifts of the free $NaClO_4$ and complexed $NaClO_4$ by 18C6 in DME solution

Temp. K	Free salt[a] $T_{2A}x10^3$(S)	Free salt[a] δ(ppm)[c]	Complexed salt[b] $T_{2B}x10^3$(S)	Complexed salt[b] δ(ppm)[c]
296.5	7.18±0.07	-7.99±0.09	4.02±0.02	-15.4±0.2
285.4	7.26±0.09	-7.92±0.09	3.89±0.02	-15.5±0.2
274.4	6.97±0.08	-7.9±0.1	3.87±0.02	-15.5±0.2
263.3	6.77±0.08	-7.8±0.1		
252.3	6.43±0.08	-7.7±0.1	3.57±0.01	-15.5±0.2
241.2	5.52±0.07	-7.3±0.1	3.26±0.01	-15.6±0.2

a. 0.0992M $NaClO_4$.
b. 0.1033M $NaClO_4$ with 0.1494M 18C6.
c. Chemical shifts are relative to that of NaCl(0.1M) in D_2O at 25.0°C.

Table 14. Sodium-23 relaxation times and chemical shifts of the free NaSCN and complexed NaSCN by 18C6 in DME solution

Temp. K	Free salt[a] $T_{2A}x10^3$(S)	Free salt[a] δ(ppm)[c]	Complexed salt[b] $T_{2B}x10^3$(S)	Complexed salt[b] δ(ppm)[c]
296.3	4.75±0.05	-2.5±0.1	2.93±0.02	-11.3±0.2
285.9	4.81±0.05	-2.5±0.1	2.82±0.02	-11.4±0.2
276.4	4.73±0.02	-2.6±0.1	2.65±0.02	-11.4±0.3
265.3	4.73±0.02	-2.6±0.1	2.49±0.02	-11.5±0.3
255.0	4.58±0.04	-2.5±0.1	2.47±0.01	-11.7±0.3
244.7	4.49±0.03	-2.7±0.1	2.12±0.02	-11.7±0.3

a. 0.0400M NaSCN.
b. 0.0400M NaSCN with 0.0844M 18C6.
c. Chemical shifts are relative to that of NaCl(0.1M) in D_2O at 25.0°C.

Table 15. The sodium ion mean lifetimes of $NaBPh_4$ with 18C6 in DME solution

Temp.	Mean life time τ (s) x 10^5				
K	1	2	3	4	5
298	10.18±0.03	6.73±0.13	6.15±0.02	6.03±0.03	3.40±0.04
290	12.26±0.04	7.67±0.12	7.45±0.02	6.94±0.03	3.98±0.04
282	14.08±0.03	9.98±0.11		7.17±0.04	4.03±0.03
278		11.99±0.09	8.59±0.03	9.07±0.04	
274	16.15±0.03	12.16±0.09	9.61±0.02	9.77±0.04	3.92±0.03
270		13.43±0.08		10.95±0.04	
267	18.88±0.04	14.20±0.08	13.31±0.02	11.08±0.04	5.65±0.04
259	39.7±0.2	17.74±0.05	19.71±0.02	11.80±0.04	7.82±0.04
251	49.9±0.1	21.70±0.06		17.52±0.04	19.80±0.06
243		19.89±0.18		19.72±0.08	17.62±0.37
235		44.53±0.90		35.30±0.63	

1. $NaBPh_4$(0.0507 M) with 18C6(0.0134 M), P_{Na^+} =0.731;
2. $NaBPh_4$(0.0532 M) with 18C6(0.0280 M), P_{Na^+} =0.476;
3. $NaBPh_4$(0.0517 M) with 18C6(0.0284 M), P_{Na^+} =0.453;
4. $NaBPh_4$(0.0500 M) with 18C6(0.0302 M), P_{Na^+} =0.400;
5. $NaBPh_4$(0.0507 M) with 18C6(0.0384 M), P_{Na^+} =0.249.

Table 15(continued)

Temperature	Mean life time τ (s) x 10^5	
K	1	2
297.5	6.31 ± 0.03	3.48 ± 0.07
293.0	6.99 ± 0.02	3.86 ± 0.14
289.0	7.63 ± 0.02	4.13 ± 0.11
285.0	8.25 ± 0.02	4.94 ± 0.10
282.0	8.87 ± 0.02	4.98 ± 0.09
278.0	9.71 ± 0.03	5.32 ± 0.12

1. $NaBPh_4$(0.0361 M) with 18C6(0.0168 M), P_{Na^+} =0.533;
2. $NaBPh_4$(0.0361 M) with 18C6(0.0212 M), P_{Na^+} =0.413.

Table 15(continued)

Temperature K	Mean life time τ (s) x 10^5
279.9	13.96 ± 0.12
290.7	14.69 ± 0.12
294.9	14.82 ± 0.11
300.4	13.34 ± 0.13
311.0	10.21 ± 0.12
318.7	8.62 ± 0.15

$NaBPh_4$(0.0375 M) with 18C6(0.0095 M), P_{Na^+} =0.747.

Table 16. The sodium ion mean lifetimes of $NaBPh_4$ with 18C6 in the mixture of DME:THF (3:1, mole fraction)

Temperature	Mean life time τ (s) x 10^4	
K	1	2
298.1	1.35 ± 0.01	0.97 ± 0.05
290.2	1.96 ± 0.01	0.8 ± 0.3
282.3	2.73 ± 0.02	2.440 ± 0.008
274.4	3.80 ± 0.03	3.352 ± 0.009
266.5	5.92 ± 0.07	4.42 ± 0.02
258.6	9.3 ± 0.1	5.90 ± 0.03
250.7	14.6 ± 0.3	8.33 ± 0.04
243.0	22.2 ± 0.6	12.3 ± 0.1

1. $NaBPh_4$(0.0491 M) with 18C6 (0.0218 M), P_{Na^+} =0.556;
2. $NaBPh_4$(0.0520 M) with 18C6 (0.0359 M), P_{Na^+} =0.348.

Table 17. The sodium ion mean lifetimes of $NaBPh_4$ with 18C6 in 1:1 (Mole fraction) DME:THF Solution

Temperature	Mean life time τ (s) x 10^4	
K	1	2
274.4	6.32 ± 0.04	2.00 ± 0.01
282.3	5.53 ± 0.03	1.94 ± 0.01
290.2	4.48 ± 0.02	1.452 ± 0.009
298.1	3.029 ± 0.007	0.904 ± 0.006
306.0	1.651 ± 0.004	0.470 ± 0.006
313.9	1.023 ± 0.002	0.482 ± 0.007

1. NaBPh4(0.0532M) with 18C6(0.0276M), P_{Na^+} =0.481;
2. NaBPh4(0.0514M) with 18C6(0.0445M), P_{Na^+} =0.134.

Table 18. The rate constants of the decomplexation of $NaBPh_4 \cdot 18C6$ complex in 1,2-DME solution

Temperature (K)	k_d (s^{-1})
234	1320 ± 40
242	1600 ± 200
250	2000 ± 200
258	2500 ± 200
266	3800 ± 600
274	4900 ± 900
282	5900 ± 1000
290	7000 ± 1000
298	8000 ± 2000

Table 19. The rate constants of the decomplexation of $NaBPh_4 \cdot 18C6$ complex in DME:THF(3:1,mole fraction) mixture

Temperature (K)	k_d (s^{-1})
243	260 ± 15
251	394 ± 4
259	600 ± 21
267	890 ± 70
274	1290 ± 150
282	1800 ± 300
290	2600 ± 500
298	3500 ± 800

Table 20. The rate constants of the decomplexation of $NaBPh_4 \cdot 18C6$ complex in DME:THF(1:1,mole fraction) mixture

Temperature (K)	k_d (s^{-1})
314	3400 ± 600
306	2500 ± 400
298	1800 ± 300
290	1200 ± 200
282	850 ± 80
274	580 ± 40

Table 21. Kinetic parameters of the decomplexation of $NaBPh_4$-18C6 complex in THF, 1,2-DME and the mixtures of THF and 1,2-DME at 298 K

	THF	DME:THF (1:1, MF)	DME:THF (3:1, MF)	1,2-DME
k_d	58.±9.	1800±300	3500±800	8000±2000
E_a [a]	12.2±0.5	7.7±0.8	6.8±0.2	4.5±0.2
$\Delta H^{\ddagger}$ [b]	11.5±0.5	7.1±0.8	6.2±0.2	3.7±0.2
$\Delta S^{\ddagger}$ [c]	-11.9±1.6	-20±1	-21.3±0.7	-28.2±0.8
$\Delta G^{\ddagger}$ [d]	15.1±0.2	13.0±0	12.6±0.1	12.1±0.1

a. E_a, activation energy, $kcal \cdot mol^{-1}$;
b. $\Delta H^{\ddagger}$, activation enthalpy, $kcal \cdot mol^{-1}$;
c. $\Delta S^{\ddagger}$, activation entropy, $cal \cdot mol^{-1} \cdot K^{-1}$;
d. $\Delta G^{\ddagger}$, activation free energy, $kcal \cdot mol^{-1}$;
e. k_d, (s^{-1}).

Table 22. The comparison of the experimentally determined kinetic parameters to those calculated

	THF	DME:THF (1:1)	DME:THF (3:1)	1,2-DME
a.	ln K_d 4.1 ± 0.2	7.5 ± 0.2	8.2 ± 0.2	9.1 ± 0.3
b.		6.6	7.9	
a.	E_a 12.2 ± 0.5	7.7 ± 0.8	6.8 ± 0.2	4.5 ± 0.2
b.		8.3	6.3	
a.	$\Delta H^{\ddagger}$ 11.5 ± 0.5	7.1 ± 0.8	6.2 ± 0.2	3.7 ± 0.2
b.		7.6	5.7	
a.	$\Delta G^{\ddagger}$ 15.1 ± 0.2	13.0 ± 0.1	12.6 ± 0.1	12.1 ± 0.1
b.		13.6	12.9	
a.	$\Delta S^{\ddagger}$ -12 ± 2	-20 ± 1	-21.3 ± 0.7	-28.2 ± 0.8
b.		-20.1	-24.1	

a. Experimental values
b. Predicted values
c. E_a, activation energy, kcal·mol^{-1};
d. $\Delta H^{\ddagger}$, activation enthalpy, kcal·mol^{-1};
e. $\Delta S^{\ddagger}$, activation entropy, cal·mol^{-1}·K^{-1};
f. $\Delta G^{\ddagger}$, activation free energy, kcal·mol^{-1}.

Table 23. The comparison of the chemical shifts and the relaxation times of $NaBph_4$ and $NaBPh_4$ Complex with 18C6 in THF, 1,2-DME and the mixture solutions

Solvents	THF	DME:THF (1:1)	DME:THF (3:1)	1,2-DME
		Mole fraction		
a. Free Salt				
Chemical Shift(ppm)	-7.55±0.02	-6.01±0.08	-4.82±0.08	-4.5±0.1
Relaxation Rate($S.^{-1}$)	81.1±10%	126.4±0.9	126.4±0.9	145.6±0.5
b. Complexed Salt				
Chemical Shift(Hz)	-15.9±0.2	-16.1±0.2	-15.5±0.1	-15.19±0.08
Relaxation Rate($S.^{-1}$)	597.±10%	351.4±0.9	237.1±0.9	116.2±0.9

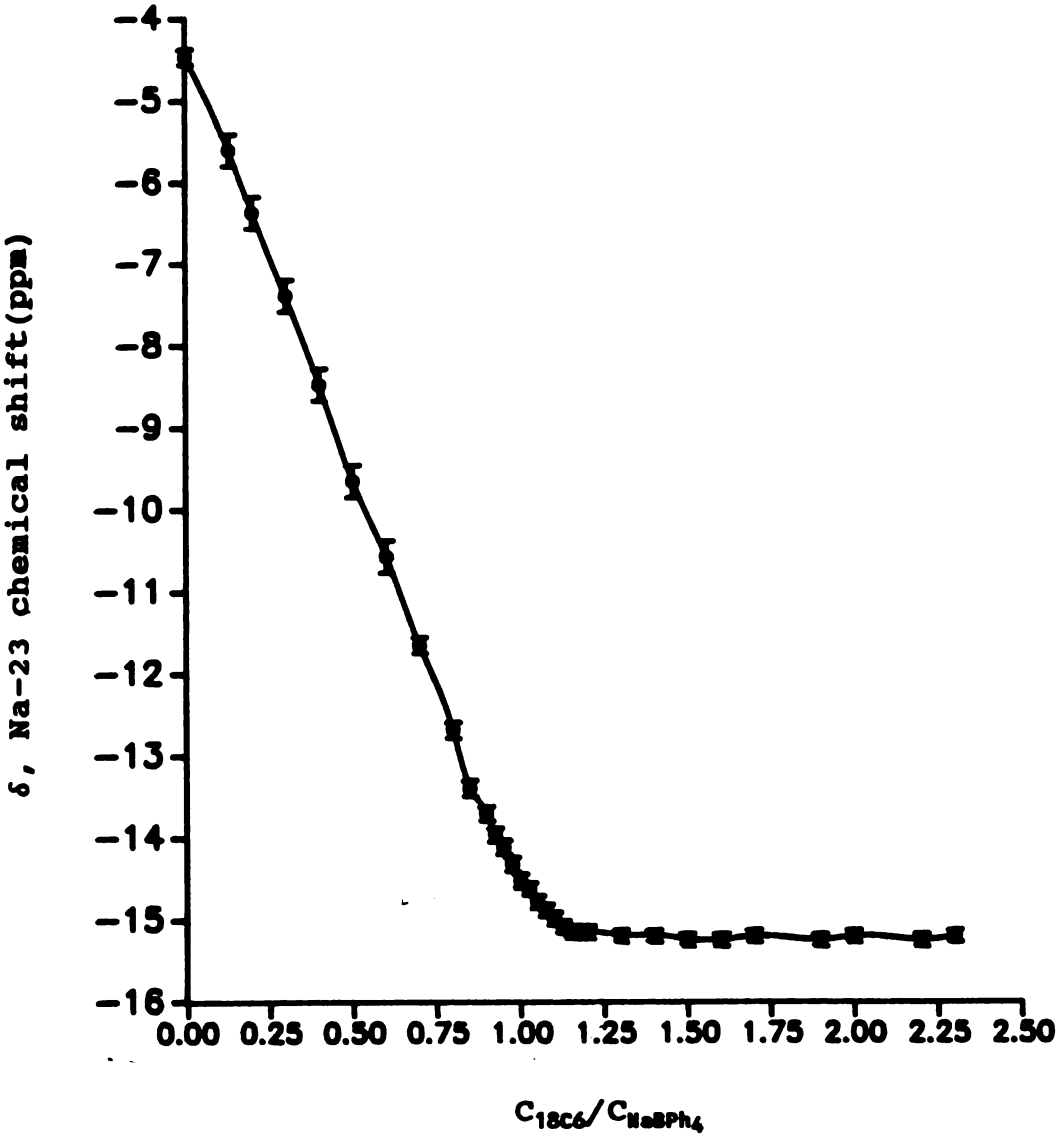

Figure 2. Na-23 chemical shift of $NaBPh_4$ as a function of the concentration of 18C6 ligand in DME solution at 25°C

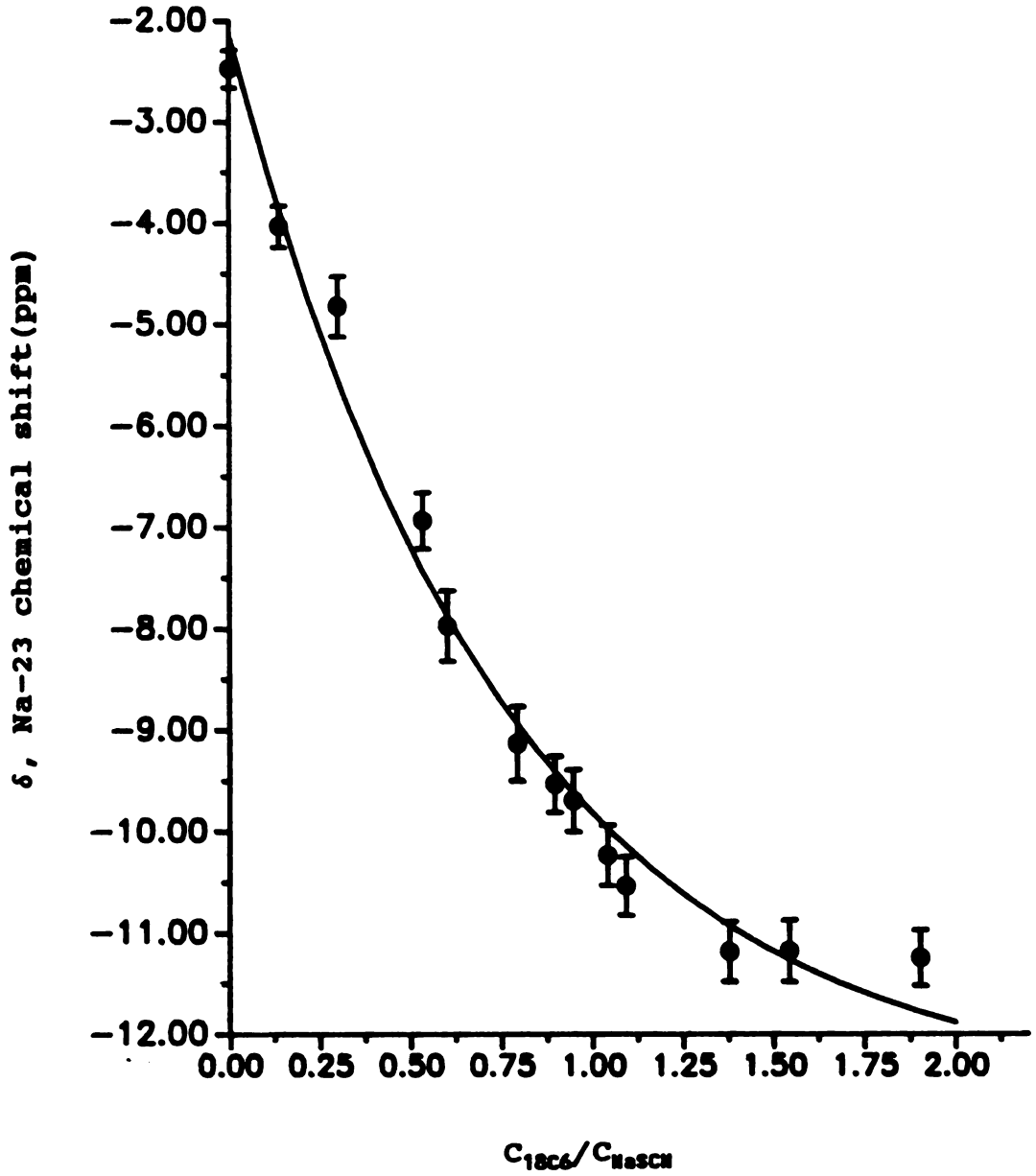

Figure 3. Na-23 chemical shift of NaSCN as a function of the concentration of 18C6 ligand in DME solution at 25°C

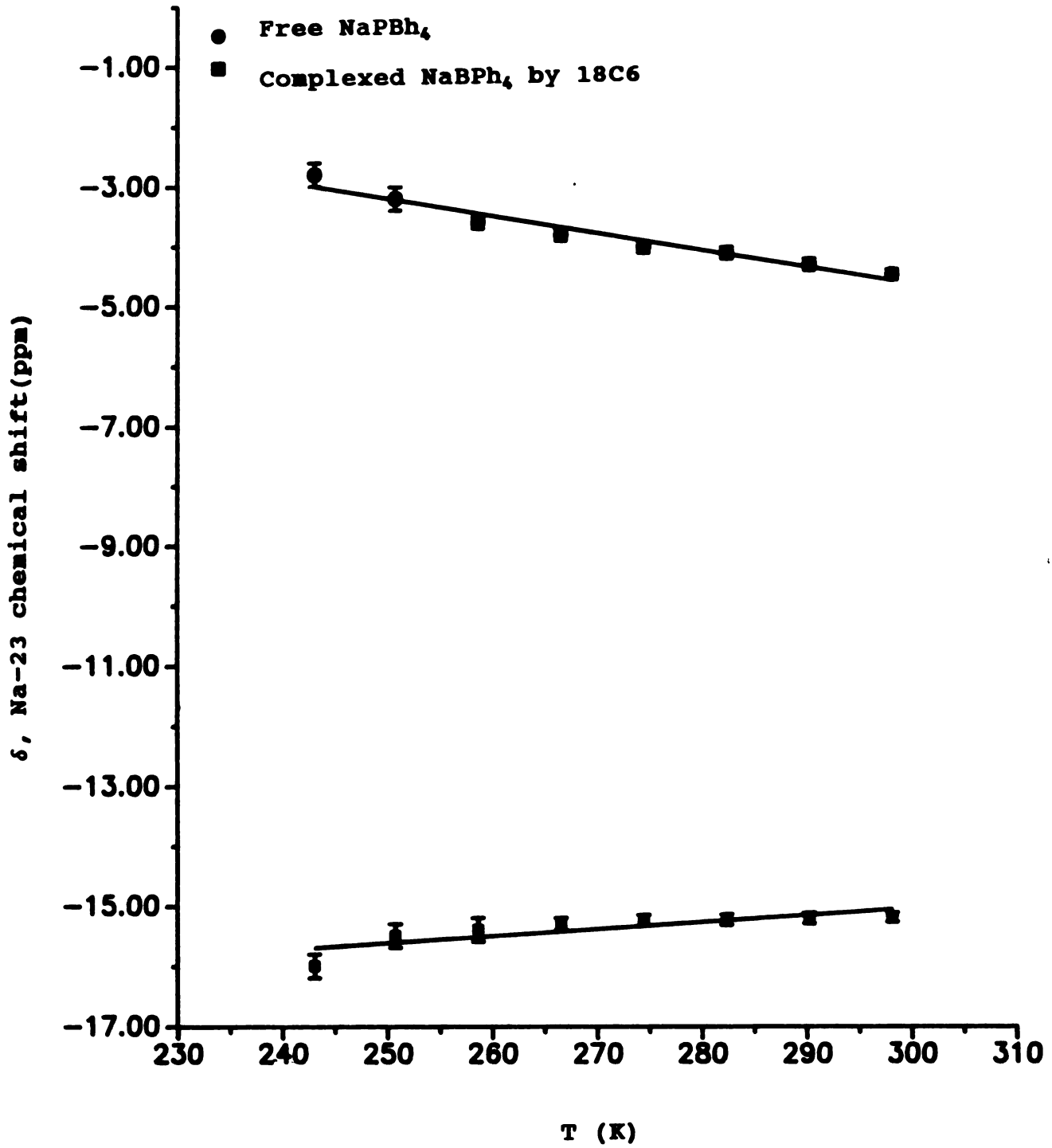

Figure 4. Na-23 chemical shifts of the uncomplexed $NaBPh_4$ and the complexed $NaBPh_4$ by 18C6 as functions of temperature in DME

the total $NaBPh_4$ concentration: 0.05M

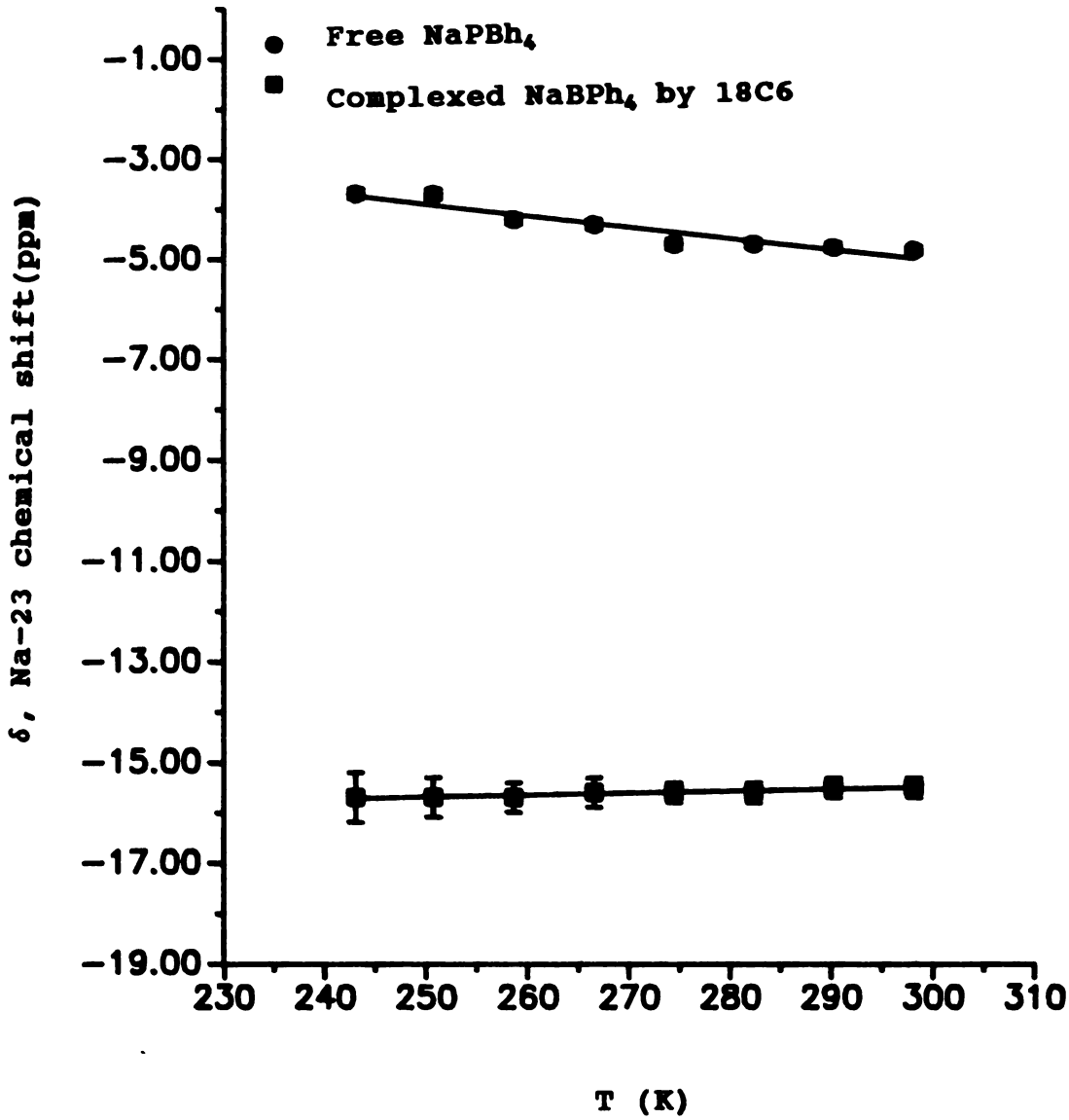

Figure 5. Na-23 chemical shifts of the uncomplexed $NaBPh_4$ and the complexed $NaBPh_4$ by 18C6 as functions of temperature in DME:THF(3:1,molar) mixture

the total $NaBPh_4$ concentration: 0.05M

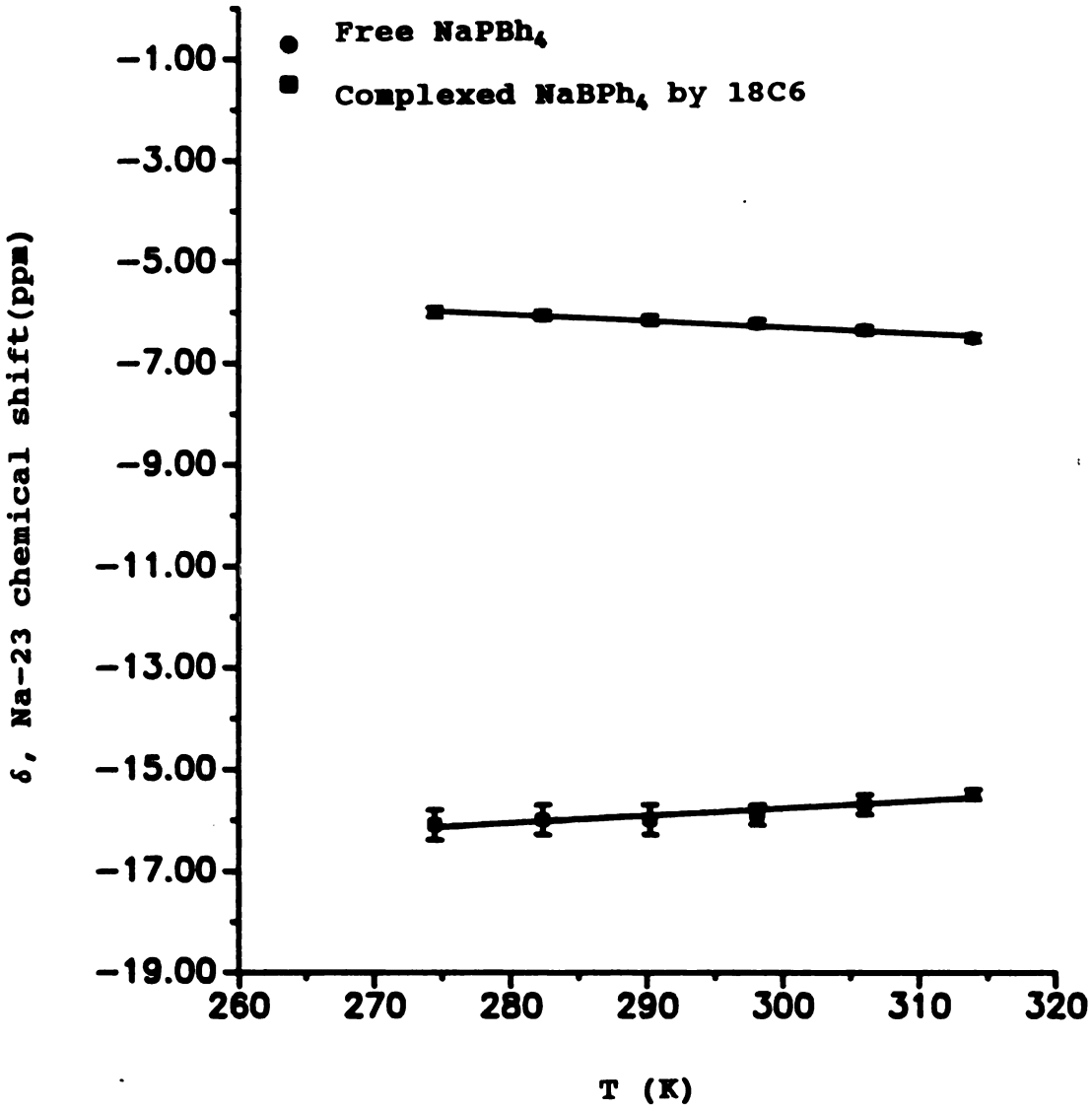

Figure 6. Na-23 chemical shifts of the uncomplexed $NaBPh_4$ and the complexed $NaBPh_4$ by 18C6 as functions of temperature in DME:THF(1:1,molar) mixture

the total $NaBPh_4$ concentration: 0.05M

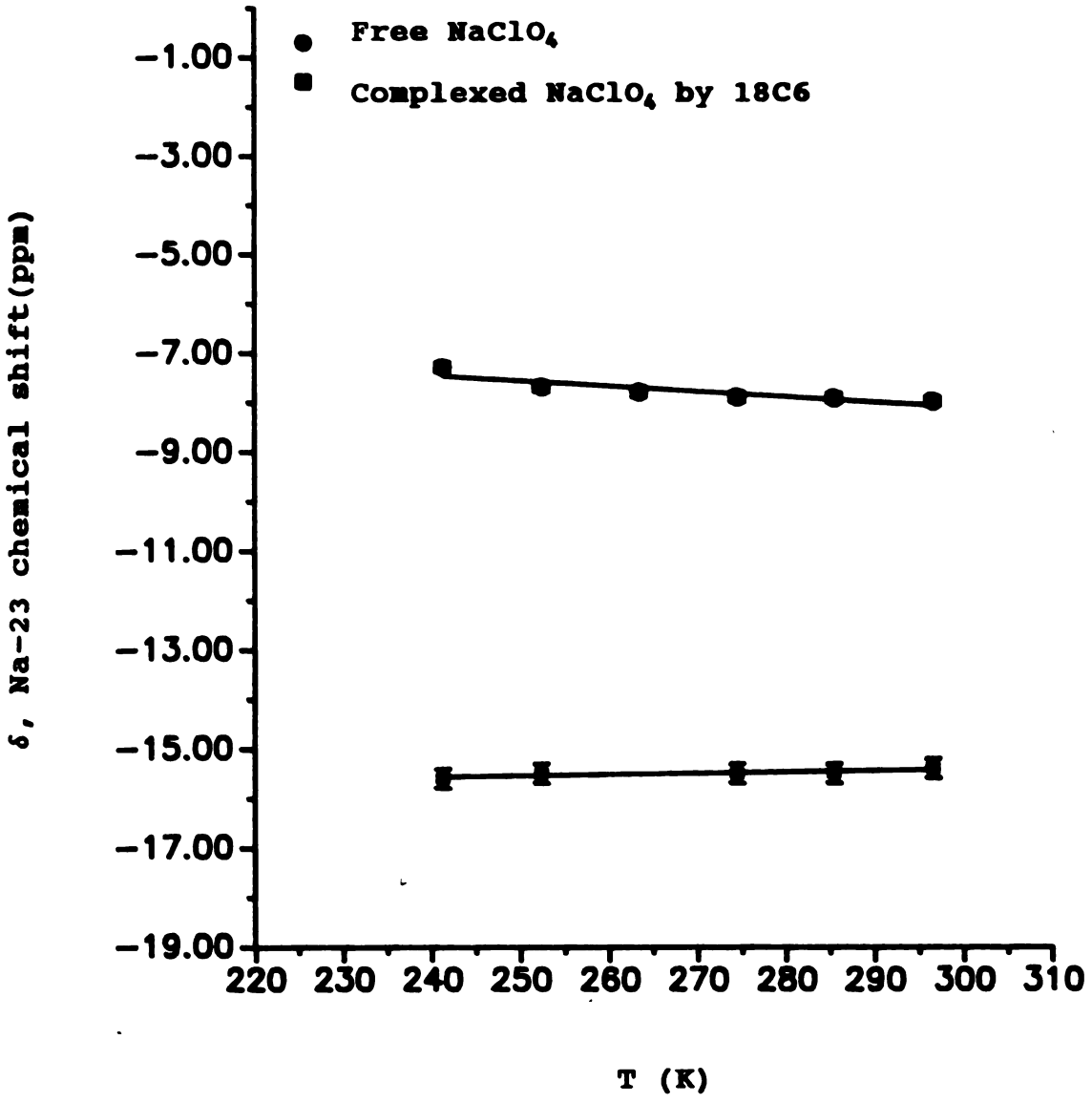

Figure 7. Na-23 chemical shifts of the uncomplexed $NaClO_4$ and the complexed $NaClO_4$ by 18C6 as functions of temperature in DME

the total $NaClO_4$ concentration: 0.1M

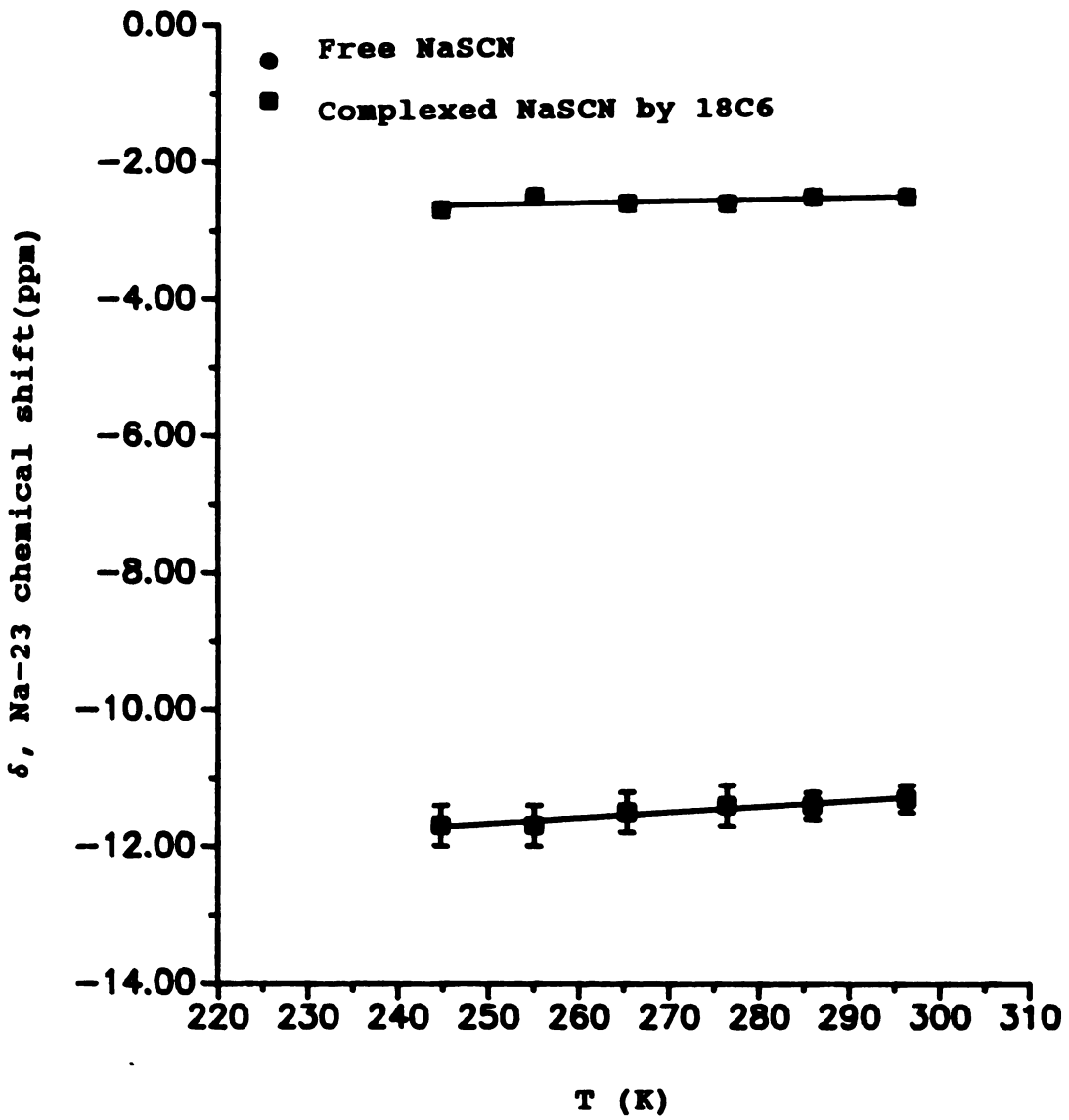

Figure 8. Na-23 chemical shifts of the uncomplexed NaSCN and the complexed NaSCN by 18C6 as functions of temperature in DME

the total NaSCN concentration: 0.04M

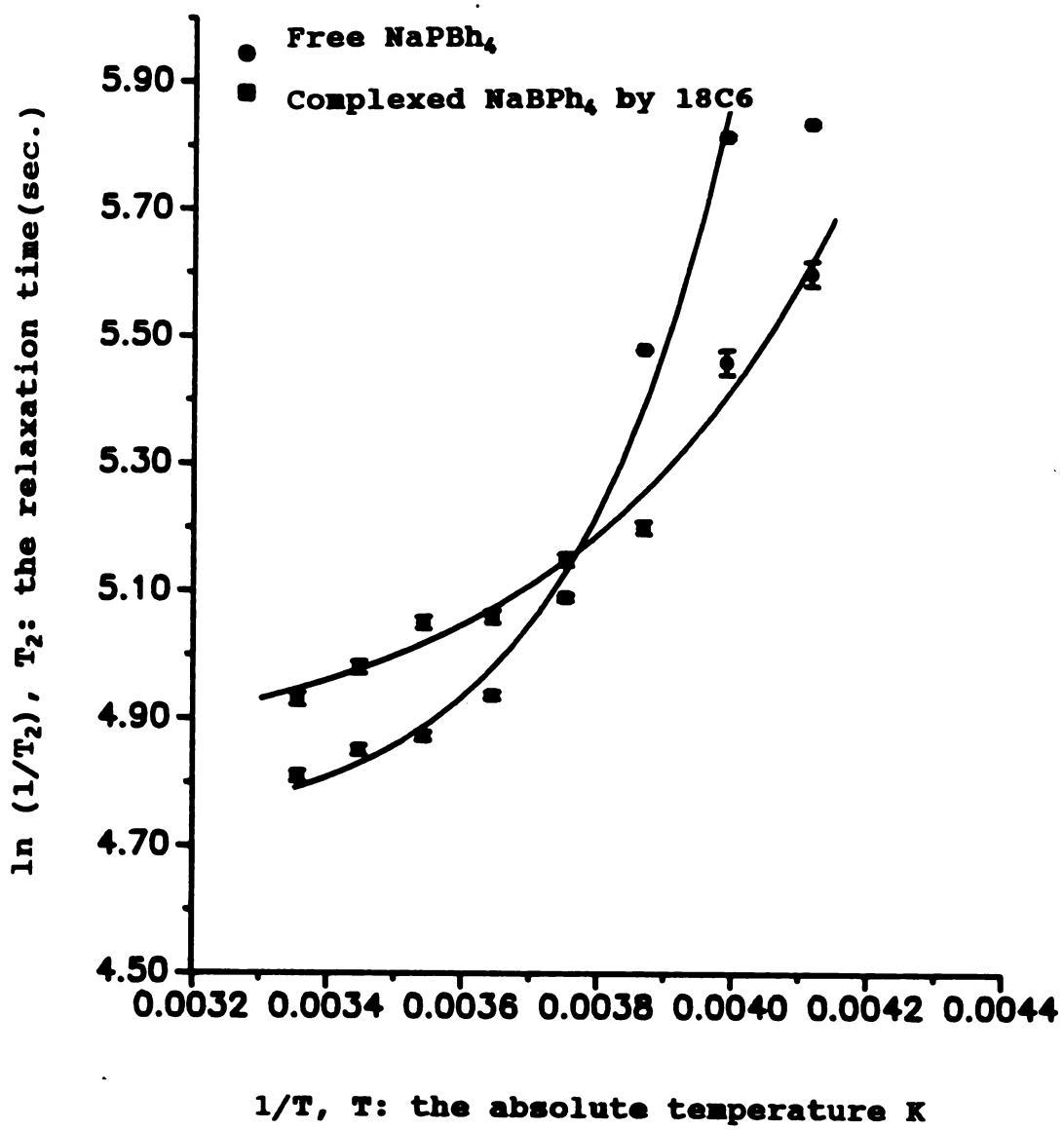

Figure 9. The relaxation rates of Na-23 of the uncomplexed $NaBPh_4$ and the complexed $NaBPh_4$ by 18C6 as functions of reciprocal temperature in DME

the total $NaBPh_4$ concentration: 0.05M

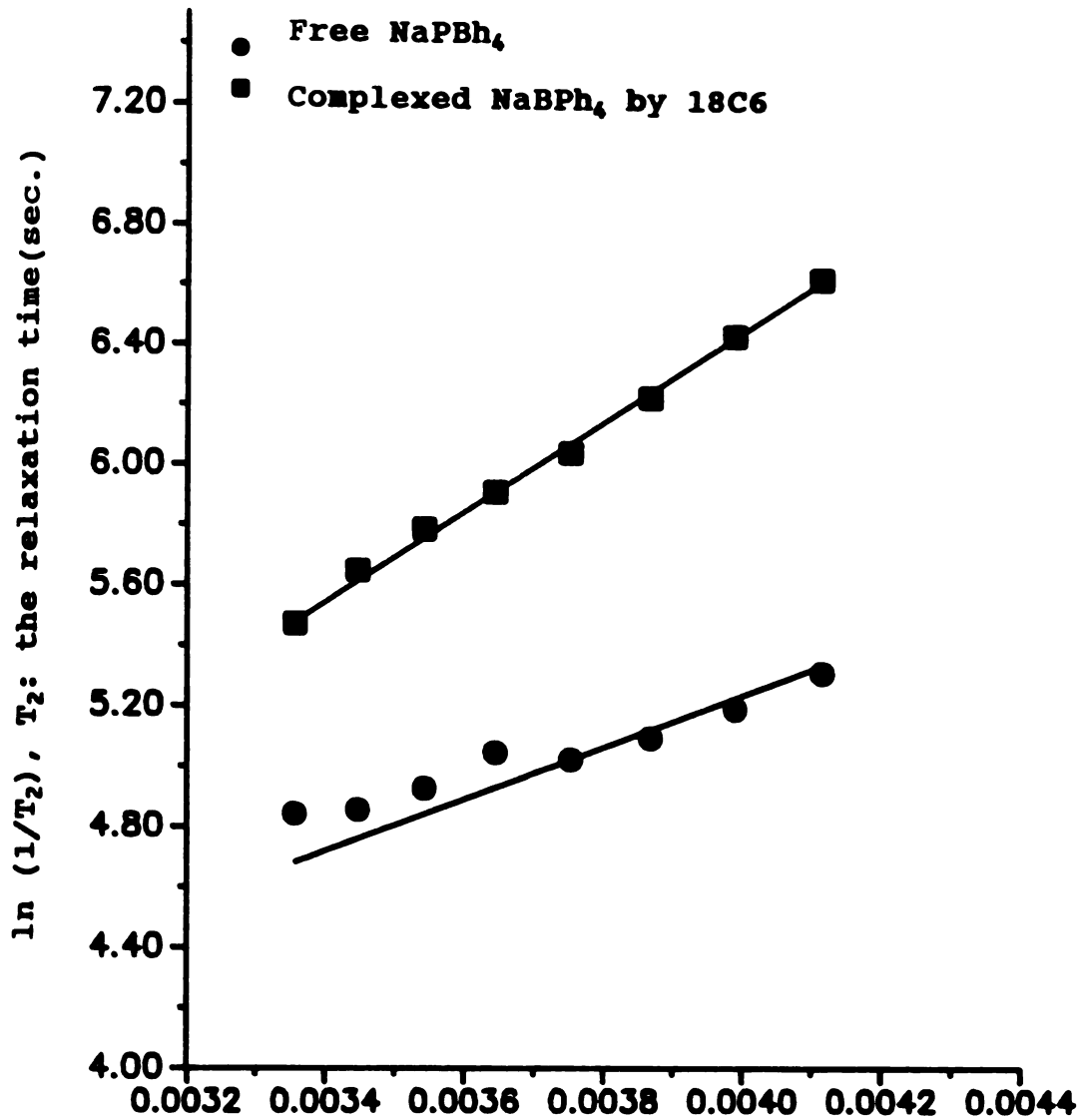

Figure 10. The relaxation rates of Na-23 of the uncomplexed $NaBPh_4$ and the complexed $NaBPh_4$ by 18C6 as functions of reciprocal temperature in DME:THF(3:1, molar) mixture

the total $NaBPh_4$ concentration: 0.05M

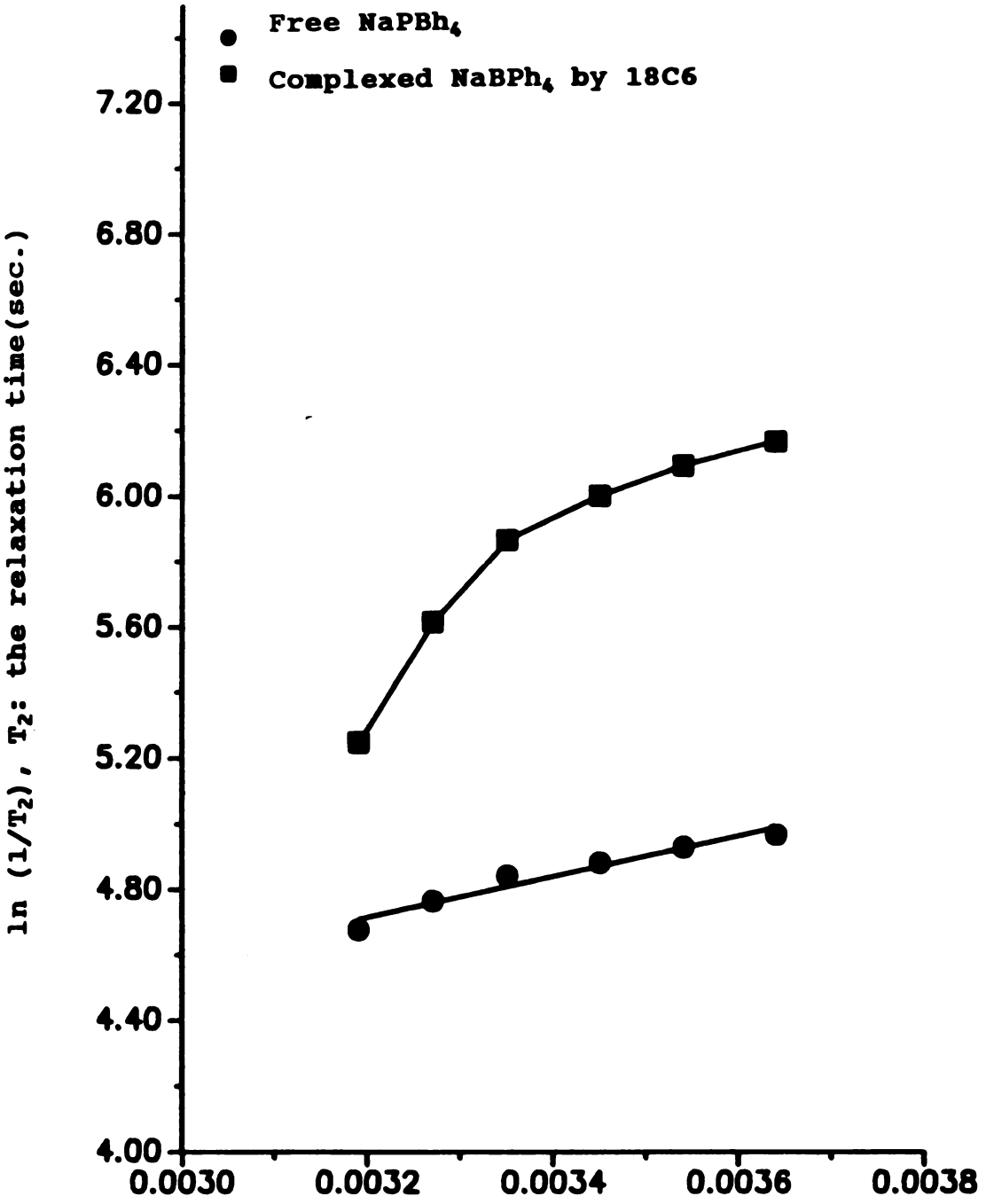

Figure 11. The relaxation rates of Na-23 of the uncomplexed $NaBPh_4$ and the complexed $NaBPh_4$ by 18C6 as functions of reciprocal temperature in DME:THF(1:1, molar) mixture

the total $NaBPh_4$ concentration: 0.05M

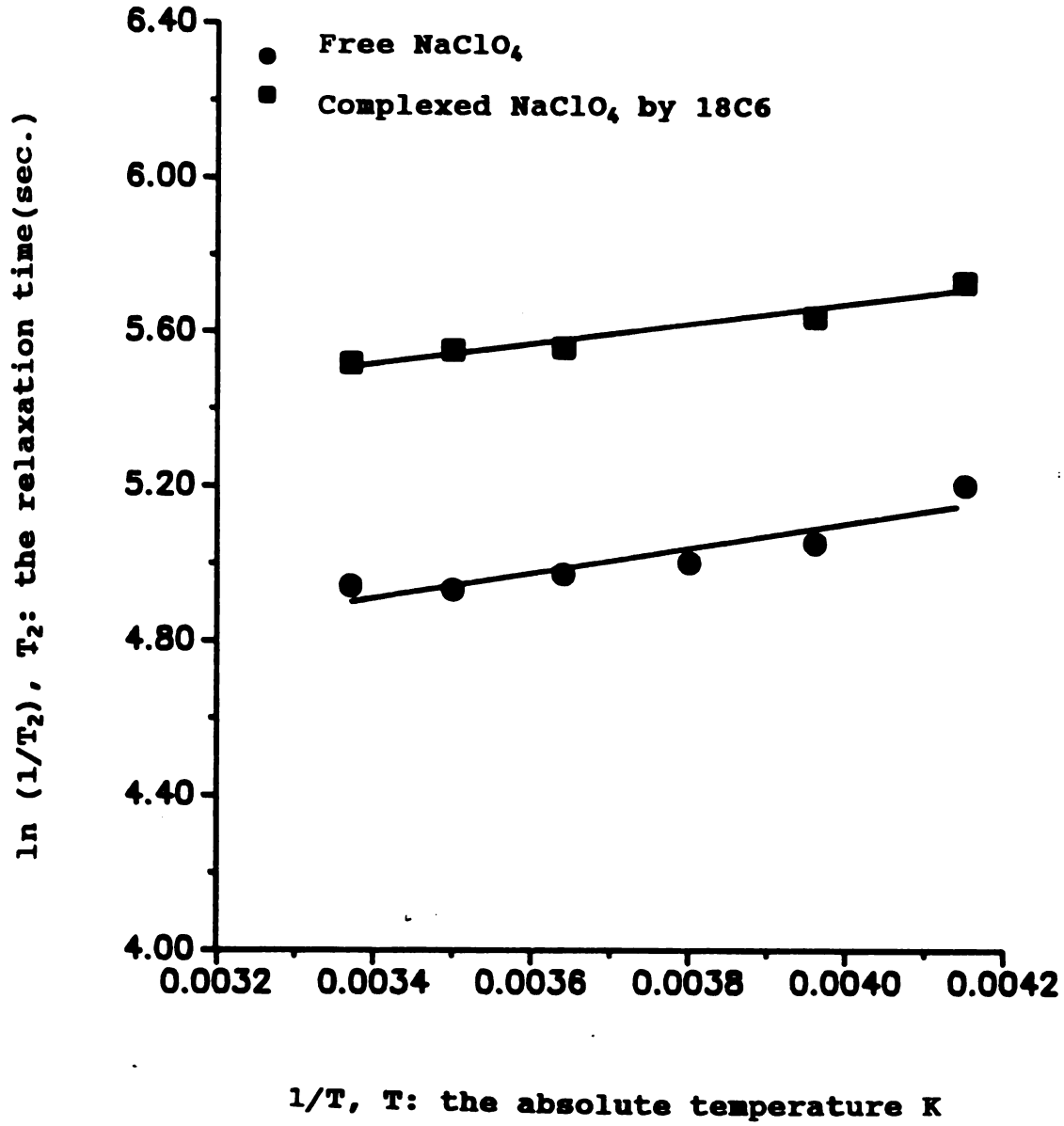

Figure 12. The relaxation rates of Na-23 of the uncomplexed $NaClO_4$ and the complexed $NaClO_4$ by 18C6 as functions of reciprocal temperature in DME

the total $NaClO_4$ concentration: 0.1M

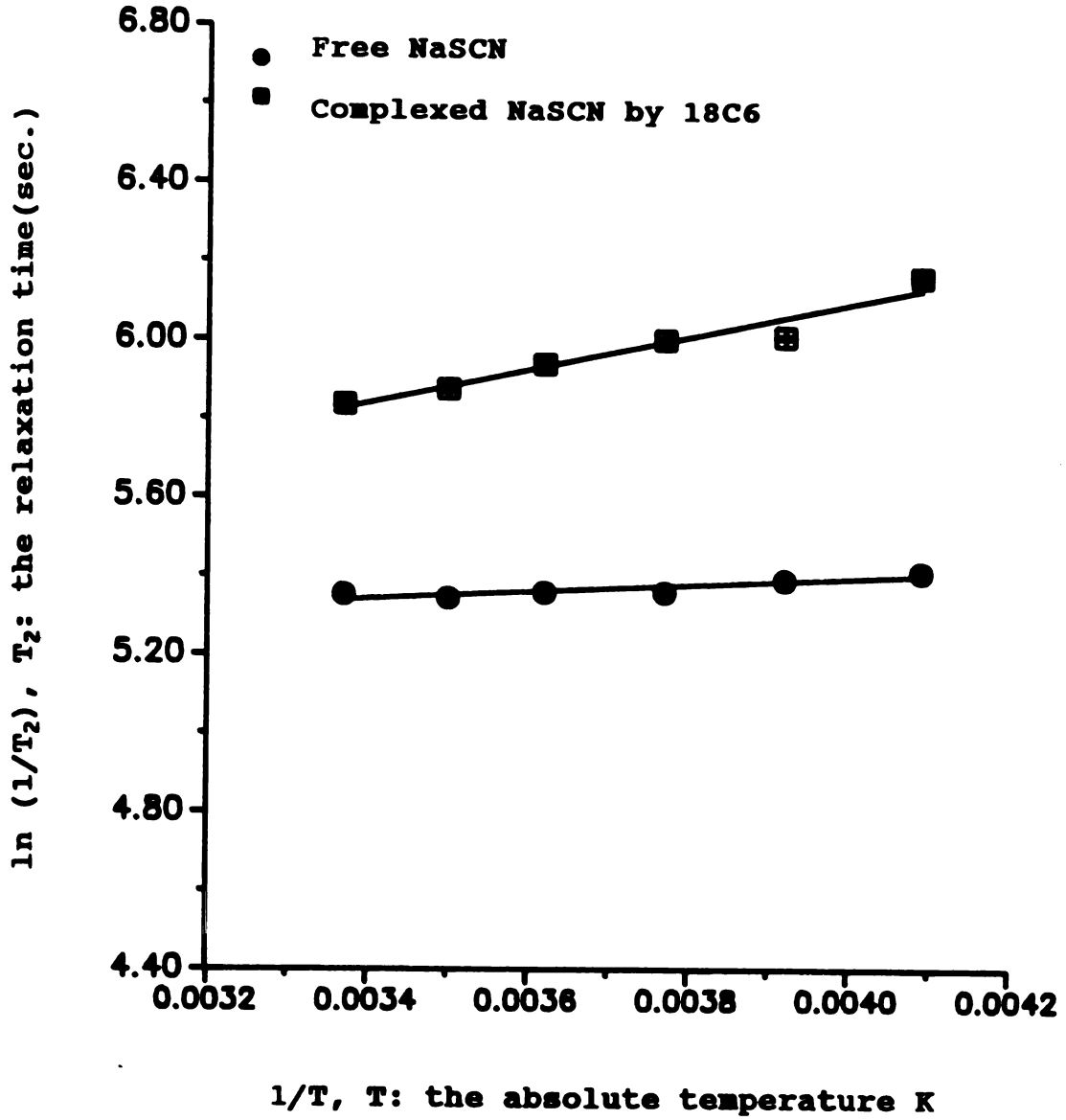

Figure 13. The relaxation rates of Na-23 of the uncomplexed NaSCN and the complexed NaSCN by 18C6 as functions of reciprocal temperature in DME

the total NaSCN concentration: 0.04M

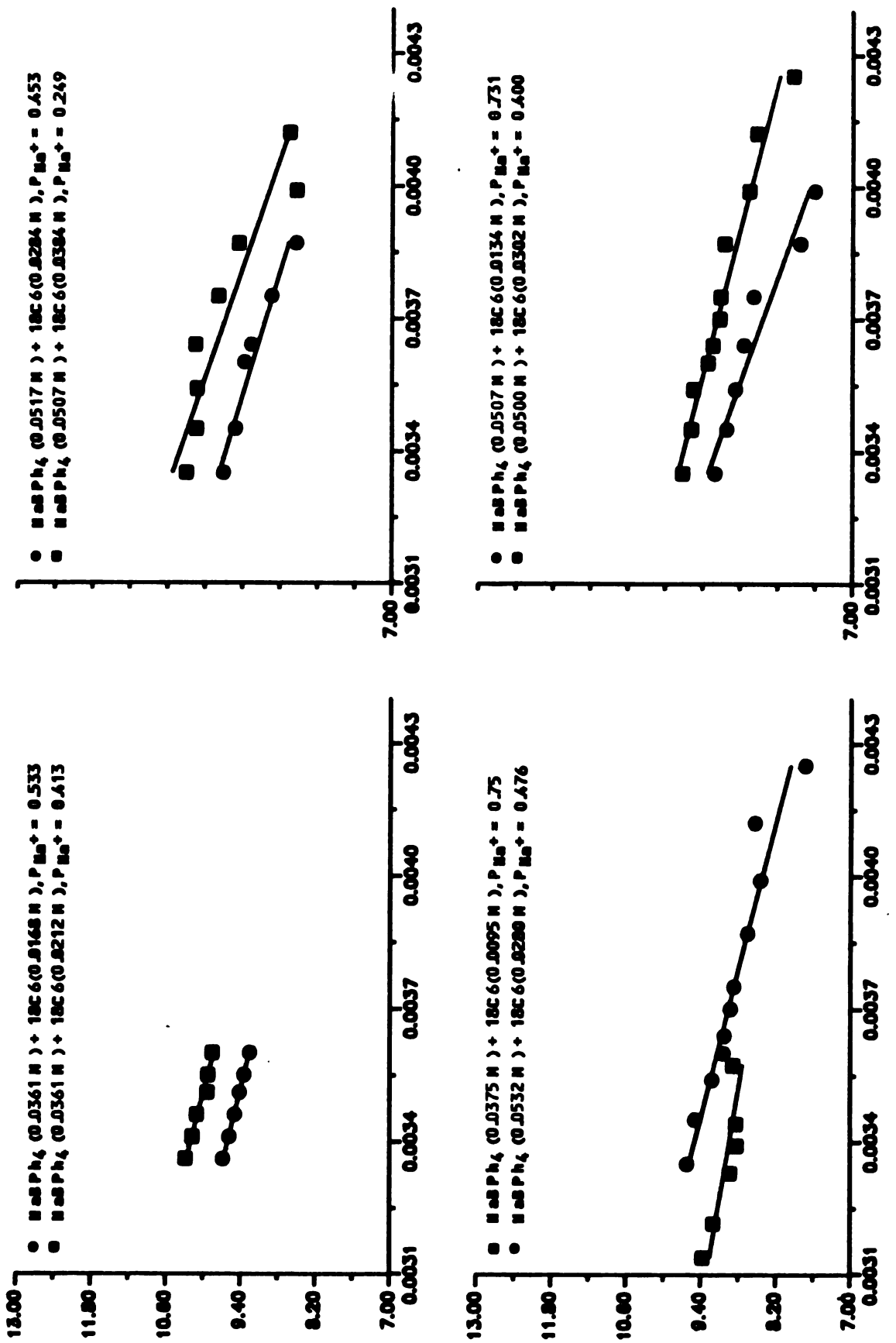

Figure 14. ln (1/τ) against 1/T for the system $NaBPh_4$ + 18C6 in DME solutions

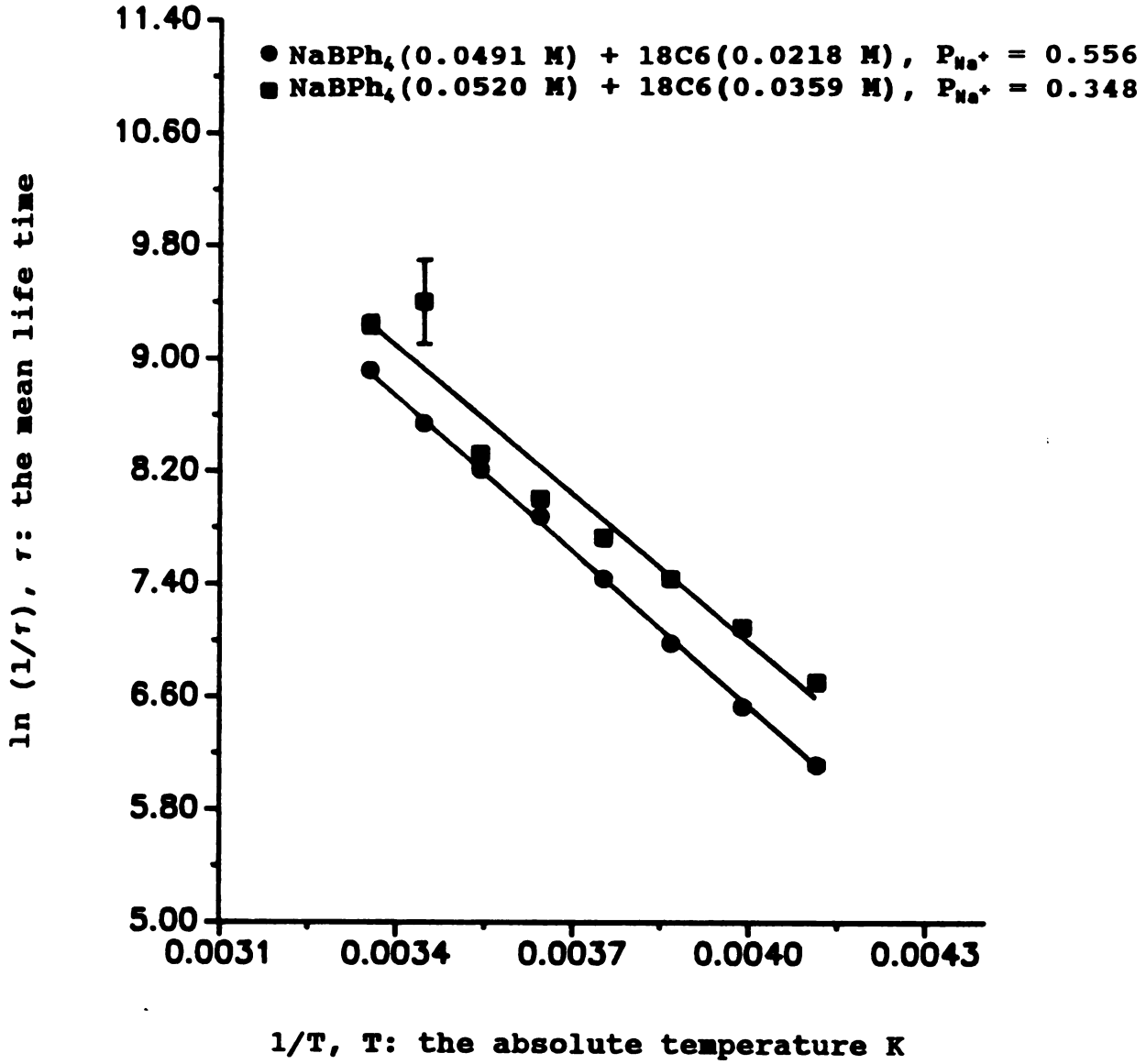

Figure 15. ln (1/τ) against 1/T for the system $NaBPh_4$ + 18C6 in DME:THF(3:1,molar) mixtures

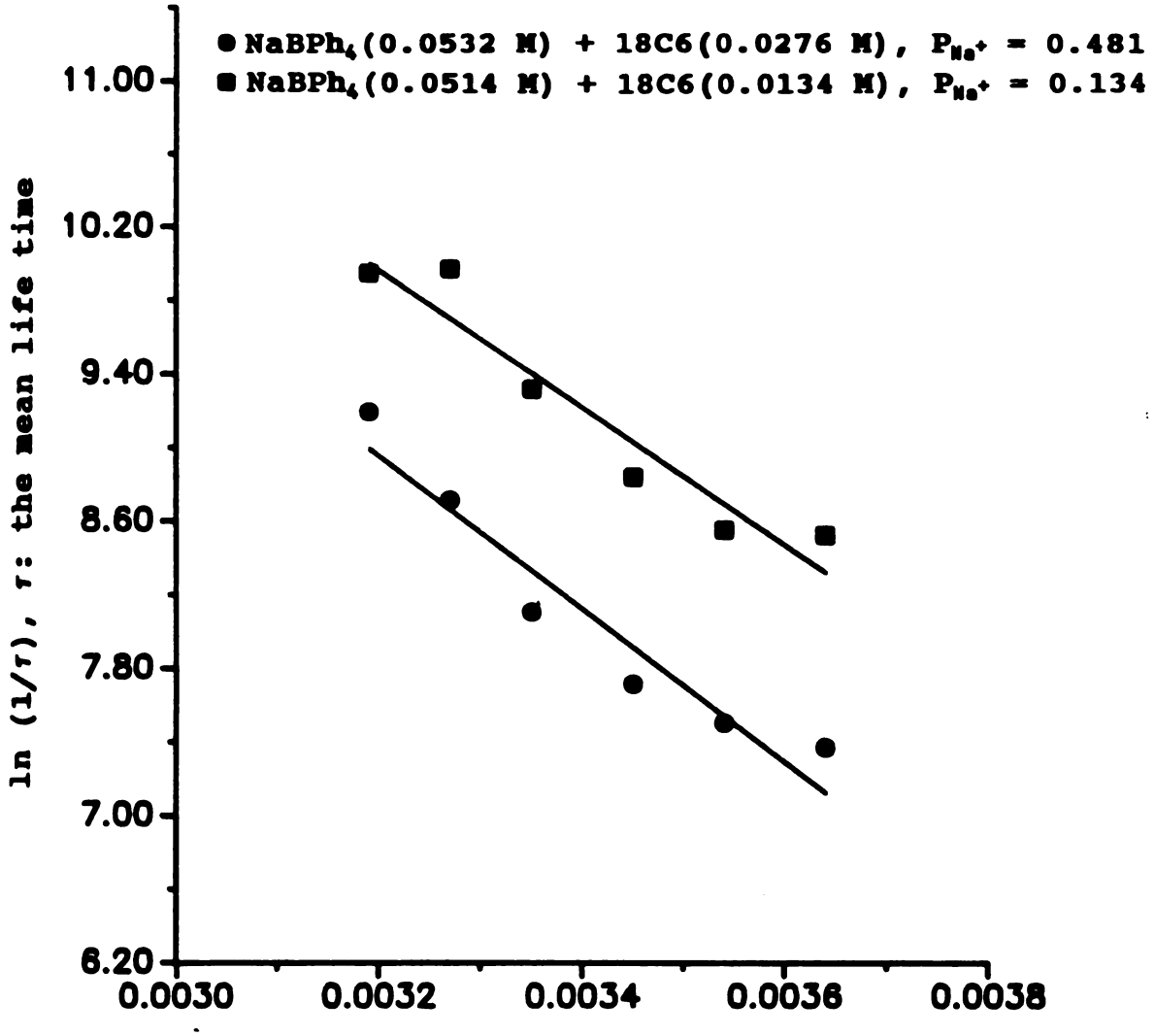

Figure 16. ln (1/τ) against 1/T for the system $NaBPh_4$ + 18C6 in DME:THF(1:1,molar) mixtures

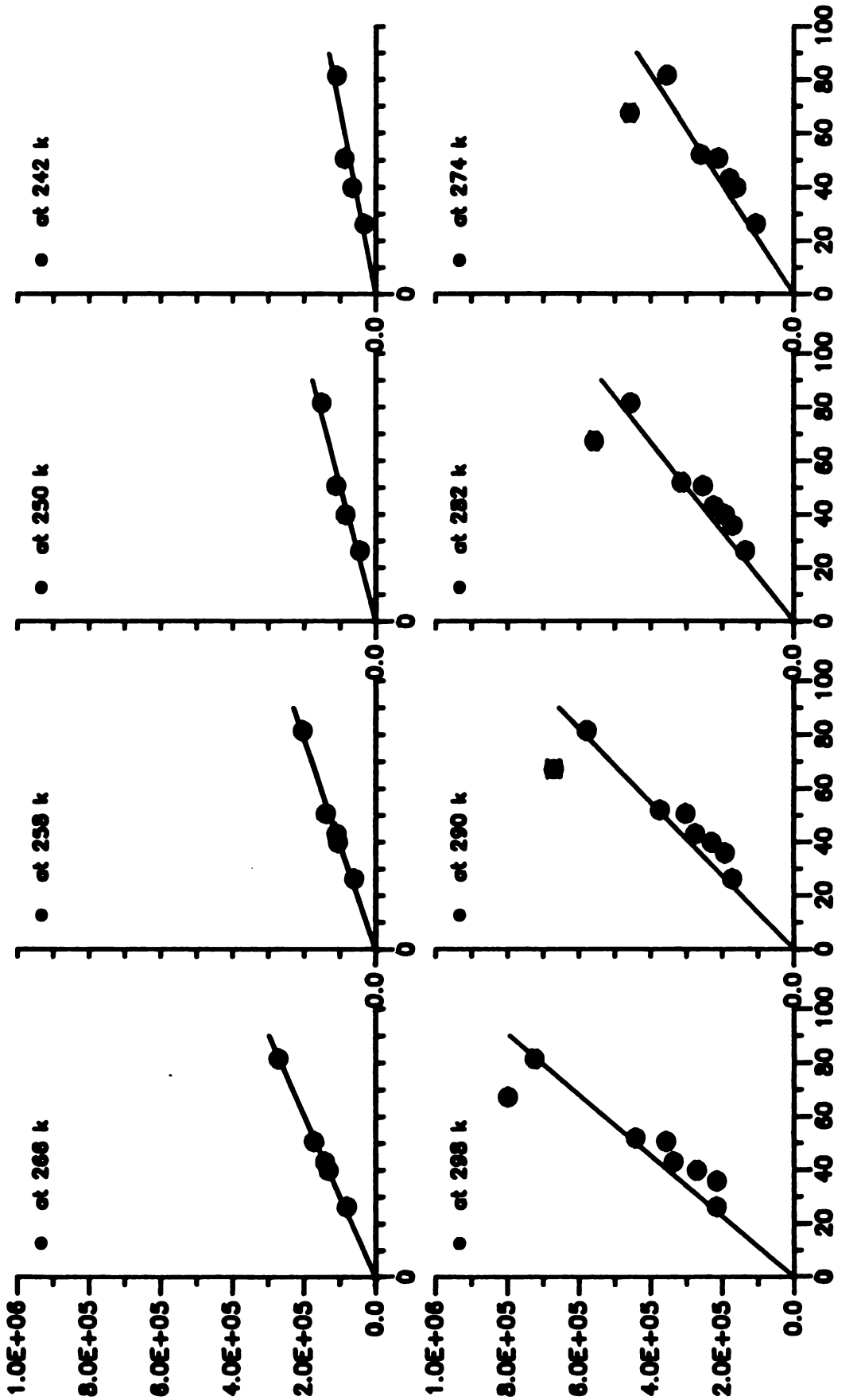

Figure 17. $1/r[Na]_T$ vs. $1/[Na^+]_f$ for $NaBPh_4$ + 18C6 in DME solution

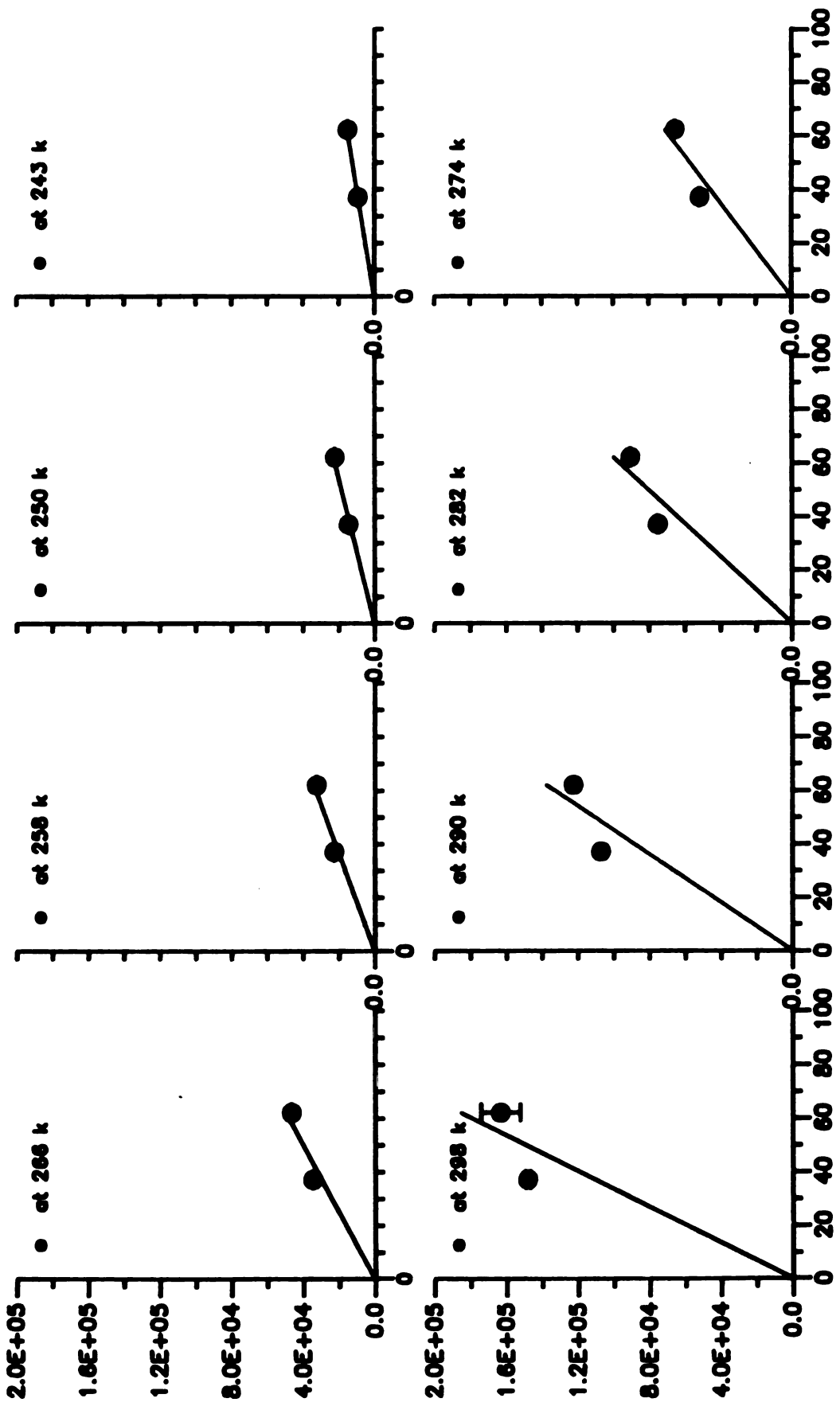

Figure 18. $1/r[Na]_T$ vs. $1/[Na^+]_f$ for $NaBPh_4$ + 18C6 in DME:THF(3:1,molar) mixture

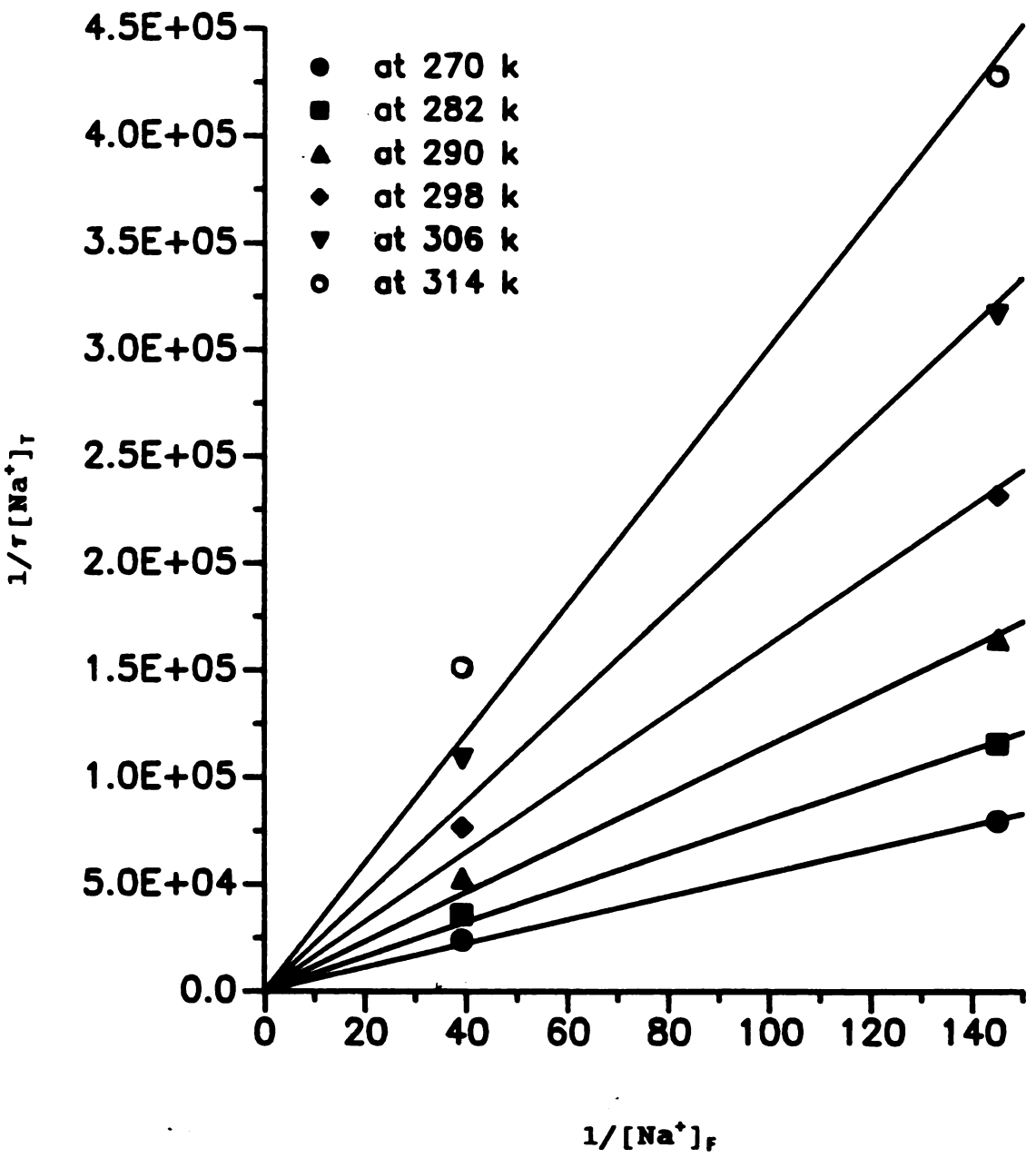

Figure 19. $1/\tau[Na]_T$ vs. $1/[Na^+]_f$ for $NaBPh_4$ + 18C6 in DME:THF(1:1,molar) mixture

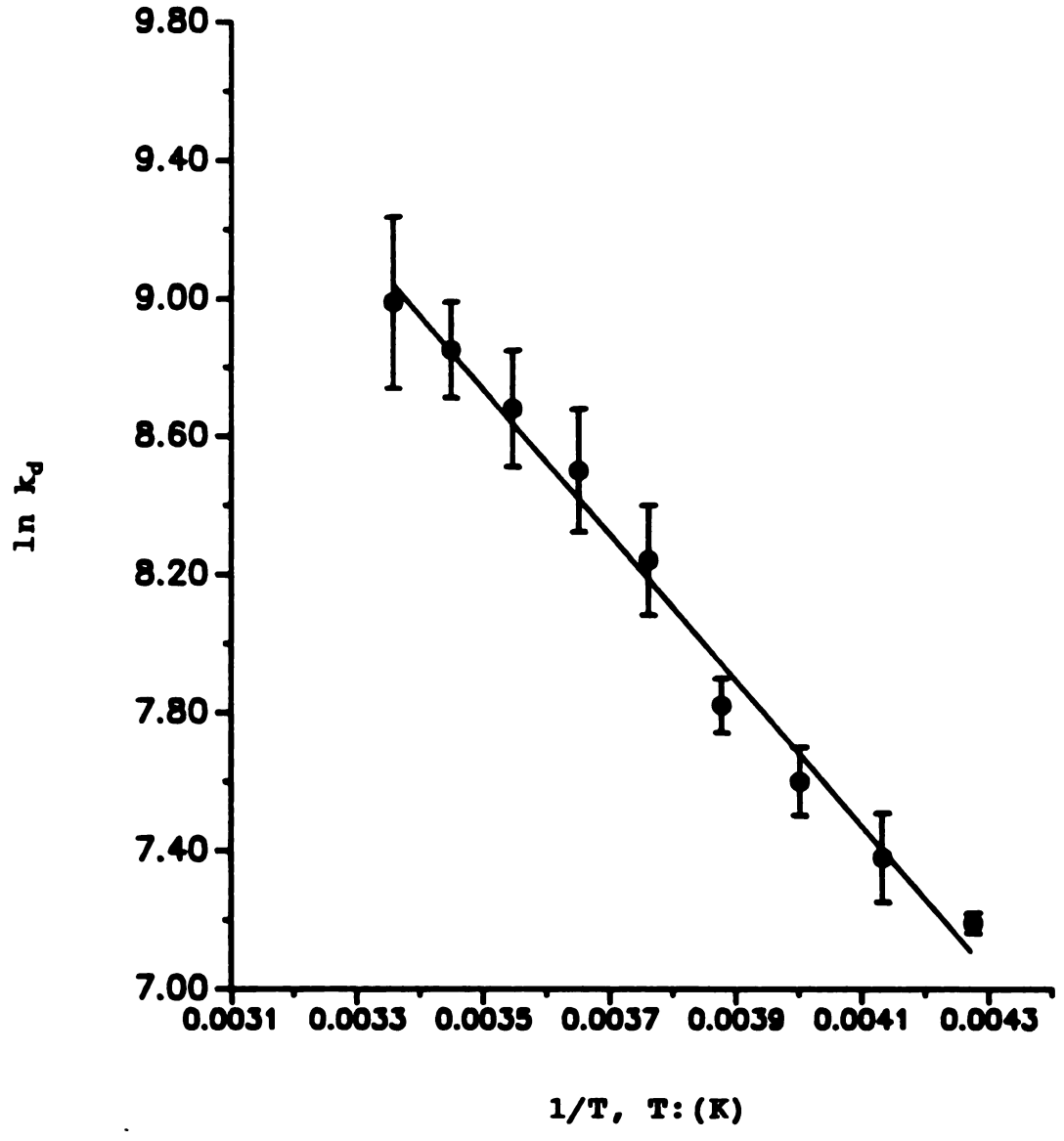

Figure 20. The Arrhenius plot for the system of $NaBPh_4$ + 18C6 in the pure DME solution. ln k_{-2} vs. 1/T

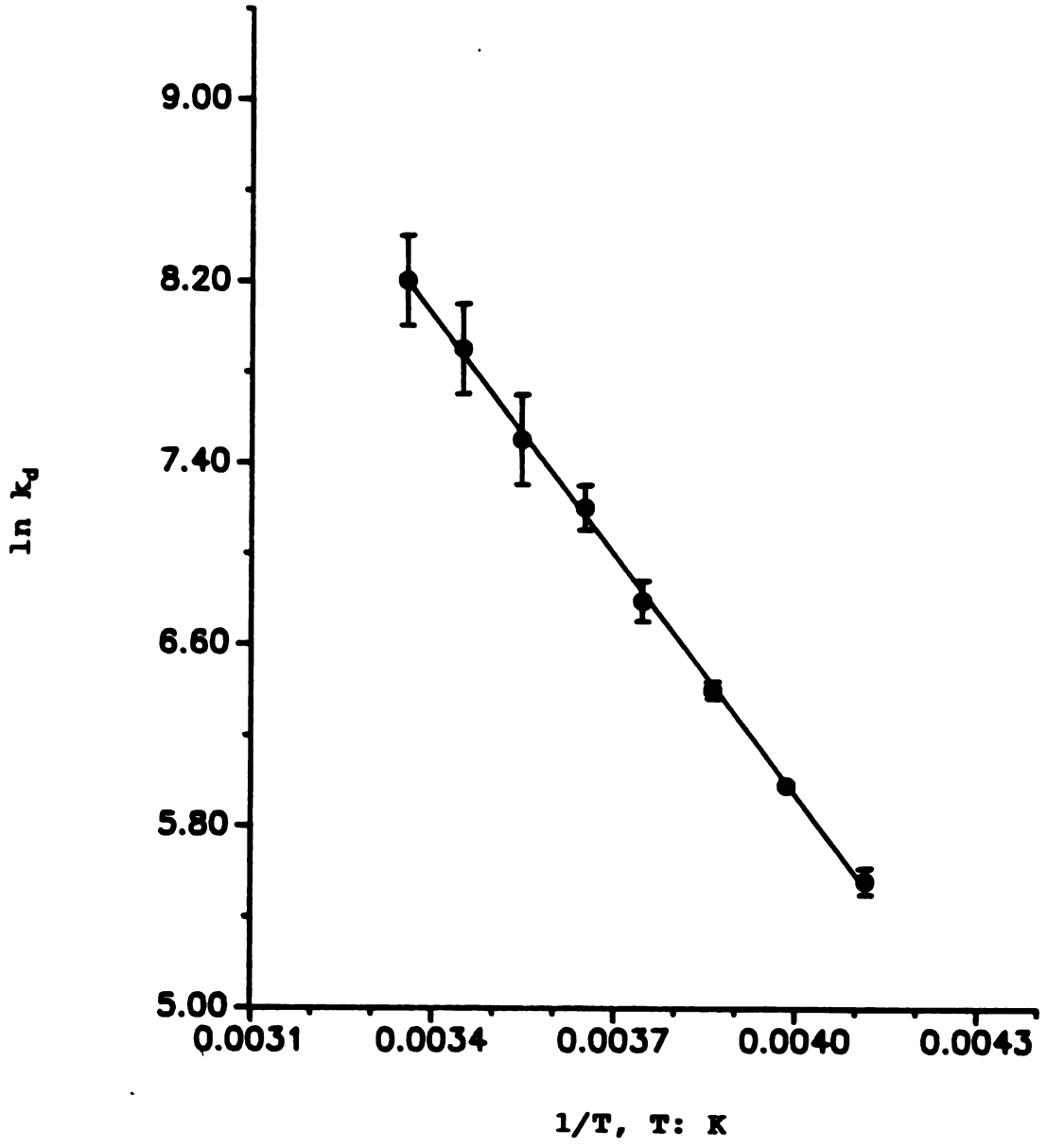

Figure 21. The Arrhenius plot for the system of $NaBPh_4$ + 18C6 in DME:THF(3:1, molar) mixture. ln k_{-2} vs. 1/T

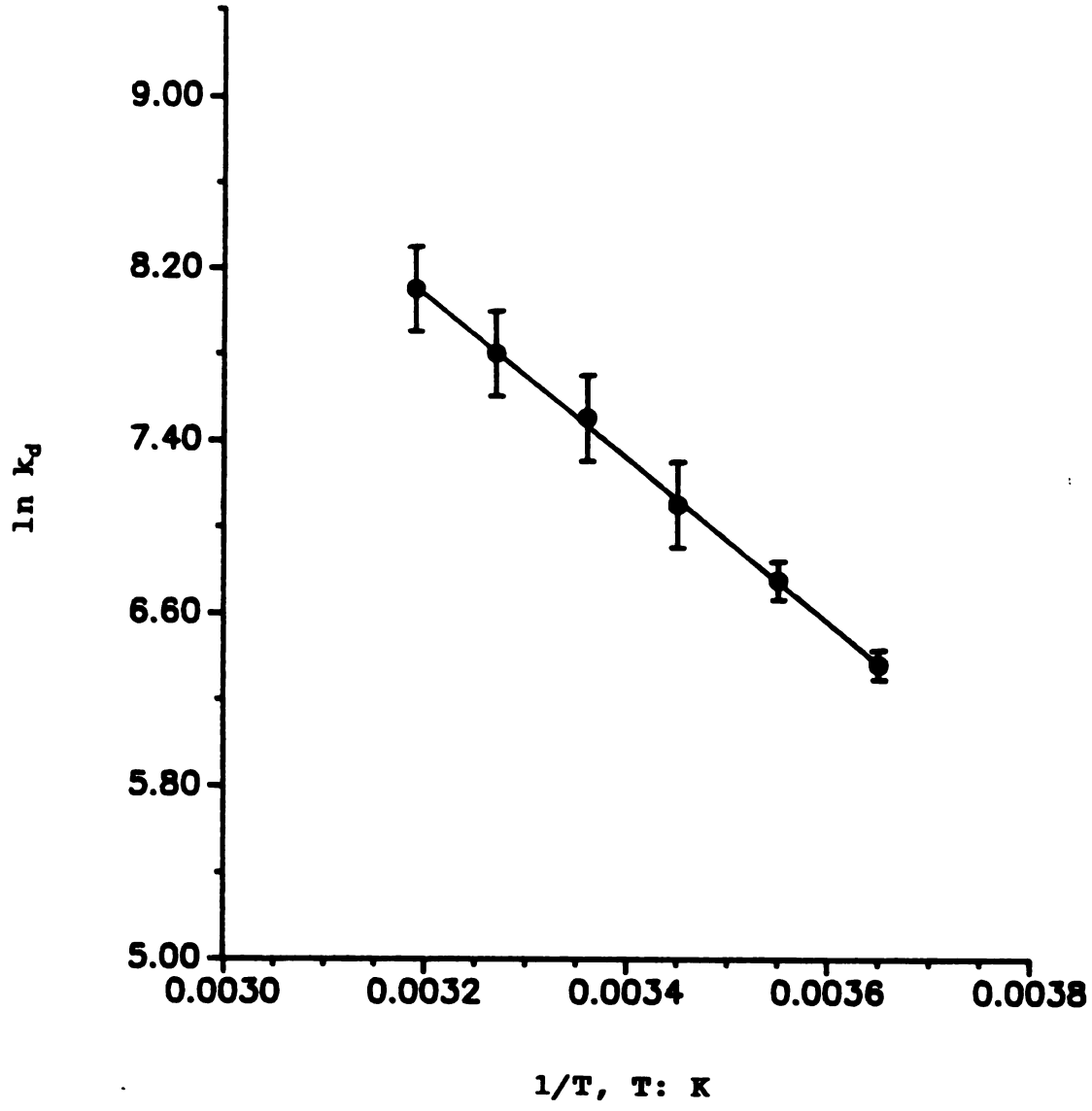

Figure 22. The Arrhenius plot for the system of $NaBPh_4$ + 18C6 in DME:THF(1:1, molar) mixture. ln k_{-2} vs. 1/T

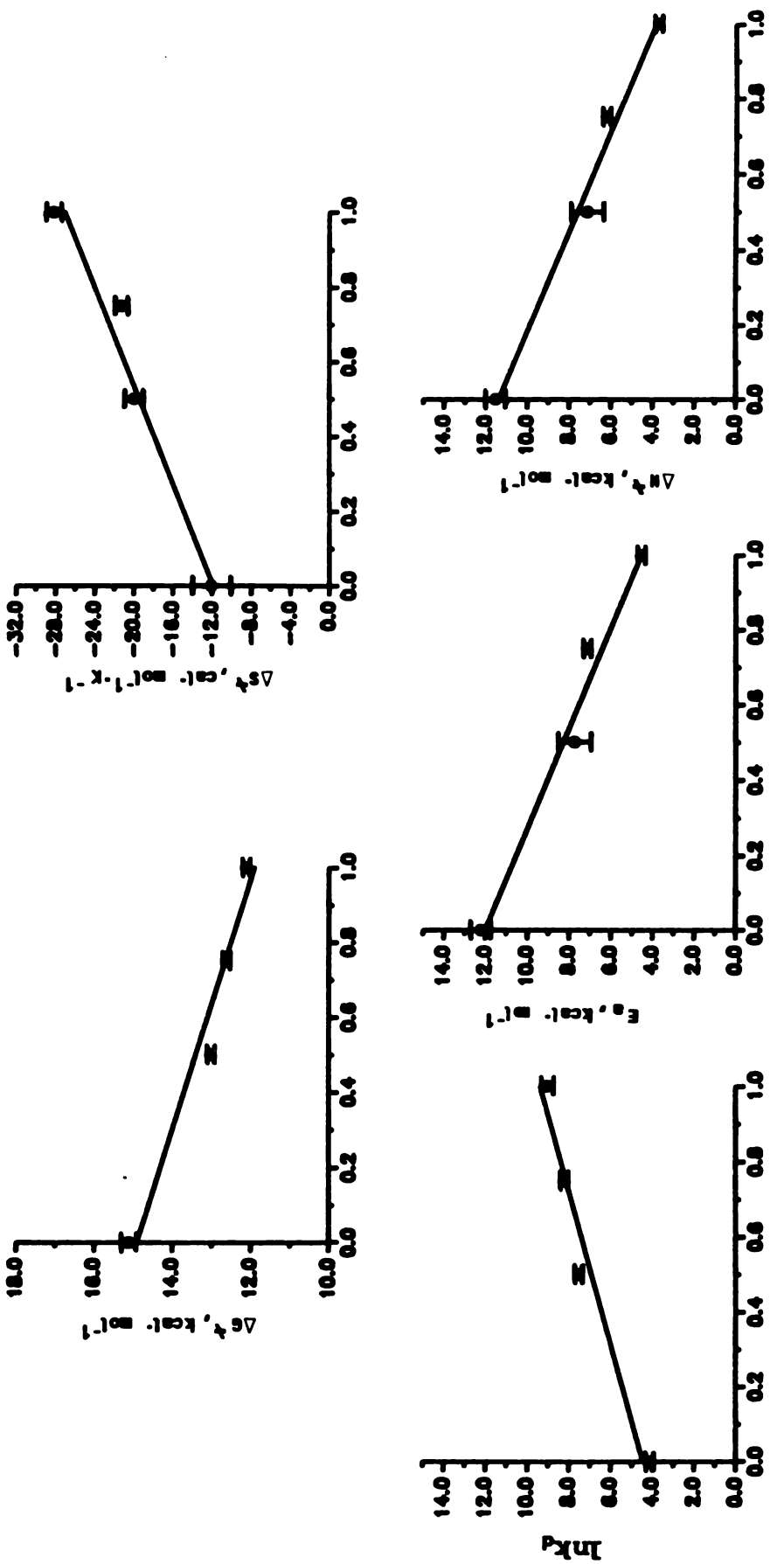

Figure 23. Activation parameters as functions of the composition of the binary mixture of DME:THF

Chapter 4

KINETIC STUDIES OF THE EXCHANGE REACTION OF THE THALLIUM ION WITH 18C6 AND PENTAGLYME IN ACETONITRILE

4.1 INTRODUCTION

As noted before, kinetic studies of complexation reactions of metal ions with macrocyclic ligands are sparse as compared to thermodynamic studies. Open chain ligands or linear ligands have even less kinetic information available, probably because most of the exchange reaction rates of metal ions between their uncomplexed sites and complexed sites are too fast to be measured by most of currently available experimental method.

Maass and coworkers,[93] describe the synthesis of a series of noncyclic neutral ionophores and studies of the complexation reactions of these ligands with alkali metal ions by . The formation rate constants are in the range of 10^7 to 10^8 $M^{-1}s^{-1}$, which are relatively high but still lower than the value of around 10^9 to 10^{10} $M^{-1}s^{-1}$ expected for a diffusion-controlled combination of alkali metal ions with complexones in methanol solutions. The reduced rates are a consequence of the stepwise replacement of the solvent molecules in the inner coordination sphere of the metal ion by the chelating atoms of the multidentated complexone. This study is one of the few that deal with the linear ligand kinetic study with metal ions.

As has been discussed in Chapter 1, the tremendously enhanced macrocyclic complex stabilities(the macrocyclic effect) compared to that of their linear ligand counterparts

are still inconclusive as to which of the two factors, enthalpy or entropy, is predominant.[35-39] Kinetic studies can provide information of complexation(k_f) and decomplexation(k_d) rates as well as on the exchange mechanism. If the stability constant K_{stab} of a complex is known, measurement of k_f and k_d can show which of the two factors, the complexation or the decomplexation, determines the stability of a complex since $K_{stab} = k_f/k_d$.[38]

Hopefully, kinetic studies of complexation reactions of ions with linear polyether ligands can yield useful kinetic information about these linear ligands and possibly help to elucidate the nature of the macrocyclic effect.

4.2 RESULTS AND DISCUSSION

4.2.1 Molecular dynamics of the uncomplexed thallium ions and the complexed thallium ions by 18-Crown-6 and pentaglyme

To perform the kinetic study of the exchange reaction kinetics, the chemical shifts and the relaxation times of both the uncomplexed and the complexed thallium salts have to be measured as functions of temperature. The results of these measurement are listed in Tables 26 to 28. The chemical shifts of all species, the uncomplexed and the complexed thallium ions by 18C6 and by pentaglyme, show very clear dependence on temperature(See Figure 24); the resonances shift up-field with decrease of temperature. The

up-field shifts of the resonances indicate a stronger solvent-cation interactions for the uncomplexed and ligand-cation and/or solvent-cation interactions for the complexed cations at lower temperatures(See Page 76). However, the relaxation times of the free thallium ion and the complexed thallium ion by 18C6 do not follow the linear relationship with the reciprocal of temperature as described by Equation 19 of Chapter 2(See Figure 25). This observation is probably due to the fact that the linewidths of the free and the complexed thallium signals are extremely narrow and any inhomogeneity of a magnetic field can cause large errors in the measurement of an extremely narrow linewidth. The inhomogeneity can be caused by the geometry configuration of the experimental arrangement of NMR tubes(lock solvent in the insert) or by the field shifting because no insert with lock solvent used to avoid the inhomogeneity caused by an insert as discussed in Chapter 2.

4.2.2 Kinetic studies of the exchange reactions of $TlClO_4$ with 18C6 and pentaglyme in acetonitrile solution

When the concentrations of the ligands are smaller than the total concentrations of the salt, thallium ion undergoes the exchange reaction between the uncomplexed and complexed forms. The mean life times of the thallium ion were measured at several temperatures. The results of this measurement at different concentrations of the thallium ion and of the

ligands are listed in Table 29 for the 18C6 and in Table 30 for the pentaglyme respectively. The results show that the mean life times of the thallium ion are approximately one order in magnitude longer with 18C6 than with pentaglyme, indicating a faster exchange reaction in the $TlClO_4$ + pentaglyme system than in the $TlClO_4$ + 18C6 system in acetonitrile.

In order to obtain the mechanisms of the exchange reactions in these two systems, $1/[Tl^+]_T\tau$ is plotted against $1/[Tl^+]_f$. In Figures 28 and Figure 29 are shown these plots for the $TlClO_4$ + 18C6 and $TlClO_4$ + pentaglyme systems in acetonitrile, respectively. Horizontal straight lines are obtained in the case of $TlClO_4$ + 18C6 at all temperatures the measurements were made, indicating that the bimolecular mechanism prevails according to Equation 6 of Chapter 2. It is evident that in the case of $TlClO_4$ + pentaglyme system the exchange reaction is a combination of the bimolecular and associative-dissociative mechanisms. With the decrease of temperature, the contribution of the associative-dissociative mechanism is gradually reduced. At 263 K, the exchange proceeds only by the bimolecular mechanism.

For pentaglyme, the plots of $1/[Tl^+]_T\tau$ vs. $1/[Tl^+]_F$ also separate the respective contribution of the two exchange reaction mechanisms to the overall reaction rates, yielding k_1 and k_{-2}(or k_d) corresponding to the bimolecular and the associative-dissociative exchange mechanisms respectively.

The above results show that the exchange mechanisms of $TlClO_4$ between its uncomplexed and complexed sites in acetonitrile solutions are different for the different ligands. The rate constants for the respective reactions for the $TlClO_4$ + 18C6 and $TlClO_4$ + pentaglyme systems are listed in Tables 31 and 32 respectively.

The Arrhenius plot (ln k_1 vs. 1/T) of the $TlClO_4$ + 18C6 system in acetonitrile is not linear(See Figure 30). Figure 26 show the plots of ln ($1/\tau$) vs 1/T for the system $TlClO_4$ + 18C6 in acetonitrile solutions at different relative ratios of $TlClO_4$ to 18C6. These plots also show a generally decreasing slope with decreasing temperature.

Figure 27 shows the plots of ln ($1/\tau$) vs 1/T for the $TlClO_4$ + pentaglyme system. The exchange reaction in this system is a combination of the associative-dissociative and bimolecular exchange mechanisms, and ln ($1/\tau$) vs 1/T plots give the activation energy of the exchange reaction only when one of the exchange mechanisms is dominant. Figures 31 and 32 show the Arrhenius plots of the two exchange mechanisms for the system $TlClO_4$ + pentaglyme in acetonitrile solution.

The activation energies E_a of reactions can be obtained from the Arrhenius plots, and then the other activation

kinetic parameters($\Delta H^{\ddagger}$, $\Delta G^{\ddagger}$, and $\Delta S^{\ddagger}$) can be calculated. According to the equation:

$$\ln k = A - \frac{E_a}{RT}$$

where k is a reaction rate constant, R and T the gas constant and temperature(k), ln k is linearly dependent on 1/T with intercepts of A and slopes of E_a/R(E_a the activation energy of the reaction). The nonlinearity of Arrhenius plots can be caused by the change of either A or E_a or both with temperature. However, it could not be justified to conclude which, A and E_a, cause the nonlinear behavior of the Arrhenius plots for the $TlClO_4$ + 18C6 and $TlClO_4$ + pentaglyme systems in acetonitrile solutions. If assuming that the A is a constant over the temperature range studied, the change of the slope of the plots of ln k against 1/T can be attributed to the variation of E_a with temperature. The purpose of this assumption is to roughly asses the solvent influence on E_a and exchange mechanisms at different temperatures, and it should not be taken literally.

For the system of $TlClO_4$ + 18C6, the activation energy decreases with the decrease of temperature. It is ~16 $kcal \cdot mol^{-1}$ at 328k, ~2 $kcal \cdot mol^{-1}$ at 298k, and ~0.3 $kcal \cdot mol^{-1}$ at 278 respectively. For $TlClO_4$ + pentaglyme, plots of ln (k_1) and ln (k_{-2}) vs 1/T give activation energies of

3.00±0.05 kcal·mol^{-1} for the bimolecular exchange mechanism, and temperature dependent activation energy for the associative-dissociative mechanism(~5 kcal·mol^{-1} at 298k and ~11 kcal·mol^{-1} at 263k). The other kinetic parameters of the exchange reactions are listed in Table 33.

Since only the exchange reaction rate constants can be determined by NMR measurement if the exchange reactions proceed by the bimolecular mechanism, the complexation and decomplexation reaction rate constants are not obtainable. It is not possible to compare the complexation and decomplexation rate constants to see which of the two dominates the stability constants. However, the enhanced stability(>100 times) of the macrocyclic complex Tl·18C6^{+}(log K_f=5.8±0.5)[80] over that of the linear complex Tl·PG^{+}(log K_f=3.65±0.05)[80] is probably a combination of the complexation and decomplexation steps.

The Tl·PG^{+} complex is less stable than the Tl·18C6^{+} complex and the decomplexation rate is faster for the former. The formation rate constant at 298 k for the Tl·PG^{+} complex is 9.8 x 10^{8} s^{-1}, as obtained in this study by using the relationship $K_f=k_f/k_d$ where K_f and k_d are known. According to Maass,[93] the formation rate constant of the Tl·PG^{+} complex is slower than the diffusion-controlled rate constants(10^{9} to 10^{10} s^{-1}). The slower formation rate constants of linear ligands than expected for the diffusion-controlled processes are a result of the step-wise substitution of the solvent

molecules in the solvation shells of cations. The more rigid pre-arrangement of the donor atoms of the macrocyclic ligands before complexation cations can more effectively replace the solvent molecules in the solvation shells of cations. It would be reasonable to expect that the complexation of the thallium ion by 18C6 is faster than the complexation by pentaglyme and may reach the diffusion-controlled limit. The faster complexation rate of the thallium ion and the slower decomplexation rate of the complexed thallium ion in the Tl^+ + 18C6 system than Tl^+ + pentaglyme system combine to give a 100-fold more stable complex for the former.

Apparently, there is an interdependence between the nature of ligands and the resulting exchange mechanisms since different mechanisms prevail for different ligands in our study. It has been discussed before, that ion-pair formations and solvating abilities of solvents greatly influence the exchange reaction rates and mechanisms.

In general, based on the electrostatic repulsions of like charges and the entropy terms, the associative-dissociative mechanism is favored over the bimolecular mechanism. This preference can be changed if the charge-charge repulsion can be substantially reduced by formation of contact-ion pairs, or strong solvent-cation interactions, and so forth. The energy barrier of the decomplexation(E_a) is also determined by the easiness of the release of the

ligand. If a ligand strongly interacts with a cation, the decomplexation will be difficult, especially in solvents of very poor solvating abilities, and the activation energy E_2 will be high.

In order to explain the different behaviors of $TlClO_4$ with 18C6 and pentaglyme in acetonitrile solutions, solvations, contact ion-pair formations, and the roles of ligands, will have to be considered. In 0.01 M thallium perchlorate acetonitrile solutions, the ion pair formation of the salt should not be significant. The solvent does not have very high solvating power, as evidenced by the low solubility of $TlClO_4$ in this solvent($\tilde{}$0.01 M). It seems that neither the ion pair formation nor the solvation of thallium ions by the solvent is able to reduce the cation-cation repulsion at the transition state of the exchange reaction intrinsic with the bimolecular mechanism.

Let us assume that the exchange reaction proceed through the associative-dissociative mechanism for a system in which ion pair formation is limited and where the solvent has a very weak solvating power. At the transition state, the ions have to be partially decomplexed, but probably not solvated by the solvent molecules due to the poor solvating power of the solvent, resulting in high energy level of transition state. For the same system, the energy level of the transition state of the bimolecular mechanism would be even higher, considering the cation-cation repulsion at this

stage. Logically, the exchange will have to follow the associative-dissociative pathway so as to avoid the higher energy requirement by the bimolecular mechanism.

If ligands can interact with cations sufficiently strongly so that the cation-cation repulsion is reduced, it is possible that the bimolecular mechanism can still exist. In acetonitrile, both the $TlClO_4 \cdot 18C6$ complex and the $TlClO_4 \cdot PG$ complex are stable but the former is about 100 times more stable than the latter. Therefore, the bimolecular mechanism becomes possible for both the Tl^+ + 18C6 and Tl^+ + pentaglyme systems. For the Tl^+ + 18C6 system, the cation-ligand interactions are so strong that the bimolecular mechanism is the only exchange pathway throughout the studied temperature range. The situation for the $TlClO_4$ + PG system in acetonitrile solutions is a little different--the two exchange mechanisms coexist at room temperature and the bimolecular exchange mechanism dominates at low temperatures. In this system, the ligand-cation interaction is not as strong as that of Tl^+-18C6, and this interaction cannot effectively offset the cation-cation repulsion at the transition state of the bimolecular mechanism. This weaker complexation of Tl^+-pentaglyme is responsible for the competition of the associative-dissociative mechanism with the bimolecular one. At low temperatures, the increase of the cation-ligand interaction can assist to decrease the cation-cation repulsion at the transition state and the bimolecular mechanism prevails.

It should be mentioned that configurations of ligands may also play an important role in determining the exchange mechanism. 18C6 is a cyclic ligand, and has a symmetrical plane for cations to approach from the both sides which makes the bimolecular mechanism likely to occur. Pentaglyme is a linear ligand and it has a more free configuration than 18C6, enhancing difficulties for the symmetrical and simultaneous bonding of cations to the ligand occurring in the transition state of the bimolecular mechanism. At lower temperatures, the structure of the ligand is more rigid and more likely to take crown-ether like configurations, leading to the more contribution of the bimolecular mechanism to the overall exchange process.

Another important factor that should be mentioned for the observed bimolecular mechanism in our study is the charge density of the Tl^+ cation. It is known that K^+ and Tl^+ have very similar sizes and therefore the similar charge densities(see Table 24). It is also known that for K^+ ion the exchange mechanism is often bimolecular. Table 25 lists some results of the kinetic studies of the complexation reactions of thallium and potassium with crown ethers. Schmidt and coworkers[65] have found the bimolecular exchange mechanism for the potassium ion between its uncomplexed form and the complexed form by 18C6 in acetone, 1,3-dioxolane, methanol solutions, and in the mixture of acetone-1,4-dioxolane(80:20 v/v). The exchange mechanism in water[94] was found to be the associative-dissociative one. In pure

acetone, methanol solutions and the mixture of acetone-1,4-dioxolane, the exchange rates were found to be in the range of 10^5 $M^{-1}s^{-1}$ to 10^6 $M^{-1}s^{-1}$ in pure 1,3-dioxolane solutions. The decomplexation rate in aqueous solutions was determined to be 10^5 to 10^6 s^{-1}.

For $Tl{\cdot}18C6^+$ complex, the exchange proceeds through the bimolecular exchange mechanism and the activation energy for the decomplexation reaction decreases with decreasing of temperature in the temperature range of 278 - 328 K. The decrease of E_a with temperature can not be explained by the increased ion-ion interactions which reduce the cation-cation repulsion at the transition state of the bimolecular exchange mechanism, and eventually reduce the activation energy, because the dielectric constant of the solvent increases with decreasing of temperature and the ion-pair formation decreases with the decrease of temperature. The only other cause that can reduce the activation energy for the decomplexation reaction is the stronger solvating power of the solvent at lower temperatures although acetonitrile has been considered as a weak solvating power solvent.

It is reasonable to imagine that the solvating powers of solvents increase with decreasing of temperature because motions of cations, solvent molecules and other particles are slowed down by decreasing temperature, and solvent molecules have longer time to interact with cations. Consequently, the change of the activation energy for the

exchange reaction with temperature could be the direct result of the better solvating power of acetonitrile solvent at the lower temperature range.

Based on the obtained resutls, a detailed exchange scheme may proposed as following:

$$Tl^{+}\cdot L + {}^{*}Tl^{+} + ns \rightleftharpoons Tl^{+}\cdots L + {}^{*}Tl^{+} + ns \quad \text{(i)}$$

$$Tl^{+}\cdots L + {}^{*}Tl^{+} + ns \rightleftharpoons Tl^{+} + L + {}^{*}Tl^{+} + ns \quad \text{(iia)}$$

$$\text{or } Tl^{+}\cdots L + {}^{*}Tl^{+} + ns \rightleftharpoons Tl^{+}\cdots\cdot L\cdots\cdot {}^{*}Tl^{+} + ns \quad \text{(iib)}$$

$$Tl^{+}\cdots\cdot L\cdots\cdot {}^{*}Tl^{+} + ns \rightleftharpoons s_{n/2}\cdots\cdot Tl^{+}\cdots\cdot L\cdots\cdot {}^{*}Tl^{+}\cdots\cdot s_{n/2} \quad \text{(iiia)}$$

$$s_{n/2}\cdots\cdot Tl^{+}\cdots\cdot L\cdots\cdot {}^{*}Tl^{+}\cdots\cdot s_{n/2} \rightleftharpoons Tl^{+} + {}^{*}Tl\cdot L + ns \quad \text{(iiib)}$$

$$\text{or } Tl^{+}\cdots\cdot L\cdots\cdot {}^{*}Tl^{+} + ns \rightleftharpoons Tl^{+} + {}^{*}Tl\cdot L + ns \quad \text{(iiic)}$$

where s is solvent and the other symbols have their usual meanings. For a poor solvent, it is unlikely that the solvent will participate in this scheme. For a weak complex, steps iiia will not occur because the complex decomplexes before the second metal ion ($^{*}Tl^{+}$) reaches it. Thus, for the $Tl^{+}\cdot$PG complex, the exchange reaction undergoes by steps i and iia resulting in an associative dissociative mechanism. On the other hand, the $Tl^{+}\cdot$18C6 complex is stronger and a bimolecular mechanism prevails for the exchange reaction. That is, at high temperatures when the solvating ability of acetonitrile is weak, the mechanism is consisted of steps i, iib, and iiic while at low temperatures when the solvating power is high the mechanism is composed of steps i, iib, iiia, and iiib.

4.3 CONCLUSIONS

By comparing the activation energies and their temperature-dependence for the exchange reactions of Tl^+ ions with 18C6 and pentaglyme, it is clear that the strengths of the cation-ligand interactions and the structures of the ligand are important factors in determining the exchange mechanism. At the kinetic points of view, the bimolecular exchange reaction mechanism is not favored by the entropy factor, but the enthalpy factor is so strongly favored that it can overcome the entropy influence and the bimolecular exchange mechanism prevails for the system of $TlClO_4$ + 18C6 in acetonitrile solutions and for the system of $TlClO_4$ + pentaglyme at low temperatures.

Because of the bimolecular exchange mechanism in the system $TlClO_4$ + 18C6, the decomplexation rate constant of the complex cannot be obtained. Thus, we are not able to compare the two systems to conclude which factor, complexation or decomplexation, determines the macrocyclic effect.

Table 24. A list of some physicochemical properties of some metal ions

Alkali metal	Crystal radius r[Å]	Charge density [Coulomb/Å^3]	Free energy of hydration	Rate constant of inner sphere substitution k[s^{-1}]
Li	0.60	0.22	122	~5 x 10^8
Na	0.95	0.088	98	~8 x 10^8
K	1.33	0.045	81	~1 x 10^9
Rb	1.48	0.036	76	~2 x 10^9
Cs	1.69	0.029	68	~5 x 10^9
Tl	1.40			

Pauling ionic radii

Table 25. Comparison of the complexations of thallium and potassium

M	Solv.	K_f M^{-1}	k_f $M^{-1}s^{-1}$	k_d s^{-1}	Ref.
DB30C10					
K^+	MeOH	$(3.7\pm0.4)\times10^4$	$(6\pm2)\times10^8$	$(1.6\pm0.5)\times10^4$	21
Tl^+	MeOH	$(3.2\pm0.4)\times10^4$	$(8\pm1)\times10^8$	$(2.5\pm0.3)\times10^4$	21
18C6					
K^+	H_2O		1.0×10^{10}	3.7×10^6	20
K^+	MeOH	1.26×10^6			95
K^+	CH_3CN	5×10^5			25,97
15C5					
K^+	H_2O	5.5 ± 0.5	4.3×10^8	7.8×10^7	24
Tl^+	H_2O	17 ± 2	8.0×10^8	5.0×10^7	24

Table 26. Tl-205 chemical shift and relaxation time of the free thallium perchlorate(0.01M) in acetonitrile

Temperature (K)	Chemical Shifts (ppm)	Relaxation Time (s)
333	-209.04±0.02	0.0180±0.0008
328	-211.11±0.02	0.0172±0.0007
323	-213.15±0.02	0.0154±0.0004
318	-215.21±0.02	0.0177±0.0004
313	-217.34±0.02	0.0171±0.0006
308	-219.84±0.02	0.0187±0.0002
303	-221.65±0.01	0.0231±0.0002
298	-223.45±0.02	0.0204±0.0002
293	-225.30±0.02	0.0170±0.0003
288	-227.87±0.03	0.0089±0.0001
278	-232.35±0.03	0.0090±0.0001
268	-237.28±0.02	0.0143±0.0002
258	-242.31±0.02	0.0138±0.0001
248	-247.20±0.02	0.0124±0.0002

The chemical shift is referenced to that of 0.1M $TlClO_4$ in D_2O.

Table 27. Tl-205 chemical shift and relaxation time of the complexed thallium perchlorate(0.01M) by 18C6 in acetonitrile

Temperature (K)	Chemical Shifts (ppm)	Relaxation Time (s)
333	-142.75±0.03	0.0101±0.0002
328	-143.83±0.03	0.0119±0.0003
323	-144.89±0.02	0.0141±0.0004
318	-146.02±0.02	0.0181±0.0004
313	-147.84±0.01	0.0232±0.0005

The chemical shift is referenced to that of 0.1M $TlClO_4$ in D_2O.

Table 28. Tl-205 chemical shift and relaxation time of the complexed thallium perchlorate(0.01M) by pentaglyme in acetonitrile

Temperature (K)	Chemical Shifts (ppm)	Relaxation Time (S)
298	-139.58±0.02	0.0150±0.0008
288	-142.20±0.03	0.0080±0.0004
278	-144.98±0.09	0.0035±0.0001
268	-148.3±0.2	0.00189±0.00007
258	-152.47±0.2	0.00123±0.00007
248	-156.59±0.3	0.00088±0.00003

The chemical shift is referenced to that of 0.1M $TlClO_4$ in D_2O.

Table 29. The mean life times of the thallium ion in the system of $TlClO_4$ with 18C6 in acetonitrile solutions

Temperature	Mean life time τ (s) x 10^6			
K	1	2	3	4
278	2.57±0.02	2.44±0.03	3.28±0.07	2.47±0.06
288	2.19±0.03	2.26±0.02	2.69±0.03	2.19±0.02
293	2.21±0.02	2.14±0.05	2.92±0.09	2.34±0.05
298	2.30±0.03	2.28±0.02	2.58±0.06	2.53±0.01
303	2.17±0.02	2.17±0.01	2.48±0.03	2.23±0.03
308	1.95±0.01	1.88±0.02	2.48±0.05	2.16±0.02
313	1.66±0.01	1.70±0.02	1.91±0.04	1.73±0.02
318	1.51±0.02	1.45±0.01	1.76±0.03	1.26±0.02
323	1.25±0.03	0.93±0.05	1.59±0.07	1.32±0.04
328	1.23±0.04	1.39±0.08	1.41±0.07	1.76±0.07

1. $TlClO_4$(0.0112M) with 18C6(0.0045M), P_{Tl^+} = 0.5946;
2. $TlClO_4$(0.0100M) with 18C6(0.0015M), P_{Tl^+} = 0.8487;
3. $TlClO_4$(0.0099M) with 18C6(0.0094M), P_{Tl^+} = 0.0894;
4. $TlClO_4$(0.0097M) with 18C6(0.0074M), P_{Tl^+} = 0.2394.

Table 30. The mean life times of the thallium ion in the system of $TlClO_4$ with pentaglyme in acetonitrile

Temperature	Mean life time τ (s) x 10^7			
K	1	2	3	4
308	2.55±0.05	2.74±0.06	2.53±0.05	2.17±0.05
298		3.80±0.05	2.87±0.05	1.94±0.04
293	3.04±0.07	3.64±0.05	2.81±0.05	2.22±0.09
288	3.53±0.06	3.19±0.03	3.77±0.03	4.27±0.06
283	5.1±0.2	3.8±0.1	3.2±0.1	3.0±0.2
278	5.1±0.1	4.0±0.1	3.4±0.1	5.3±0.2
273	3.3±0.2	4.9±0.2	4.6±0.2	3.2±0.3
263	8.5±0.5	7.0±0.3	6.4±0.3	6.2±0.5

1. $TlClO_4$(0.0107M) with pentaglyme(0.0034M), P_{Tl^+} = 0.6822;
2. $TlClO_4$(0.0095M) with pentaglyme(0.0041M), P_{Tl^+} = 0.5653;
3. $TlClO_4$(0.0099M) with pentaglyme(0.0056M), P_{Tl^+} = 0.4311;
3. $TlClO_4$(0.0097M) with pentaglyme(0.0081M), P_{Tl^+} = 0.1678.

Table 31. The exchange rate constants(k_1) of the thallium ion in the system of $TlClO_4$ with pentaglyme in acetonitrile via the bimolecular exchange mechanism and the exchange or the decomplexation rate constant(k_d or k_{-2}) via the associative-dissociative mechanism, $TlClO_4$:0.01M

Temperature (k)	$k_1 \times 10^{-8}$ $M^{-1} \cdot s^{-1}$	$k_{-2} \times 10^{-5}$ s^{-1}
308	3.5 ± 0.1	3.1 ± 0.4
298	3.0 ± 0.1	2.2 ± 0.4
293	2.7 ± 0.1	1.9 ± 0.4
288	2.5 ± 0.2	1.6 ± 0.4
283	2.3 ± 0.3	1.3 ± 0.5
278	2.1 ± 0.2	1.0 ± 0.5
273	1.9 ± 0.2	0.8 ± 0.5
263	1.5 ± 0.2	0.4 ± 0.6

Table 32. The exchange rate constants of the thallium ion in the system of $TlClO_4$ with 18C6 in acetonitrile, $TlClO_4$:0.01M

Temperature (k)	$k_1 \times 10^{-7}$ $M^{-1}s^{-1}$
278	3.7 ± 0.5
288	4.2 ± 0.4
293	4.1 ± 0.5
298	4.1 ± 0.2
303	4.4 ± 0.3
308	4.7 ± 0.4
313	5.6 ± 0.3
318	7. ± 1.
323	8. ± 2.
328	6.8 ± 0.6

Table 33. The kinetic information of the exchange reactions of $TlClO_4$ in acetonitrile solutions with 18C6 and pentaglyme at 298k

k	E_a	$\Delta H^{\ddagger}$	$\Delta S^{\ddagger}$	$\Delta G^{\ddagger}$
18-Crown-6				
$(4.1\pm0.2)\times10^{7}$	~2	~1.4	~-19	7.06±0.03
Pentaglyme				
A				
$(3.0\pm0.1)\times10^{8}$	3.00±0.05	2.41±0.05	-11.6±0.2	5.88±0.02
B				
$(2.2\pm0.4)\times10^{5}$	~5	~4.4	~-19	10.2±0.1

a. E_a, $\Delta H^{\ddagger}$, and $\Delta G^{\ddagger}$, in units of kcal·mol^{-1}; $\Delta S^{\ddagger}$ in the units of cal·mole^{-1}·K^{-1};
b. k: the decomplexation rate constant k_d corresponding to the associative-dissociative mechanism in acetonitrile solutions with the units of s^{-1}; or the exchange reaction rate constant k_1 of the bimolecular exchange mechanism in nitromethane solutions with the units of $S^{-1}\cdot M^{-1}$;
c. AN is an abbreviation for acetonitrile and nitromethane respectively;
d. The bimolecular exchange mechanism: 18-Crown-6 and pentaglyme(A); the associative-dissociative mechanism: pentaglyme(B).

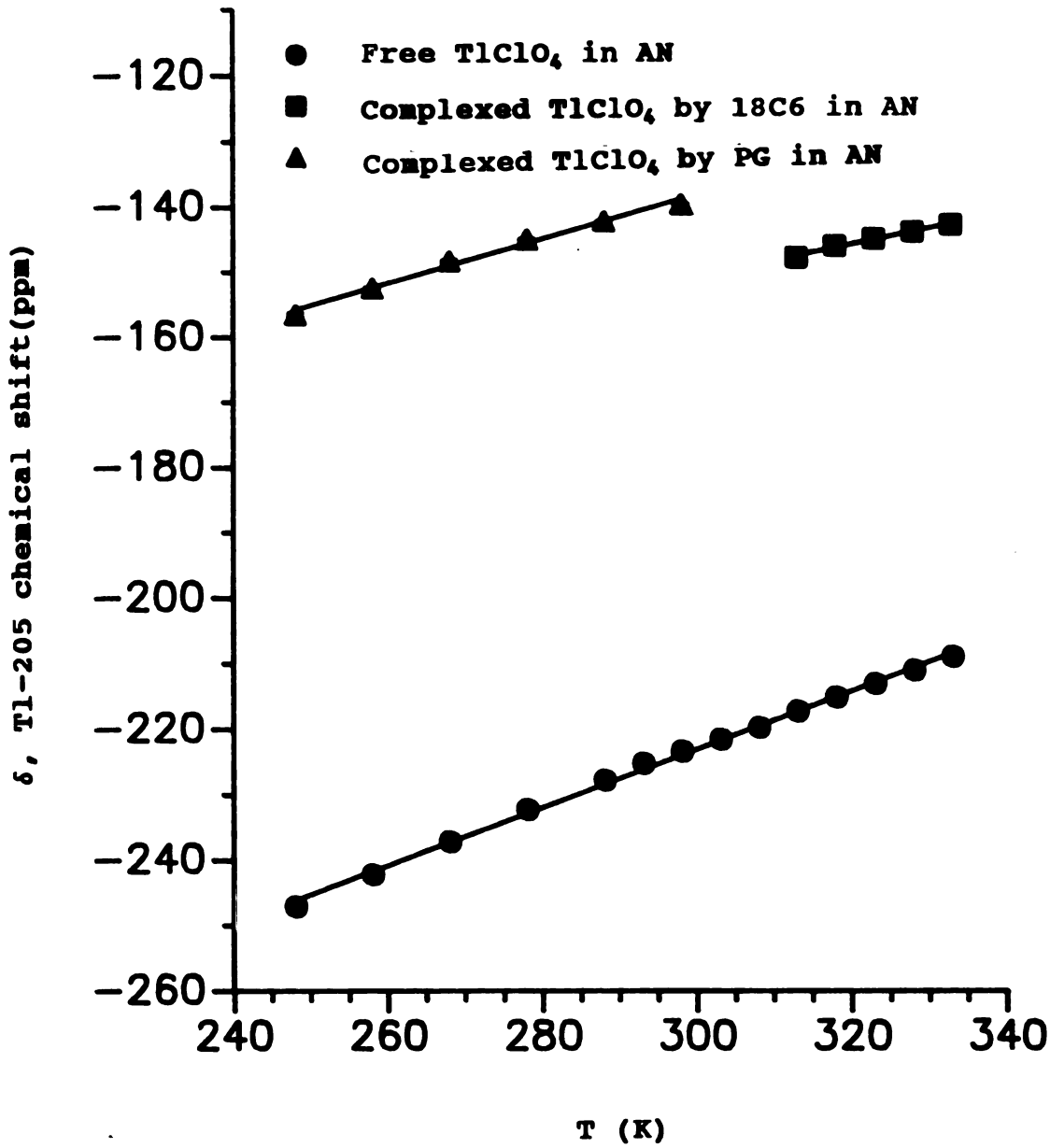

Figure 24. Tl-205 chemical shifts of the uncomplexed $TlClO_4$ and the complexed $TlClO_4$ by 18C6 and pentaglyme ligands in acetonitrile solutions as functions of temperature

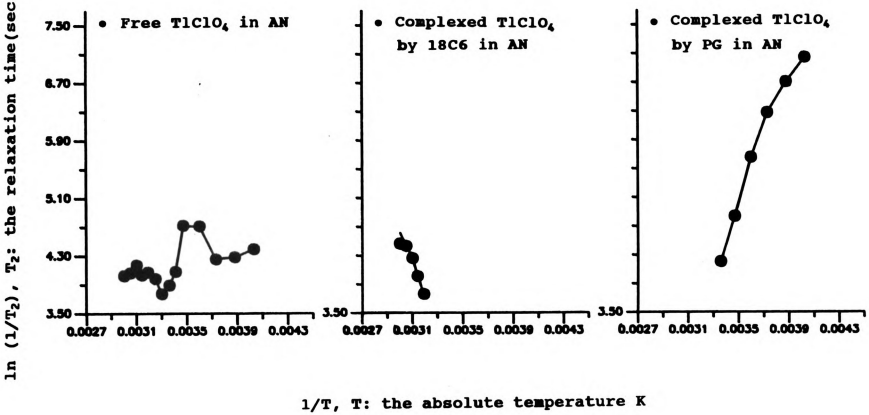

Figure 25. Tl-205 relaxation rates of the uncomplexed $TlClO_4$ and the complexed $TlClO_4$ by 18C6 and pentaglyme ligands in acetonitrile solutions as functions of temperature

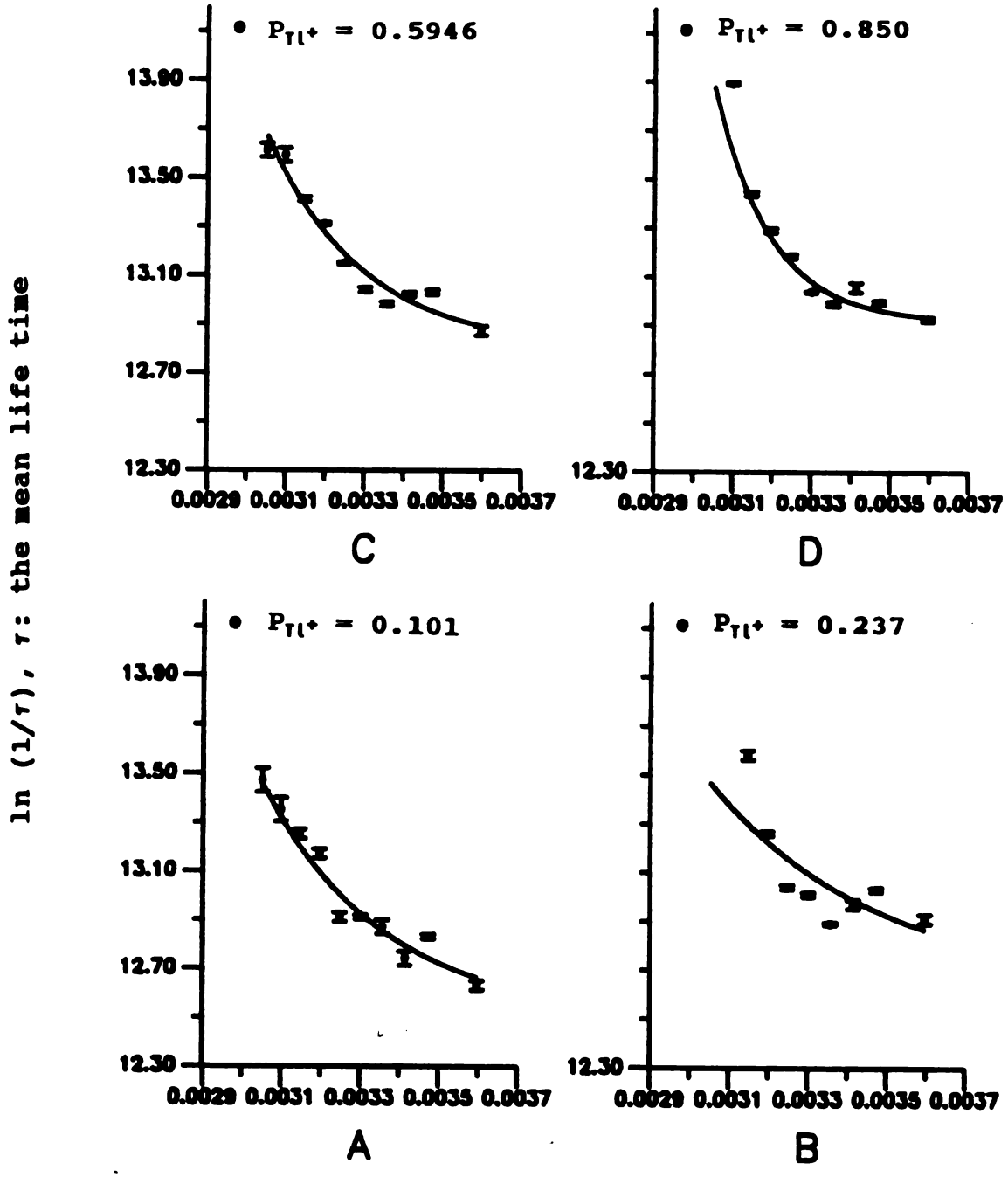

Figure 26. ln (1/τ) vs. 1/T for the system $TlClO_4$ + 18C6 in acetonitrile solution
τ: the mean life time(s) of the thallium ions in the exchange reaction; T: temperature in K;
A. 0.0099M $TlClO_4$ + 0.0089M 18C6, P_{Tl^+} = 0.101;
B. 0.0097M $TlClO_4$ + 0.0074M 18C6, P_{Tl^+} = 0.237;
C. 0.0112M $TlClO_4$ + 0.0045M 18C6, P_{Tl^+} = 0.5946;
D. 0.0100M $TlClO_4$ + 0.0015M 18C6, P_{Tl^+} = 0.850.

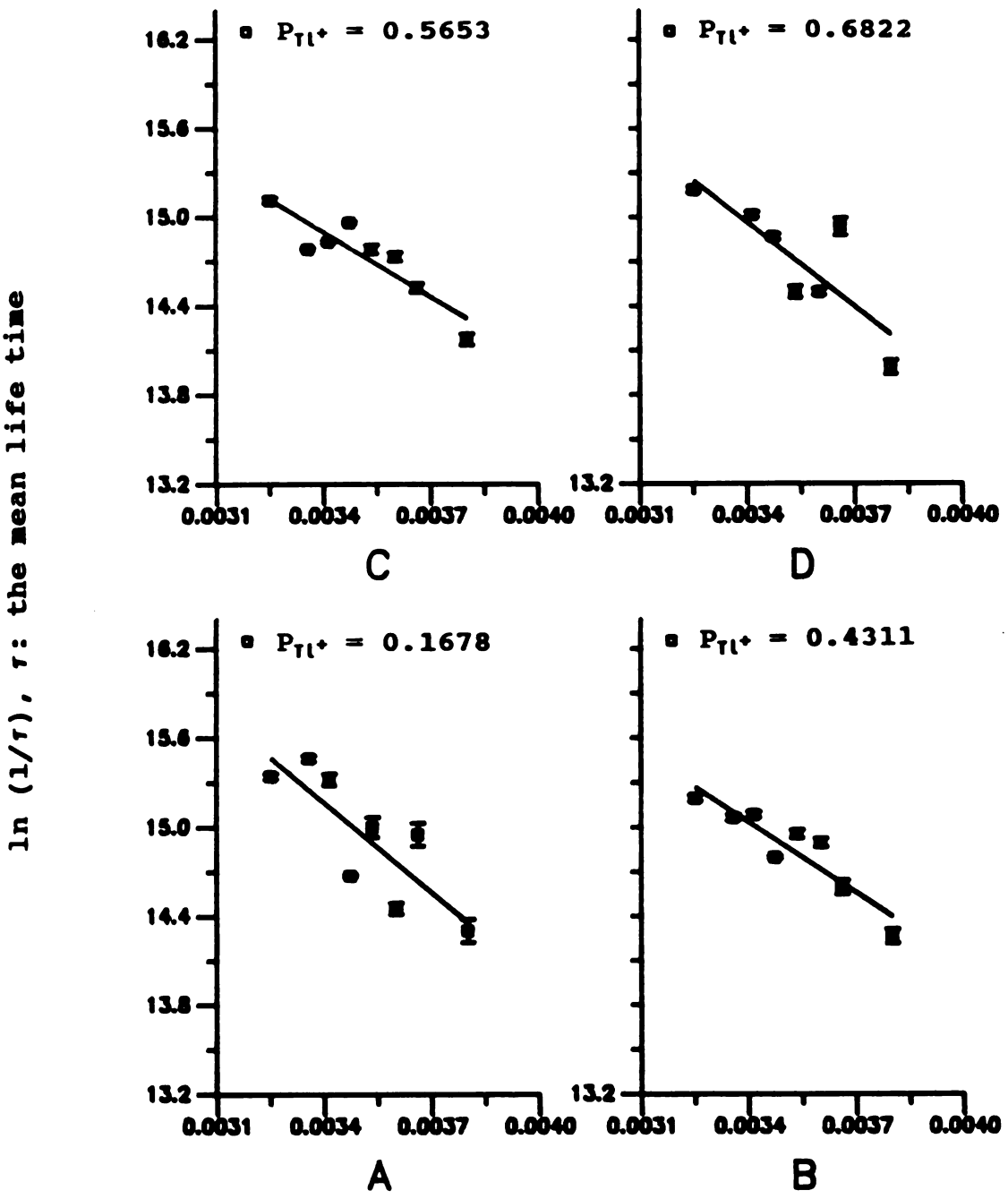

Figure 27. ln (1/τ) vs. 1/T for the system $TlClO_4$ + pentaglyme in acetonitrile solution.
τ: the mean life time(s) of the thallium ions in the exchange reaction; T: temperature in K;
A. 0.0097M $TlClO_4$ + 0.0081M PG, P_{Tl^+} = 0.1678;
B. 0.0099M $TlClO_4$ + 0.0056M PG, P_{Tl^+} = 0.4311;
C. 0.0095M $TlClO_4$ + 0.0041M PG, P_{Tl^+} = 0.5653;
D. 0.0107M $TlClO_4$ + 0.0034M PG, P_{Tl^+} = 0.6822.

Figure 28. $1/\tau[Tl^+]_T$ **vs.** $1/[Tl^+]_F$ **for the system** $TlClO_4$ **+ 18C6 in acetonitrile solution at several temperatures**
τ: the mean life time of the thallium ions in the exchange reaction(s); $[Tl^+]_T$ and $[Tl^+]_F$: the concentrations of the total and free thallium ions respectively

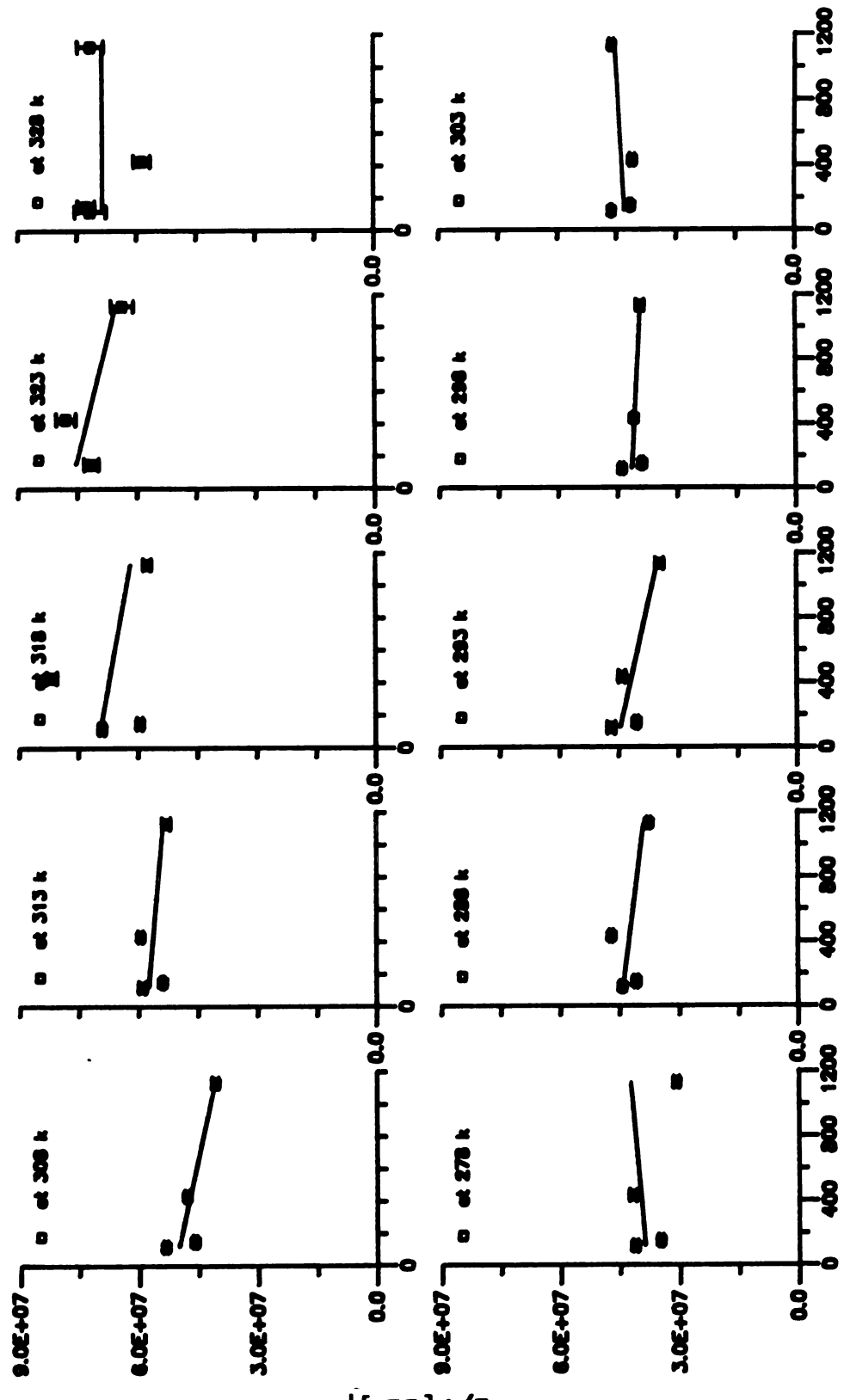
1/r [Tl+]T
1/[Tl+]F
9.0E+07
6.0E+07
3.0E+07
0.0
0
400
800
1200

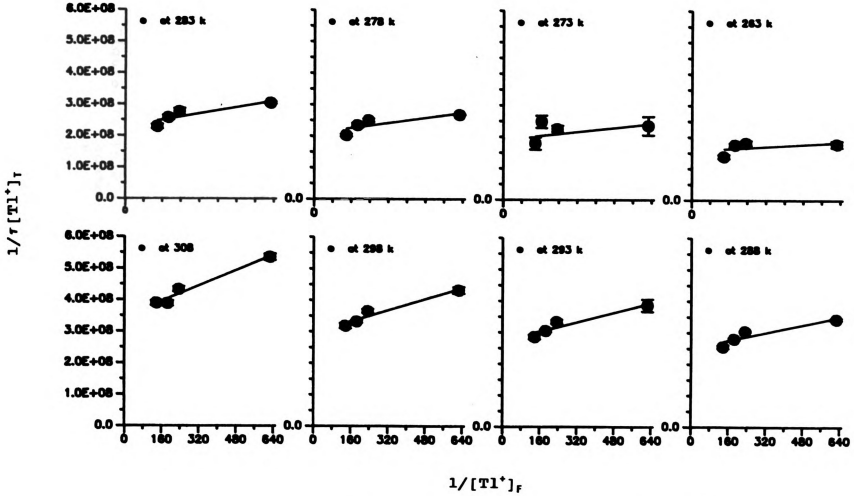

Figure 29. $1/\tau[Tl^+]_T$ vs. $1/[Tl^+]_F$ for the system $TlClO_4$ + pentaglyme in acetonitrile solution at several temperatures
τ: the mean life time of the thallium ions in the exchange reaction(s); $[Tl^+]_T$ and $[Tl^+]_F$: the concentrations of the total and free thallium ions respectively

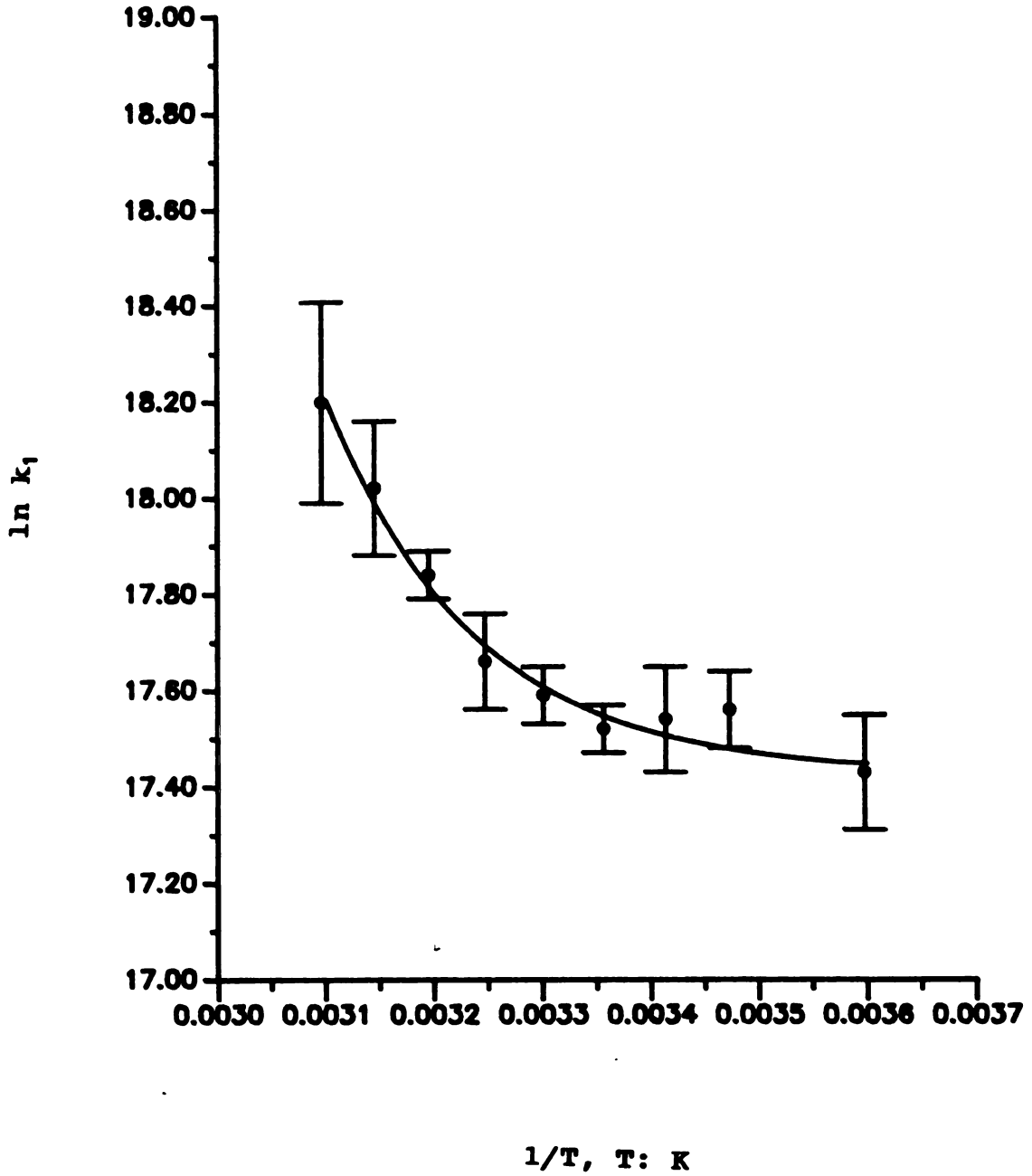

Figure 30. ln k_1 vs. 1/T for the system $TlClO_4$ + 18C6 in acetonitrile solution.
k_1: the exchange rate constant of the thallium ions by the bimolecular mechanism; T: temperature in K

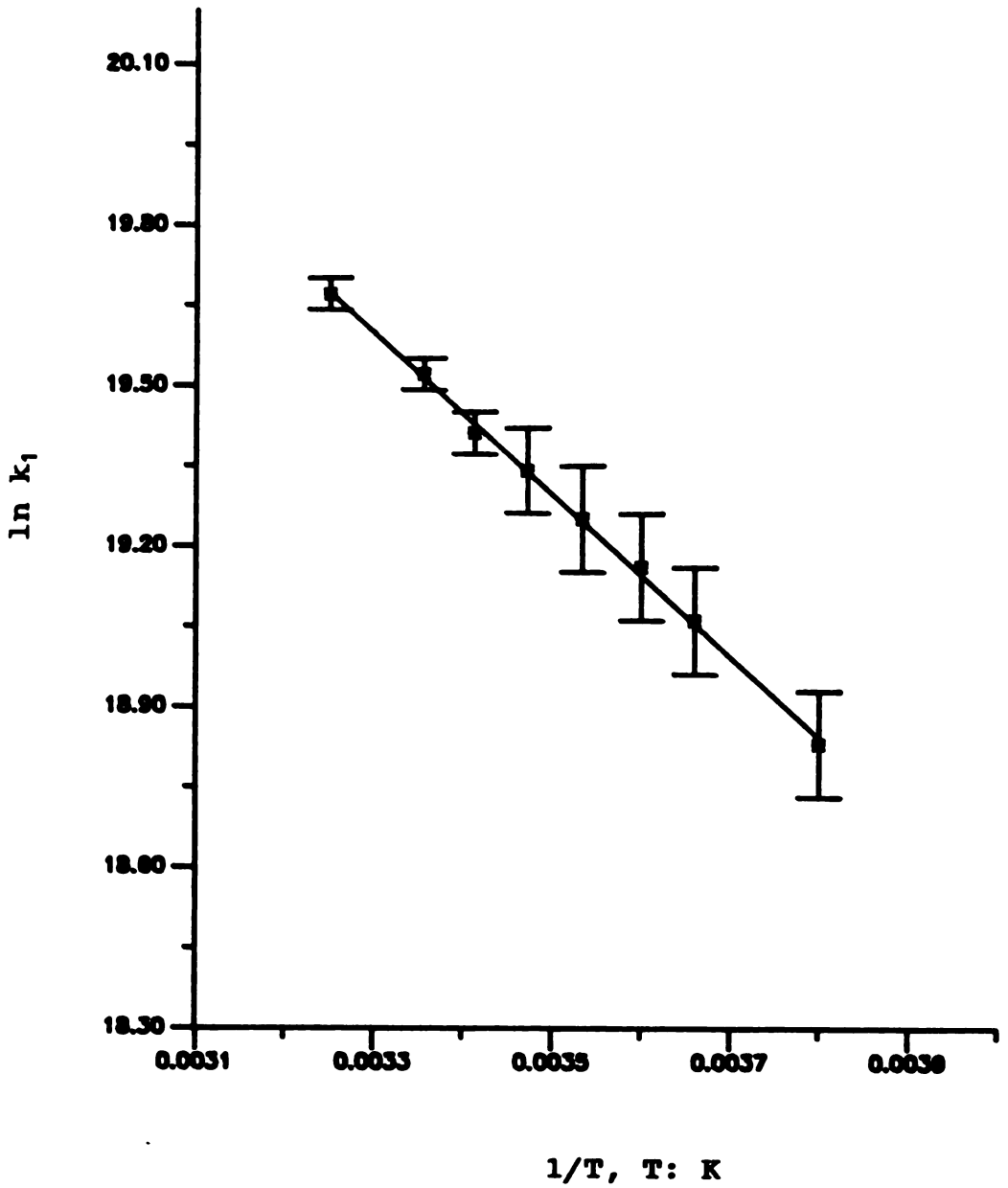

Figure 31. ln k_1 vs. 1/T for the bimolecular exchange mechanism in the system $TlClO_4$ + pentaglyme in acetonitrile solution
k_1: the exchange reaction rate constant of the thallium ions by the bimolecular exchange mechanism; T: temperature in K

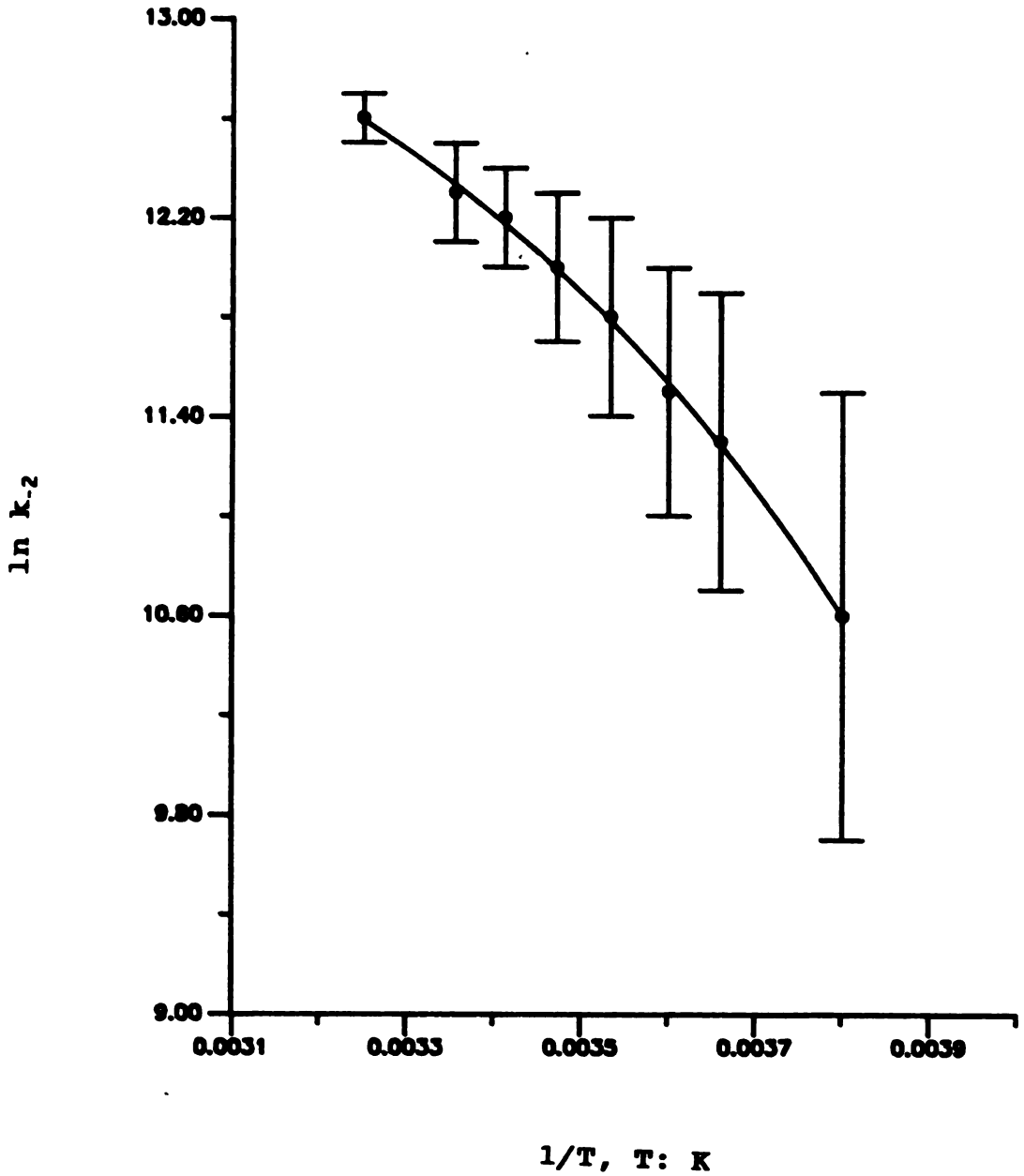

Figure 32. ln k_{-2} vs. 1/T for the associative-dissociative mechanism in the system $TlClO_4$ + pentaglyme in acetonitrile solution
k_{-2}: the exchange or the decomplexation rate constant of $TlClO_4$·Pentaglyme complex by the associative-dissociative exchange mechanism; T: temperature in K

Chapter 5

KINETIC STUDIES OF LITHIUM PERCHLORATE COMPLEX BY 15-CROWN-5 IN ACETONITRILE AND NITROMETHANE

5.1 INTRODUCTION

Kinetics of the exchange reaction between the free lithium salts and their complexes by macrocyclic polyethers have been studied much less than those of the other alkali ions. The lack of kinetic information for Li^+ again can be attributed to the experimental difficulties encountered in the measurement. The acquisition of kinetic information by the NMR technique involves measurements of the relaxation times of the free and of the complexed metal ions, as well as obtaining the spectra of the nuclei of the metal ions under exchange conditions. It is very difficult to accurately obtain the information mentioned above when the line widths of the measured signals are very narrow. Without exchange, lithium line-widths are typically between 1 to 2 Hz and they are 5 to 8 Hz with exchange. In addition to the measuring difficulties, the fact that the lithium ion forms only a few stable crown ether complexes , e.g. with 12C4, and 15C5, and in only a few solvents, such as acetonitrile and nitromethane, limits the kinetic studies to a small number of systems with high enough complex stabilities and slow enough decomplexation rates for dynamic NMR measurement.

Previous studies on sodium, potassium, and cesium ions have helped to understand the mechanisms of exchange

kinetics. The exchange reactions basically occur through two different mechanisms, bimolecular and unimolecular(or associative-dissociative) mechanisms. The lack of the kinetic information about the lithium ion makes it difficult to draw any conclusions about how cations would influence the exchange reactions. It is our goal to study the exchange kinetics of lithium salts in order to see the influence of the cations on the exchange reactions.

5.2 RESULTS AND DISCUSIONS

5.2.1 Molecular dynamics of the uncomplexed lithium perchlorate and the complexed lithium perchlorate by 15C5 in acetonitrile and nitromethane solutions

Tables 34 to 35 contain relaxation times and chemical shifts for the Li^+ + 15C5 system in acetonitrile and nitromethane solutions respectively. These data are plotted as functions of temperature in Figures 33 to 34. All species show that the chemical shifts move upfield with decreasing temperature, indicating stronger solvations for the uncomplexed lithium ions and stronger ligand-cation interactions for the complexed lithium ions respectively at lower temperatures. For the free salt in both solutions, the relaxation rates (ln $(1/T_2)$) follow the dependence on temperature predicted by Equation 19 of Chapter 2, that is, increasing with decreasing of temperature. For the complexed form in the solutions, the relaxation times are more or less

randomly distributed with temperature. This temperature randomness of the relaxation times for both the free and the complexed sites by cryptands was also observed in other solvents, such as pyridine, dimethyl sulfoxide, and dimethylformamide, formamide, and water.[66] The cause for this observation may result from a good number of factors, such as solvations of the cations, ligand-cation interactions, the viscosities of the solutions and so forth, which all change with temperature in a variety of ways.

5.2.2 The kinetics of the exchange reactions of lithium salts in acetonitrile and nitromethane solutions

Tables 36 to 37 list the mean life times of lithium perchlorate undergoing exchange reactions between its free and complexed sites, at various free and the complexed concentrations of the salt in acetonitrile and nitromethane solutions respectively. The plots of $1/\tau[Li^+]_T$ vs. $1/[Li^+]_F$ show the very strong characteristics of the unimolecular or dissociative-associative exchange mechanism in acetonitrile solutions(Figure 35), while in nitromethane solutions the bimolecular exchange mechanism is followed(Figure 36). The exchange reactions undergo different mechanisms in different solvents, namely, the associative-dissociative mechanism(Equation 4, Chapter 1) in AN and bimolecular mechanism(Equation 5, Chapter 1) in NM. From the plots of $1/\tau[Li^+]_T$ against $1/[Li^+]_F$ shown in Figures 35 and 36, the rate constants for the respective exchange reactions are

obtained according to Equation 6 of Chapter 2--namely, the intercepts and the slopes of these plots are obtained as the rate constants for the bimolecular and the associative-dissociative mechanisms respectively. These rate constants are listed in Tables 38 to 39.

Figures 37 to 38 show the plots of the natural logarithm of the reciprocal of the mean life times(ln $(1/\tau)$) against the reciprocal of the absolute temperature(1/T). The activation energy for the decomplexation of the $LiClO_4 \cdot 15C5$ complex in acetonitrile and the activation energy for the exchange reactions in nitromethane are 4.83±0.03 $kcal \cdot mol^{-1}$ in acetonitrile solutions and 4.98±0.09 $kcal \cdot mol^{-1}$ in nitromethane solutions respectively. The activation energies can also be obtained by plotting ln k vs. 1/T (Arrhenius plots)(see Figures 39 and 40), where k is the rate constant and T is the temperature(K). When only one exchange mechanism is operative for exchange reactions, plots of ln $(1/\tau)$ vs. 1/T differ from plots of ln k vs. 1/T only by a constant while the slopes are the same. The activation energies are listed in Table 40 together with the other kinetic parameters: $\Delta H^{\ddagger}$, $\Delta S^{\ddagger}$, and $\Delta G^{\ddagger}$.

The study of the exchange kinetics of the lithium complexes by 12-Crown-4 has also been attempted, but the reaction rate was so fast that it was not possible to measure the mean life times of the complex in the temperature range studied.

As can be seen, lithium ion complexation by 15C5 in acetonitrile and nitromethane is very fast(the mean life times are in the range of 10^{-3} to 10^{-4} seconds)(see Tables 36 and 37). The activation energies are small, compared to those of the lithium-cryptand complexes,[66] which are usually in the range of 10 to 20 kcal·mol^{-1}. As usual, the smaller activation energies for the decomplexation is a result of weaker lithium-crown ether complexes than the lithium-cryptand complexes. Naturally, 3-dimensional cryptand macrocyclic ligands have better complexing abilities toward metal ions(the "cryptand effect") The decomplexation of the cryptand complexes is more difficult compared to the 2-dimensional crown ether complexes in which the complexed cations are still exposed to the solvent molecules. Among crown ethers, lithium salts form the strongest complexes with 15C5 ligand because the cation size is closest to that of the 15C5 ligand cavity(see Table 1). The logarithm of the stability constant log K_f for the lithium perchlorate complex with 15C5 in nitromethane and acetonitrile solutions is greater than 4.[98] Generally, other lithium-crown ether complexes are less stable and the decomplexation rates are very fast--to a degree that the mean life time of the lithium species can not be measured.

Summarizing the kinetic results of the exchange reactions involving the alkali ions and some crown ethers in acetonitrile and nitromethane solutions, we can see two

interesting patterns of the exchange mechanisms for the alkali ions in these two solvents.

The exchange of the lithium ions between its uncomplexed site and the complexed site by 15C5 in acetonitrile and nitromethane solutions proceeds by the two different mechanisms: the associative-dissociative and the bimolecular one respectively.

In a study of Detellier and coworker,[76] the exchange mechanism of the sodium ion with DB18C6 and DB24C8 in acetonitrile was shown to be the associative-dissociative one and in nitromethane the associative-dissociative and the bimolecular exchange routes are competing with each other.[76]

For the potassium ion complexed by crown ethers, no exchange kinetic information is available in acetonitrile and nitromethane solutions. But the thallium ion resembles the potassium ion in the charge density, and can be used as a substitute for the potassium ion for the purpose of comparing the influences of cations of the alkali family in kinetic studies as discussed in Chapter 1 and Chapter 4. According to the results presented in Chapter 4, the thallium ion undergoes exchange in acetonitrile solutions between the uncomplexed and the complexed sites through the bimolecular exchange mechanism when the ligand is 18C6, and the combination of the associative-dissociative and the bimolecular mechanisms while the ligand is pentaglyme.

Shamsipur[64] has reported on the kinetics of the exchange reactions of Cs^+ with DB30C10 in acetonitrile and nitromethane solutions. The associative-dissociative mechanism is a predominant one in nitromethane solutions whilst the bimolecular exchange path way is a prevailing process in acetonitrile medium.

Clearly, the results mentioned above show that in acetonitrile solutions the exchange mechanism changes from the associative-dissociative one for the lithium ion to the bimolecular one for the cesium ion. The change of the exchange mechanism in nitromethane solutions follows the opposite direction, namely, the bimolecular mechanism for the lithium ion and the associative-dissociative mechanism for the cesium ion.

In order to understand the different patterns of the exchange mechanisms for the alkali ions in acetonitrile and nitromethane solutions, we first invoke the discussions about the roles of the ion pair formation and the solvating powers of the solvents.

Solvents of good solvating powers as well as contact ion pairs can effectively reduce the cation-cation repulsion encountered in the transition state of the bimolecular exchange reactions as noted by Shamsipur[64] and Strasser,[50] because the presence of solvents and anions in the immediate vicinity of cations can partially offset the charge densities of the cations. Usually, contact ion pairs tend to

form more easily in solvents of poor solvating abilities because ionic species can be solvated by solvents of strong solvating abilities to prevent the formation of contact ion pairs. The Gutmann donor number for acetonitrile is 14.7, substantially higher than that of nitromethane(2.7), while the dielectric constants of acetonitrile(38) and nitromethane(36) are comparable. The combined effect of a slightly lower dielectric constant and a much smaller solvating strength of nitromethane than acetonitrile is that electrolytes tend to form more contact ion pairs in nitromethane solutions and cations are more solvated in acetonitrile solutions.

As discussed previously, the associative-dissociative mechanism is favored over the bimolecular mechanism on the grounds of entropy and cation-cation repulsions. Which one of the two exchange mechanisms dominates in acetonitrile and nitromethane varies from cation to cation and depends on the strength of solvations of cations and ligands, and the amount of the contact ion pair.

Naturally, it is more difficult to form contact ion pairs for the lithium ion than for the other alkali ions since it is strongly solvated due to its high charge density. Contact ion pairs are increasingly formed as one goes from lithium to cesium, and the exchange mechanism leans more and more to the bimolecular process. This is exactly what was observed in acetonitrile solutions: the

associative-dissociative mechanism for the lithium sodium ions and the bimolecular mechanisms for the potassium(resembled by Tl^+) and cesium ions.

Since it was reported that in acetonitrile lithium perchlorate forms a contact ion pair,[99] it is logical to expect that lithium perchlorate also forms contact ion pairs in nitromethane solutions. Consequently, for the lithium ion an appreciable amount of the contact ion pairs formed in nitromethane solutions would help to diminish the cation-cation repulsion so that the bimolecular exchange mechanism can prevail.

However, the pattern of the change of the exchange mechanisms for the alkali metal ions between their uncomplexed sites and their complexed sites by the crown ethers in nitromethane solutions contradicts the above assertion of the influence of contact ion pairs on the exchange mechanisms. If purely following the argument of contact ion pairs to explain the exchange mechanism, we will be unable to conclude why the exchange mechanism in nitromethane solutions is the associative-dissociative one in the Cs^+ + DB30C10 system and the bimolecular one for the Li^+ + 15C5 system since Cs^+ should form more contact ion pair than Li^+ due to the lower charge density of the former. Thus, the influence of other factors need to be considered for the exchange mechanisms.

Shamsipur[64] assumed that for the cesium ion the solvent with stronger solvating power(acetonitrile) helps reduce the cation-cation repulsion in the transition state of the bimolecular exchange mechanism and in the solvent of a poor solvating ability(nitromethane) the associative-dissociative mechanism is preferred. This argument cannot be extended to the lithium ion in acetonitrile solutions because Li^+ is more strongly solvated than the cesium ion and should undergo the exchange reactions by the bimolecular exchange mechanism, which is in contrary to the obtained results.

Neither the formation of contact ion pairs nor the solvation of the cations can be used alone to explain the patterns of the change of the exchange mechanisms of the ions throughout the family of the alkali metals in acetonitrile and nitromethane solutions. Usually, when interpreting the exchange kinetics, the roles of ligands are ignored. However, Boss[100] has reported that some crown ethers and linear ligands react with some solvent molecules to form adducts. The results of the complexation are tabulated in Table 41. From these results, some trends among the studied ligands can be roughly recognized: a) the larger ligand are more solvated; b) the crown ethers are more solvated than the linear ones; c) the ligands are more solvated in nitromethane than in acetonitrile; d) the benzene-substituted crown ether is more solvated than the un-substituted counter part in acetonitrile and it is the opposite in nitromethane. Without doubt, the complexation of

ligands with solvents(or solvations of ligands) will have influences on the exchange kinetics. Solvations of ligands stabilize the partially decomplexed ligands at the transition state of the associative-dissociative mechanism, contributing to the existence of this mechanism or the competition of this mechanism with the bimolecular one.

Exchange kinetics and exchange mechanisms are complicated by ion pair formations, and by solvation of both cations and ligands. To explain the observed results, only preliminary speculations can be made. Further investigations are badly needed to achieve a better understanding. The lithium ion is highly solvated in acetonitrile solutions due to its high charge density, and contact ion pairs are formed in nitromethane due to the low dielectric constant and the low solvating ability of the solvent. As the result, the associative-dissociative mechanism prevails in acetonitrile solutions while the bimolecular mechanism is favored in nitromethane solutions. The sodium ion still prefers the associative-dissociative mechanism in acetonitrile solutions because of the solvation of DB18C6 and DB24C8 and because the charge density of the sodium ion is still high; in nitromethane solutions the two exchange mechanisms coexist because of the more contact ion pairs formed due to the lower dielectric constant and the less benzene-substituted ligand-solvent interactions. The results for the thallium ion were shown above and in Chapter 4, namely, the bimolecular exchange for the ligand 18C6 and the mixture of

the two mechanisms for the ligand pentaglyme because of the preferred ligand geometry of 18C6 for the bimolecular mechanism and the decreased charge density of the thallium ion. For the cesium ion, the more contact ion pairs formed and the bigger and more symmetric DB30C10 ligand prefers the bimolecular mechanism in acetonitrile solutions while the weaker solvation of the cesium ion in nitromethane solution leads to the associative-dissociative mechanism.

5.3 CONCLUSION

It is clear that the exchange reactions for the lithium ions in these two solvents undergo totally two different mechanisms. Doubtless, both charge densities of cations and properties of the solvents have significant influences on the exchange reaction kinetics as evidenced by the patterns of the exchange reactions associated with each alkali cation in acetonitrile and nitromethane solutions. From lithium to sodium, potassium and then to cesium ions, the exchange mechanism goes in acetonitrile solutions from the associative-dissociative to the bimolecular exchange mechanism, while in nitromethane solutions it is a bimolecular one the lithium ion and a associative-dissociative one for the cesium ion. These patterns are tentatively explained by the currently available knowledge of the influences of the ion pairs of electrolytes and the solvations of the ligands and cations.

Table 34. Lithium-7 relaxation times and chemical shifts of the free $LiClO_4$ and complexed $LiClO_4$ by 15C5 in acetonitrile solutions

Free salt[a]			Complexed salt[b]		
Temp. (K)	T_{2A} (s)	δ^c (ppm)	Temp. (K)	T_{2B} (s)	δ^c (ppm)
297	0.122±0.007	-2.359±0.004	300	0.107±0.005	-1.758±0.004
285	0.107±0.006	-2.502±0.004	290	0.114±0.006	-1.915±0.004
275	0.092±0.005	-2.616±0.005	280	0.103±0.007	-2.044±0.004
265	0.081±0.003	-2.731±0.006	270	0.099±0.006	-2.187±0.005
255	0.070±0.003	-2.845±0.007	260	0.113±0.004	-2.345±0.004
			250	0.100±0.006	-2.502±0.005

a. 0.0991M $LiClO_4$ in the acetonitrile solution;
b. 0.1010M $LiClO_4$ with 0.1528M 15C5 in the acetonitrile solution;
c. Chemical shifts are referenced to that of LiCl(1%) in D_2O at 25 °C.

Table 35. Lithium-7 relaxation times and chemical shifts of the free $LiClO_4$ and complexed $LiClO_4$ by 15C5 in nitromethane solutions

Temp.	Free salt[a]		Complexed salt[b]	
K	T_{2A} (S)	δ(ppm)[c]	T_{2B} (S)	δ(ppm)[c]
298	0.120±0.005	-0.640±0.004	0.108±0.002	-1.488±0.004
290	0.107±0.006	-0.715±0.004	0.107±0.007	-1.587±0.004
282	0.101±0.006	-0.798±0.005	0.109±0.007	-1.660±0.004
274	0.103±0.005	-0.876±0.004	0.122±0.007	-1.750±0.004
266	0.099±0.005	-0.964±0.005	0.072±0.003	-1.841±0.006
258	0.095±0.006	-1.052±0.006	0.106±0.003	-1.917±0.001

a. 0.0498M $LiClO_4$ in the nitromethane solution;
b. 0.0500M $LiClO_4$ with 0.0683M 15C5 in the nitromethane solution;
c. Chemical shifts are referenced to that of LiCl(1%) in D_2O at 25 °C.

Table 36. The lithium ion mean life times of $LiClO_4$ with 15C5 in acetonitrile solutions at different relative concentrations of the salt to the ligand

Temperature	Mean life time τ (s) x 10^4		
K	1	2	3
300	2.0±0.1	5.5±0.2	-----
290	1.8±0.1	5.8±0.4	-----
280	2.6±0.2	8.6±0.3	2.1±0.2
270	4.2±0.2	19.0±0.6	2.5±0.2
260	7.3±0.3	22.9±0.6	3.9±0.3
250	10±1	29±2	5.4±0.4

1. $LiClO_4$(0.1020M) with 15C5(0.0506M) in the acetonitrile Solution, P_{Li^+} = 0.504;
2. $LiClO_4$(0.1039M) with 15C5(0.0350M) in the acetonitrile Solution, P_{Li^+} = 0.663;
3. $LiClO_4$(0.1020M) with 15C5(0.0720M) in the acetonitrile Solution, P_{Li^+} = 0.294.

Table 37. The lithium ion mean life times of $LiClO_4$ with 15C5 in nitromethane solutions at different relative concentrations of the salt to the ligand

Temperature	Mean life time τ (s) x 10^4			
K	1	2	3	4
298	1.0±0.1	2.2±0.2	2.7±0.3	0.8±0.2
290	1.2±0.1	3.2±0.2	3.2±0.2	1.1±0.3
282	1.4±0.1	3.7±0.3	3.8±0.2	1.3±0.2
274	1.7±0.2	4.3±0.2	4.6±0.3	1.8±0.2
266	1.9±0.2	4.9±0.2	5.8±0.3	2.4±0.2
258	3.0±0.1	74.±0.2	10.1±0.4	3.1±0.2

1. $LiClO_4$(0.0521M) with 15C5(0.0216M) in the nitromethane solution, P_{Li^+} = 0.586;
2. $LiClO_4$(0.0465M) with 15C5(0.0366M) in the nitromethane solution, P_{Li^+} = 0.215;
3. $LiClO_4$(0.0334M) with 15C5(0.0277M) in the nitromethane solution, P_{Li^+} = 0.170;
4. $LiClO_4$(0.0766M) with 15C5(0.0175M) in the nitromethane solution, P_{Li^+} = 0.772.

Table 38. The decomplexation rate constants of $LiClO_4$ complex by 15C5 in acetonitrile solutions at different temperatures

Temperature (k)	$k_d \times 10^{-3}$
300	2.5 ± 0.4
290	1.9 ± 0.3
280	1.4 ± 0.2
270	1.0 ± 0.1
260	0.7 ± 0.1
250	0.49 ± 0.08

Table 39. The exchange reaction rate constants of $LiClO_4$ complex by 15C5 in nitromethane solutions at different temperatures

Temperature (K)	$k_1 \times 10^{-4}$
298	15 ± 4
290	12 ± 3
282	9 ± 2
274	7 ± 1
266	5.3 ± 0.9
258	4.0 ± 0.6

Table 40. The kinetic information of the exchange reactions of $LiClO_4$ in acetonitrile and nitromethane solutions when 15C5 is present at 298 K

Sol.	K	E_a	$\Delta H^{\ddagger}$	$\Delta S^{\ddagger}$	$\Delta G^{\ddagger}$
AN	$(2.5\pm0.4)\times10^{3}$	4.83±0.01	4.24±0.01	-24.3±0.3	11.45±0.09
NM	$(15\pm4)\times10^{4}$	4.98±0.09	4.39±0.09	-20.1±0.2	10.4±0.2

a. E_a, $\Delta H^{\ddagger}$, and $\Delta G^{\ddagger}$, in units of $kcal\cdot mol^{-1}$; $\Delta S^{\ddagger}$ in the units of $cal\cdot mole^{-1}\cdot K^{-1}$;
b. k: the decomplexation rate constant k_d corresponding to the associative-dissociative mechanism in acetonitrile solutions with the units of s^{-1}; or the exchange reaction rate constant k_1 of the bimolecular exchange mechanism in nitromethane solutions with the units of $s^{-1}\cdot M^{-1}$;
c. AN, NM are abbreviations for acetonitrile and nitromethane respectively.

Table 41. Complexations of some ligands with neutral organic molecules in benzene at 298 K

Host	Guest	Association Constant ($m.f^{-1}$)	Guest	Association Constant ($m.f^{-1}$)
15C5	MeCN	$K_{1:1}$=4.5±0.2	$MeNO_2$	$K_{1:1}$=5.2±0.9
B15C5	MeCN	$K_{1:1}$=5.1±0.6	$MeNO_2$	$K_{1:1}$=2.5±0.6
18C6	MeCN	$K_{1:1}$=12±2 $K_{1:2}$=2.9±0.5	$MeNO_2$	$K_{1:1}$=15±2 $K_{1:2}$=16±3
21C7	MeCN	$K_{1:1}$=13±1		
TG	MeCN	$K_{1:1}$=4.3±0.2	$MeNO_2$	$K_{1:1}$=5.0±0.5
PG	MeCN	$K_{1:1}$=7.1±0.2		

Reference 100
TG: tetraglyme; PG: pentaglyme.

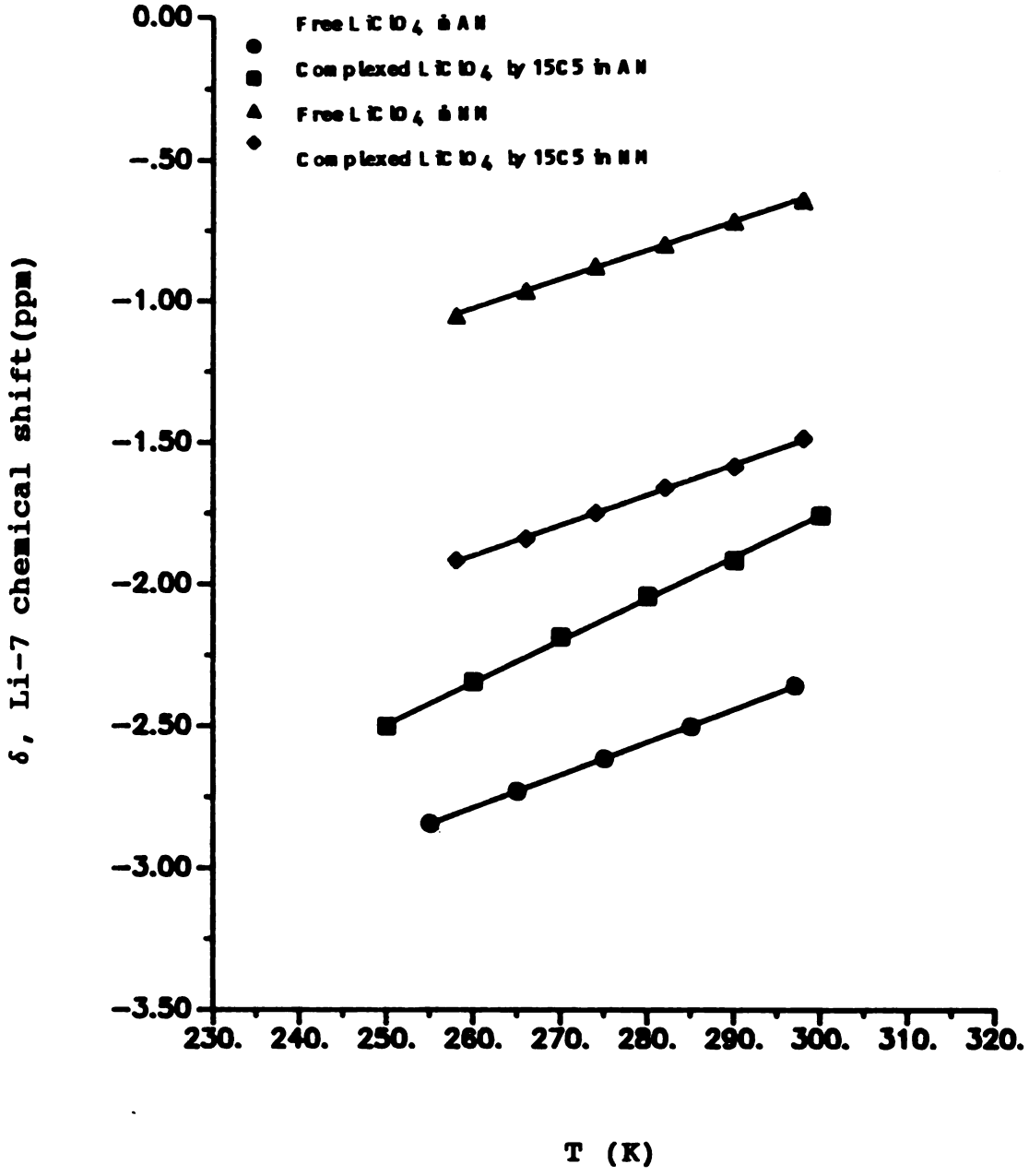

Figure 33. Li-7 chemical shifts of the uncomplexed $LiClO_4$ and the complexed $LiClO_4$ by 15C5 as functions of temperature in acetonitrile and nitromethane solutions
the total $LiClO_4$ concentration: 0.05M

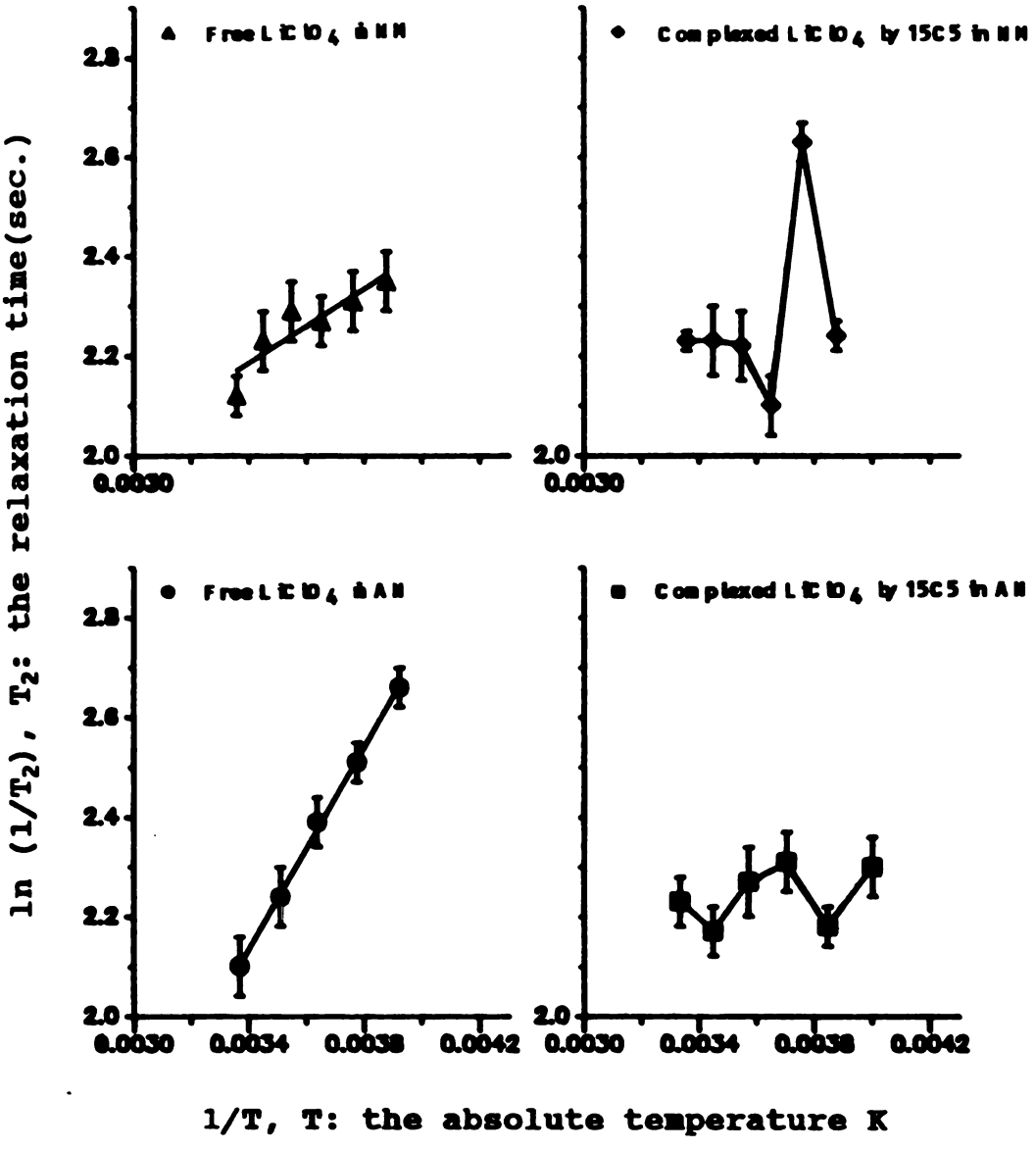

Figure 34. The relaxation rates of Li-7 of the uncomplexed $LiClO_4$ and the complexed $LiClO_4$ by 15C5 as functions of the reciprocal temperature in acetonitrile and nitromethane solutions
the total $LiClO_4$ concentration: 0.05M

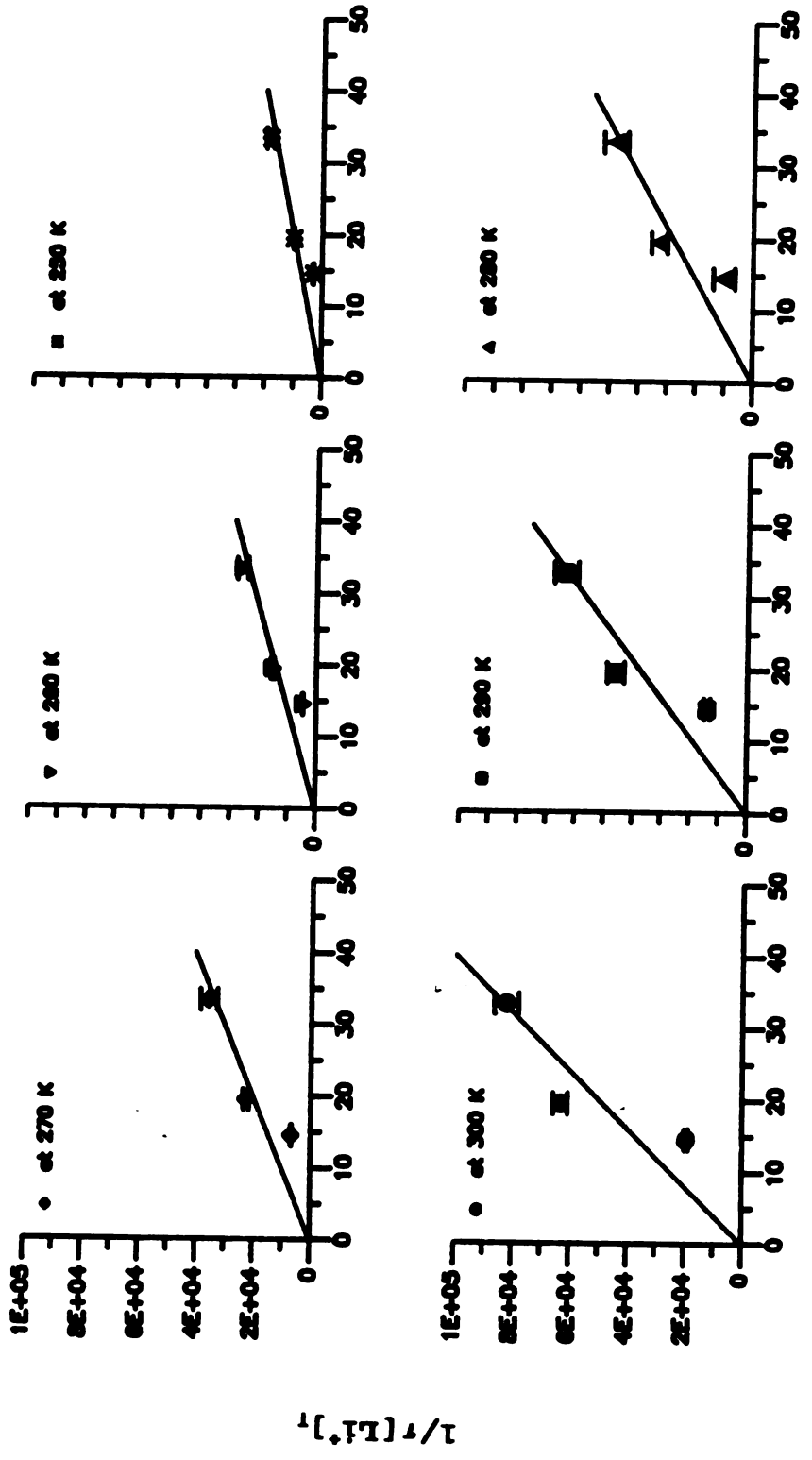

Figure 35. $1/r[Li^+]_I$ vs. $1/[Li^+]_f$ for $LiClO_4$ + 15C5 in acetonitrile solution

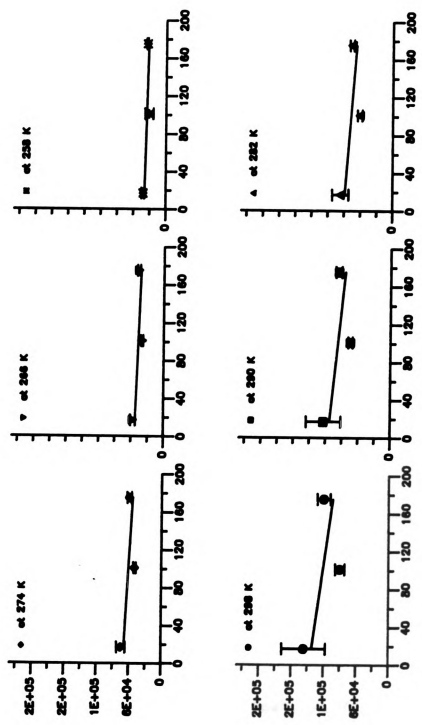

Figure 36. $1/r[Li^+]_T$ vs. $1/[Li^+]_f$ for $LiClO_4$ + 15C5 in nitromethane solution

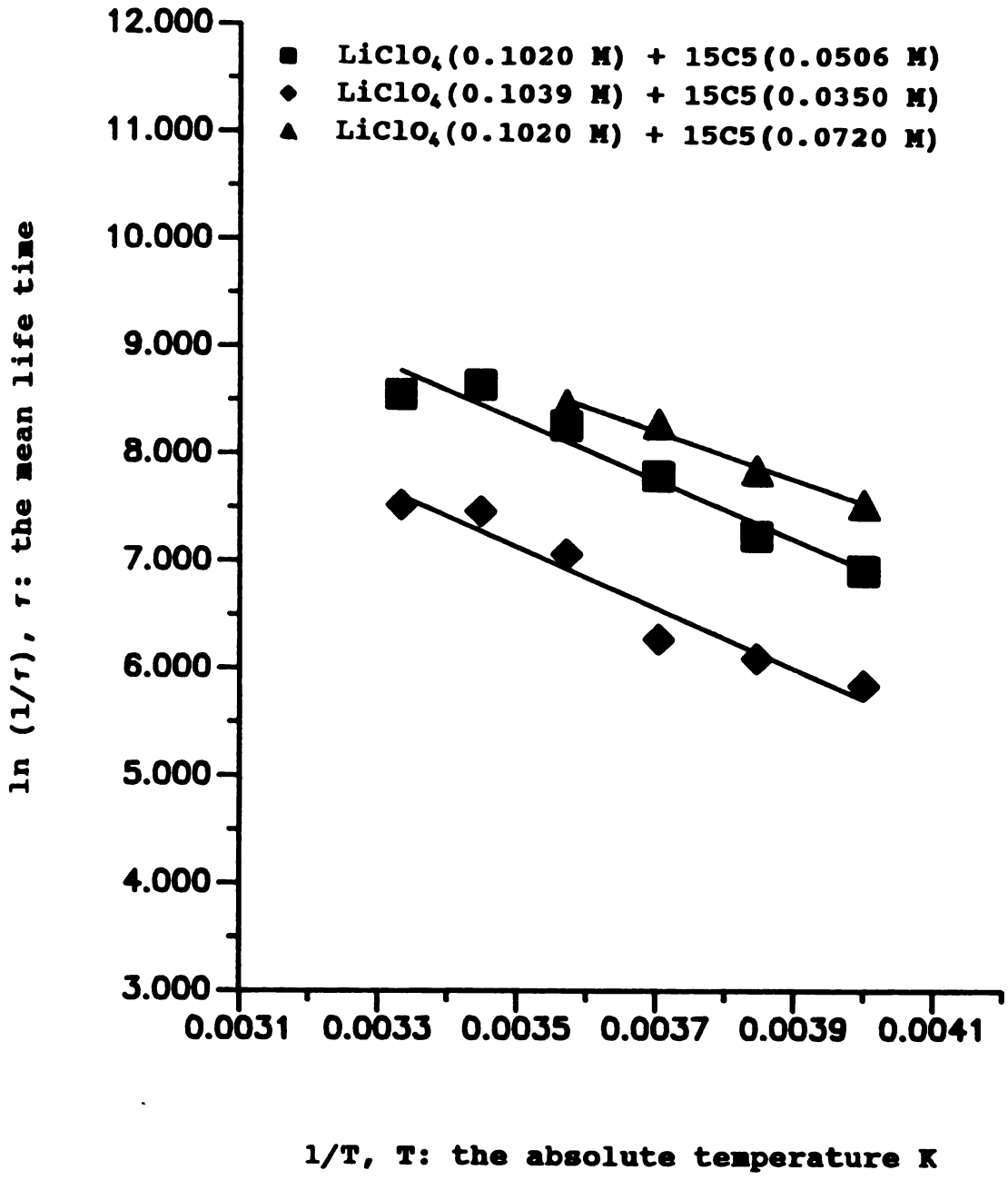

Figure 37. ln (1/τ) against 1/T for the system $LiClO_4$ + 15C5 in acetonitrile solutions

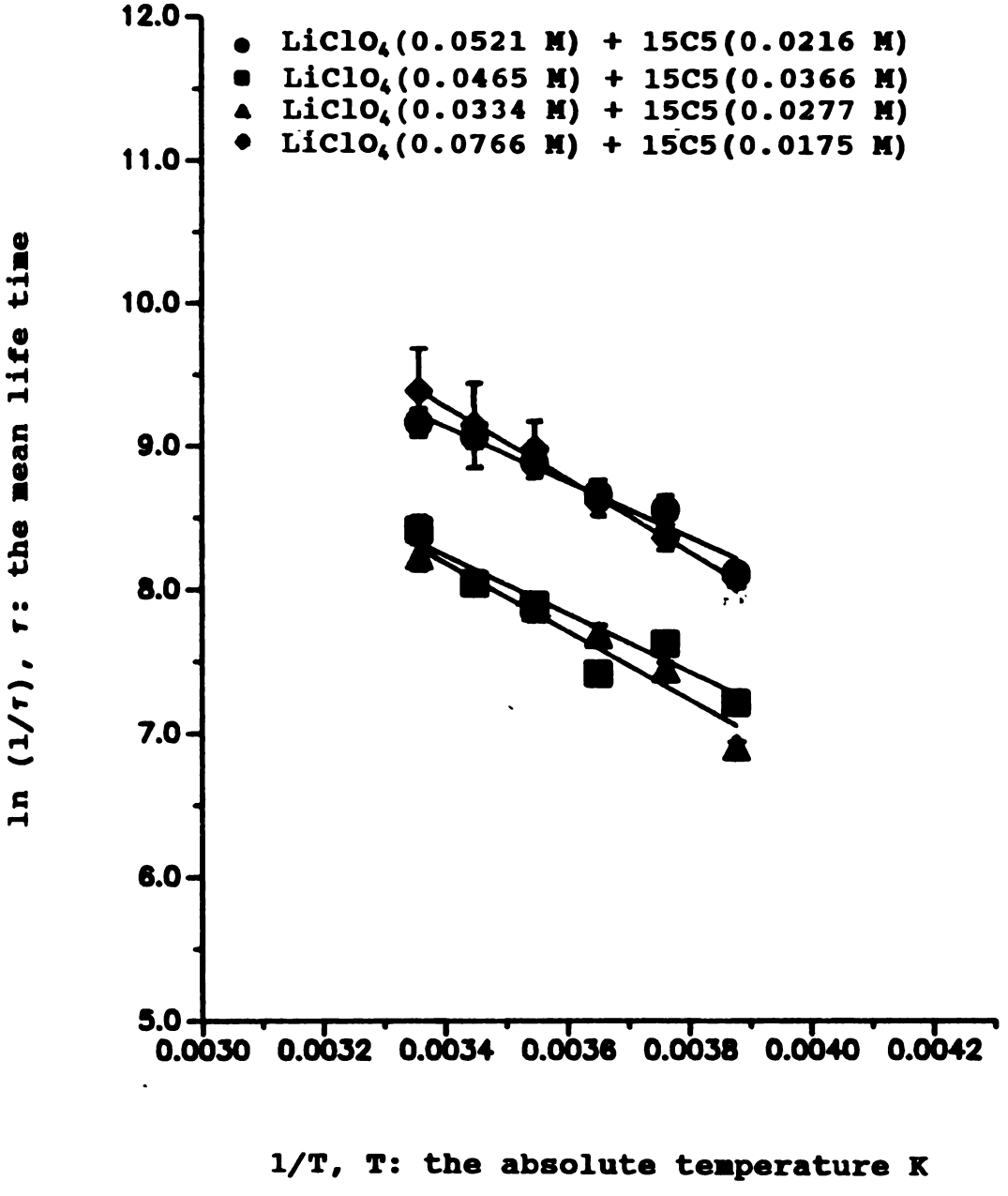

Figure 38. ln (1/τ) against 1/T for the system $LiClO_4$ + 15C5 in nitromethane solutions

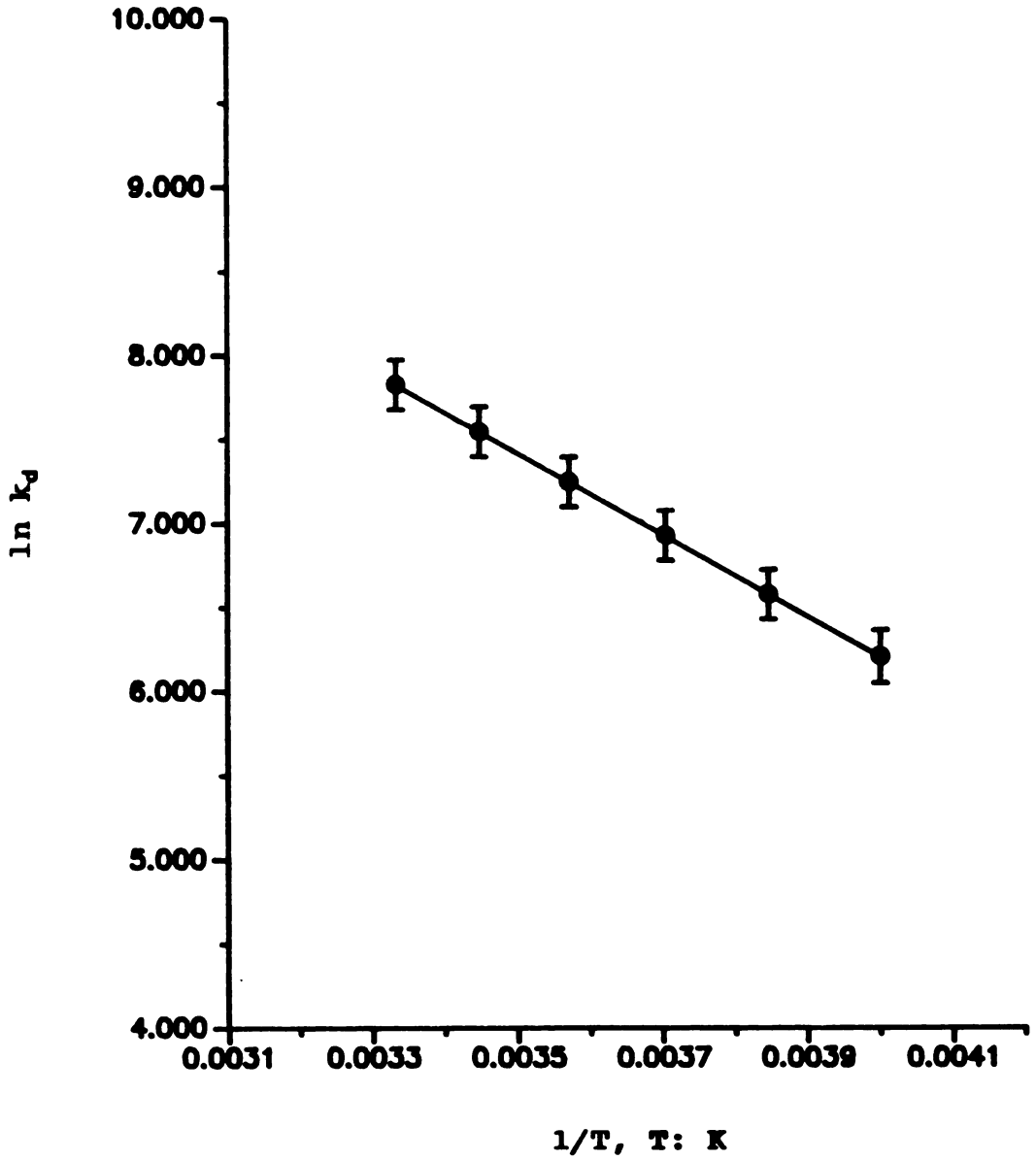

Figure 39. ln k_d against 1/T for the system $LiClO_4$ + 15C5 in acetonitrile solutions

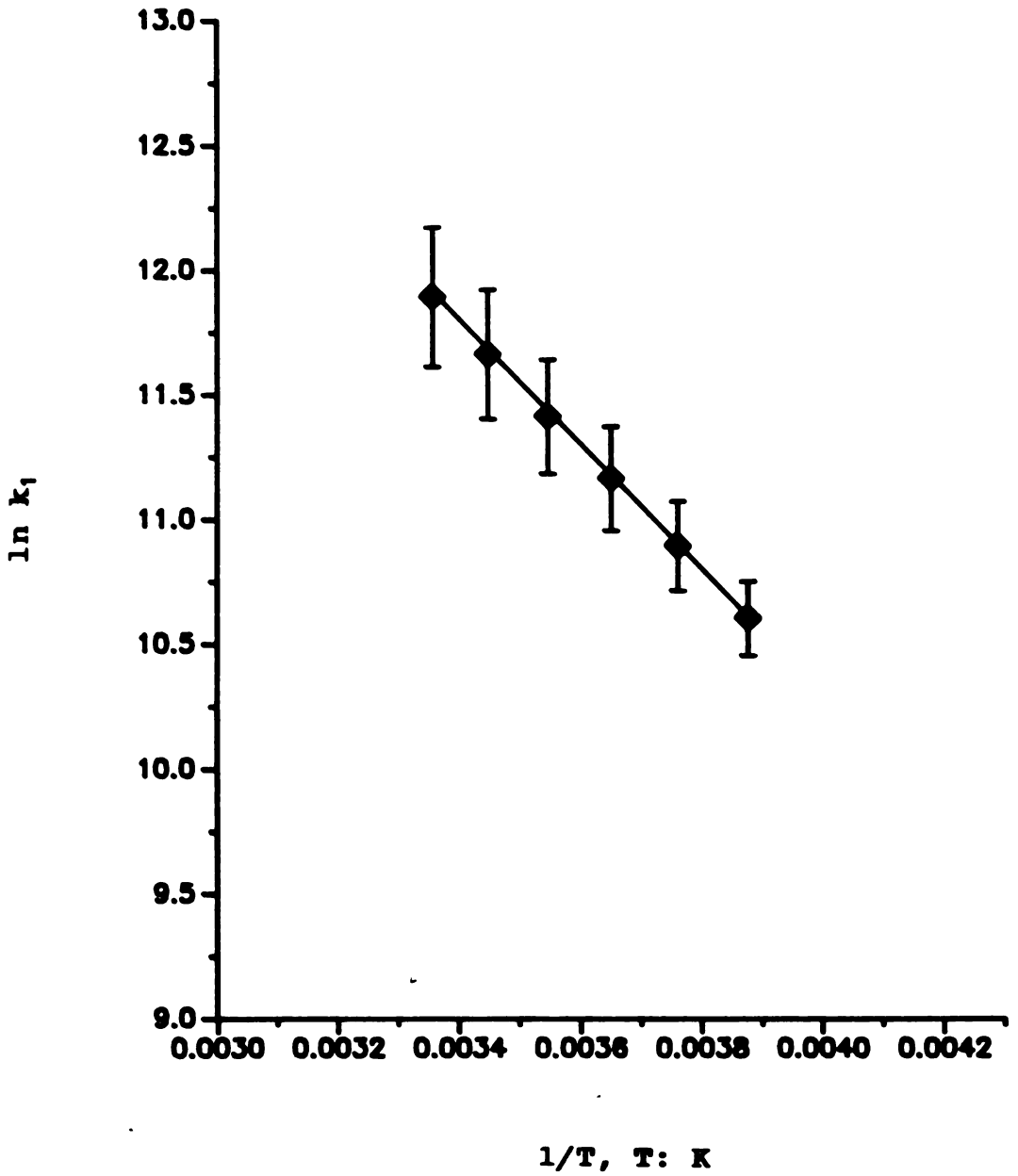

Figure 40. ln k_1 against 1/T for the system $LiClO_4$ + 15C5 in nitromethane solutions

APPENDICES

Appendix A

DATA TRANSFER

Following the next few steps to transfer a data file from the Bruker-180 spectrometer to the VAX system:

1. On the VAX system, open a file that the data are to be transferred:

(T)* RUN [Z]GETNMR

(R)* GETNMR-Version 20-Apr-1987

(R) TARGET FILE: (T)TEST.DAT

2. On Bruker-180, run the data transfer program:

(T) RUN NTCTDL

(R) DATA-TRANSFER PROGRAM VERSION #10903

(R) COMMAND:

(R) BI,BO,CP,AP,AR,KB,LP,LR,MO,TL,TT?

(T) BO

(R) WHAT FORMAT(A=ASCII, B=BINAR)?

(T) A

(R) WHAT PARITY(E, O, M, N)?

(T) N

(R) MAXIMUM RECORD LENGTH = 64 (Return)

(R) PROMPT = (T)12

(R) ENTER TERMINAL MODE (Y, N)?

(T) N(at this point, the data are being transferred)

3. On the VAX system, type '$' to exit the file TEST.DAT. Now the transfer is finished, and the data are stored in a file named TEST.DAT on the VAX system.

4. On Bruker-180, exit the data transfer program.

(R) COMMAND:

(R) BI,BO,CP,AP,AR,KB,LP,LR,MO,TL,TT?

(Y) MO

Data transfer is finished.

*. Throughout the appendix sections, (T) and (R) are used in front of each of the steps to indicate the strings that immediately follow (T) and (R) to be typed(T) by users or to be the response(R) from the computers, when describing the computer operational procedures.

Appendix B

GETNMR.FOR

```
            PROGRAM GETNMR
C=====================================================================
C
C       Title: GETNMR.FOR  -  Get a data set from the Nicolet 180
C
C       Author:  T V Atkinson
C                Chemistry Dept.
C                Michigan State University
C                East Lansing, MI 48824
C
C       DATE: 16-APR-1987
C
C=====================================================================
C
        PARAMETER (MAXREC=80)           ! Maximum length record
C
        INTEGER*2 IOSB(4)               ! QIO return status block
        INTEGER*2 LUNOUT                ! Unit to receive output
        INTEGER*2 IOFUNC                ! OR'ED IOFUNCTION CODE
        INTEGER*2 LUNTI                 ! Unit for TT:
        INTEGER*2 NBYTES                ! Number of bytes in record
        INTEGER*4 STATUS                ! QIO status return
        INTEGER*2 PLCHAN                ! QIO Channel
C
        LOGICAL*1 STRING(80)            ! Input string buffer
        LOGICAL*1 OUTKIN(4)             ! Extension for KINFIT file
        LOGICAL*1 NMRREC(MAXREC)        ! Buffer to receive info from NIC180
        LOGICAL*1 PBUFF(1)              ! Prompt for NIC180
C
        CHARACTER LUNNMR*2/'TT'/        ! Device to NIC180
C
        INCLUDE '($IODEF)'
        INCLUDE '($SSDEF)'
        INTEGER*4 SYS$QIOW,SYS$ASSIGN,SYS$DASSGN
```

```
C
C
      DATA PBUFF/015/, LUNTI/5/, LUNOUT/1/
C
C-----------------------------------------------------------------
C
C       Entry Point
C
C-----------------------------------------------------------------
C
      WRITE (LUNTI,8500)
 8500 FORMAT  (' GETNMR - Version 20-APR-1987')
C
      STATUS = SYS$ASSIGN( LUNNMR, PLCHAN,, ) ! Get a channel.
      IF ( STATUS .NE. 1 ) THEN               ! If failure, then give the
          TYPE 1001                   ! user some idea what it is.
          CALL LIB$SIGNAL( %VAL( STATUS ))    ! Give the VMS official reason
          STOP                                ! and bail out.
          END IF
C
C-----------------------------
C
C       Get file name
C
C-----------------------------
C
      IOFUNC=(IO$M_NOECHO .OR. IO$_READPROMPT)
 50   WRITE (LUNTI,8510)
 8510 FORMAT ('$TARGET FILE: ')
      READ (LUNTI,8000,ERR=50,END=999) LSTRNG,STRING
 8000 FORMAT (Q,80A1)
      STRING(LSTRNG+1) = 0
      OPEN (UNIT=LUNOUT,NAME=STRING,TYPE='NEW',ERR=50,
      1 CARRIAGECONTROL='LIST')
C
C-------------------------------------------------
C
C       Get next record
C
C-------------------------------------------------
C
C     Prompt with PBUFF, read response.
C
```

```
 100    NBYTES = MAXREC
        STATUS = SYS$QIOW( %VAL(3), %VAL(PLCHAN),%VAL(IOFUNC),
        1 %REF(IOSB),,, %REF(NMRREC), %VAL(NBYTES),,, PBUFF, %VAL(1))
                                              ! Read a byte from digitizer.
        IF ( STATUS .NE. 1 ) THEN             ! If failure, then give the
            TYPE 1003                   ! user some idea what it is.
            CALL LIB$SIGNAL( %VAL( STATUS ))  ! Give the VMS official reason
            GOTO 200
            END IF
        NBYTES = IOSB(2)
C
C-----------------------------
C
C       Translate record and store
C
C-----------------------------
C
        IF ( NMRREC(1) .EQ. '$' ) GOTO 200
        WRITE (LUNOUT,8520) (NMRREC(K),K=1,NBYTES)
 8520   FORMAT (80A1)
        GOTO 100
C
C     Invoke the system service $DASSGN to deassign the channel to the
C
 200    STATUS = SYS$DASSGN( %VAL( PLCHAN ))  ! De-assign channel.
        IF ( STATUS .NE. 1 ) THEN             ! If failure, then give the
            TYPE 1000,STATUS                  ! user some idea what it is.
            CALL LIB$SIGNAL( %VAL( STATUS ))  ! Give the VMS official reason
            STOP                              ! and bail out.
            END IF
 999    STOP 'GETNMR'
C
1000  FORMAT (//,' *** Error de-assigning the Nicolet 180: ***')
1001  FORMAT (//,' *** Error assigning the Nicolet 180:')
1003  FORMAT (//,' *** Error in prompted-read from Nicolet 180:')
1006  FORMAT (' IOSB=',4I7)
      END
```

Appendix C

Data Transformation

A data file can be transformed into a KINFIT workable format by doing the following:

(T) RUN [Z]NIC180

(R) NIC180 (Version:21-Jan-1986)

(R) Should the output be in KINFIT Format?[Y/N] (T)Y

(R) Input File: (T)TEST.DAT

(R) NSKIP,XVAR,YVAR:(T)0,0.000001,1

(R) XINIT,XDELTA[D:0,1]: (T)-21.000,9.800

(R) 88 points are transformed.(Transformation is done.)

When running this program, a few parameters need to be provided by users: NSKIP is the number of data from the input data file to be skipped; XVAR and YVAR are the variances of data in x and y; XINIT and XDELTA are the initial value of the data file and the interval between each data point respectively in frequency(hz). In this example, no points(0) were skipped and the variances in x and y are 0.000001 and 1 respectively, the frequency for the first data point of the file was -21.000 hz and the interval between each point was 9.800 hz.

Appendix D

NIC180--Data formatting programs

```
$ !=====================================================================
$ !
$ !     NIC180.COM  -  Build NIC180, a program for reformatting NMR data
$ !
$ !     T V Atkinson
$ !     Department of Chemistry
$ !     Michigan State University
$ !     East Lansing, MI 48824
$ !
$ !     Date: 03-JUL-85
$ !
$ !=====================================================================
$ !
$ COMPOPT :== /LIST/NOI4
$ LINKOPT :== /MAP
$ DELETE DIRVMS.LIS;*,DIRVMS.OBJ;*
$ FORTRAN'COMPOPT' DIRVMS
$ DELETE NIC180.LIS;*,NIC180.OBJ;*
$ FORTRAN'COMPLIST' NIC180
$ DELETE NIC180.MAP;*,NIC180.EXE;*
$ LINK'LINKOPT' NIC180,DIRVMS

               PROGRAM NIC180
C=====================================================================
C
C       Title: NIC180.FTN  -  Process data from Nicolet 180 NMR
C
C       Author:  T V Atkinson
C                Chemistry Dept.
C                Michigan State University
C                East Lansing, MI 48824
C
C       DATE: 18-JUL-85
C
```

```
C=====================================================================
C
C
C       variable definitions
C
        LOGICAL*1 STRING(80)            ! Input string buffer
        LOGICAL*1 OUTKIN(4)             ! Extension for KINFIT file
        LOGICAL*1 OUTEXT(4)             ! Extention for MULPLT file
        LOGICAL*1 INDDIR
        LOGICAL*1 BLANK
        LOGICAL*1 ICR
        LOGICAL*1 ATSIGN
        LOGICAL*1 PERIOD
        LOGICAL*1 KINFIT
        LOGICAL*1 COMMA
        LOGICAL*1 ICY                   ! ASCII "Y"
        LOGICAL*1 ICYLC                 ! ASCII "y"
        LOGICAL*1 IGNORE                ! Flag for ignore this line
        LOGICAL*1 DOLLAR                ! ASCII "$"
C
        INTEGER*2 NPLINE                ! Number of data points per line
        INTEGER*2 NPOINT                ! Number of points loaded
        INTEGER*2 MAXPNT                ! Maximum number of points allowed
C
        REAL*4 YDATA(1000)              ! Array to hold y data
C
        DATA LUNTI,LUNIN,LUNOUT,LUNDIR/5,1,2,3/
        DATA BLANK/"40/, ICR/"15/, ATSIGN/1H

        DATA OUTKIN/'K','I','N',' '/, OUTEXT/'N','M','R',' '/
        DATA PERIOD/'.'/, ICY/'Y'/, ICYLC/'y'/
        DATA COMMA/','/,DOLLAR/'$'/
        DATA NPLINE/8/,MAXPNT/1000/
C
C---------------------------------------------------------------------
C
C       Entry Point
C
C---------------------------------------------------------------------
C
        WRITE (LUNTI,8500)
C
C---------------------------------------------------------------------
```

```
C
C       command point
C
C-------------------------------------------------------------------
C
 100    WRITE (LUNTI,8510)
        READ (LUNTI,8000,ERR=320,END=320) LSTRNG,STRING
        KINFIT = (STRING(1) .EQ. ICY) .OR. (STRING(1) .EQ. ICYLC)
C
        WRITE (LUNTI,8530)
        READ (LUNTI,8000,ERR=320,END=320) LSTRNG,STRING
        IF (.NOT. KINFIT) GO TO 110
C
        WRITE (LUNTI,8540)
        READ  (LUNTI,8550,END=320) NSKIP,XVAR,YVAR
        IF (NSKIP .LT. 0) NSKIP = 0
        INCR1 = NSKIP + 1
        INCR2 = 2*INCR1
 110    CONTINUE
C
C-------------------------------------------------------------------
C
C       Setup for a list of files
C
C-------------------------------------------------------------------
C
 120    INDDIR = STRING(1) .EQ. ATSIGN
        IF (.NOT.INDDIR) GO TO 140
        CALL DIRVMS(0,LUNDIR,LUNEL,STRING(2),LSTRNG-1,LDEVN,LVERS,IERR)
        IF (IERR.NE.0) GO TO 310
C
C-----------------------------
C
C       Process the next file
C
C-----------------------------
C
 130    CALL DIRVMS (1,LUNDIR,LUNEL,STRING,LSTRNG,LDEVN,LVERS,IERR)
        IF (IERR.EQ.-1) GO TO 230
        IF (IERR.GT.0) GO TO 310
        IF (INDDIR) WRITE (LUNTI,8560) (STRING(K),K=1,LSTRNG)
C
 140    WRITE (LUNTI,8570)
```

```
      READ  (LUNTI,8020,END=320) XINIT,XDELTA
      IF (XDELTA .EQ. 0.0) XDELTA = 1.0
C
 150  STRING(LSTRNG+1) = 0
      OPEN (UNIT=LUNIN,NAME=STRING,TYPE='OLD',ERR=210,
     1 CARRIAGECONTROL='LIST',READONLY)
      K1 = -NPLINE + 1
C
C-----------------------------
C
C     Change the extention
C
C-----------------------------
C
C     Parse the file spec
C
      DO 160 I=1,LSTRNG
 160  IF (STRING(I) .EQ. PERIOD) IPER = I
      I1 = IPER + 1
      I2 = IPER + 3
      J = 0
C
C     Put in ".NMR"
C
      IF (KINFIT) GO TO 180
      DO 170 I=I1,I2
      J = J + 1
 170  STRING(I) = OUTEXT(J)
      GOTO 200
C
C     Put in ".KIN"
C
 180  DO 190 I=I1,I2
      J = J + 1
 190  STRING(I) = OUTKIN(J)
C
 200  OPEN (UNIT=LUNOUT,NAME=STRING,TYPE='NEW',ERR=220,
      1 CARRIAGECONTROL='LIST')
C
C-------------------------------------------------------------------
C
C     Process the next record
C
```

```
C-----------------------------------------------------------------------
C
 240    READ (LUNIN,8000,END=300) LSTRN,STRING
C
C       Discard null lines
C
        IGNORE = .FALSE.
        DO 241 I=1,LSTRN
        IF (STRING(I) .EQ. DOLLAR) IGNORE = .TRUE.
 241    CONTINUE
        IF (IGNORE) GOTO 240
        IF (LSTRN .LE. 0) GOTO 240
C
C       Convert extraneous <CR> to blank
C
        DO 250 I=1,80
 250    IF (STRING(I) .EQ. ICR) STRING(I) = BLANK
C
C       Find end of line
C
        DO 260 I=1,80
        NCHAR = 80 - I + 1
        IF (STRING(NCHAR) .NE. BLANK) GO TO 270
 260    CONTINUE
C
C       Convert spaces to commas
C
 270    DO 265 I=1,NCHAR
        IF (STRING(I) .EQ. BLANK) STRING(I) = COMMA
 265    CONTINUE
C
C       Decode and Load into YDATA
C
        K1 = K1 + NPLINE
        IF (K1 .GT. MAXPNT) GOTO 299
        NPOINT = MIN0( (K1 + NPLINE - 1), MAXPNT)
        DECODE (NCHAR,8020,STRING) (YDATA(K),K=K1,NPOINT)
        GOTO 240
C
C       Data load terminated due to overflow
C
 299    WRITE (LUNTI,8685)
C
```

```
C       End of input file
C
 300    CLOSE (UNIT=LUNIN)
        WRITE (LUNTI,8680) NPOINT
C
C-----------------------------
C
C       Write a MULPLT file
C
C-----------------------------
C
        IF (KINFIT) GO TO 280
        DO 1310 I=1,NPOINT
        X1 = XINIT + I*XDELTA
 1310   WRITE (LUNOUT,8620) X1,YDATA(I)
        GOTO 400
C
C-----------------------------
C
C       Write a KINFIT file
C
C-----------------------------
C
 280    DO 1350 I=1,NPOINT,INCR2
        I2 = I + INCR1
        X1 = XINIT + I*XDELTA
        X2 = XINIT + I2*XDELTA
        WRITE (LUNOUT,8630) X1,XVAR,YDATA(I),YVAR,X2,XVAR,YDATA(I2)
        1,YVAR
 1350   CONTINUE
C
C-----------------------------
C
C       End of output file
C
C-----------------------------
C
 400    CLOSE (UNIT=LUNOUT)
        IF (INDDIR) GOTO 130
        GOTO 100
C
C       End of all files
C
```

```
 310    CLOSE (UNIT=LUNDIR)
        GOTO 100
C
C-----------------------------------------------------------------
C
C       STOP
C
C-----------------------------------------------------------------
C
 320    STOP 'NIC180'
C
C-----------------------------------------------------------------
C
C       Error Handlers
C
C-----------------------------------------------------------------
C
 210    WRITE (LUNTI,8580) (STRING(I),I=1,LSTRNG)
        GOTO 310
 220    WRITE (LUNTI,8590) (STRING(I),I=1,LSTRNG)
        GOTO 310
 230    WRITE (LUNTI,8600)
        GO TO 310
C
C-----------------------------------------------------------------------
C
C       Formats
C
C-----------------------------------------------------------------------
C
 8000   FORMAT (Q,80A1)
 8020   FORMAT (10F16.0)
C
 8500   FORMAT (//' NIC180  (Version: 21-JAN-1986)')
 8510   FORMAT ('$Should the output be in KINFIT format? [Y/N]')
 8530   FORMAT('$INPUT FILE: ')
 8540   FORMAT ('$NSKIP,XVAR,YVAR: ')
 8550   FORMAT (I8,2E15.0)
 8560   FORMAT (1X,80A1)
 8570   FORMAT ('$XINIT,XDELTA [D: 0,1]: ')
 8580   FORMAT(' Can''t open input file: ',80A1)
 8590   FORMAT(' Can''t open output file: ',80A1)
 8600   FORMAT (' Error in DIRVMS')
```

```
8620   FORMAT ('RD ',F10.3,',',F10.0)
8630   FORMAT (4(F10.3,',',E10.3,','))
8680   FORMAT (' Number of points loaded: ',I8)
8685   FORMAT (' Data load truncated - Too many points: ')
       END
```

Appendix E

EXAMPLES OF DATA FILES

E.1 TEST.DAT

```
10588 11022 11388 11613 11738 11933 12367 13071
13914 14789 15650 16469 17248 18072 19079 20322
21752 23296 24888 26431 27906 29511 31528 34054
36991 40311 44152 48584 53553 59044 65161 71950
79385 87556 96737 107105 118731 131830 146742 163635
182572 203707 226285 246743 258716 256744 240785 216394
190559 167451 147892 131437 117685 106130 96050 86965
78831 71677 65350 59705 54735 50395 46571 43188
40214 37566 35105 32803 30722 28848 27111 25555
24282 23247 22200 20983 19602 18133 16677 15470
14780 14559 14399 13918 13100 12190 11397 10815
```

This is the digitized format of the intensity of an NMR signal of the species undergoing the exchange reactions, transferred from the Bruker-180 spectrometer. In order to perform KINFIT, this data file has to be rewritten into a KINFIT readable file by adding the frequency intervals between each data point, and variances in frequency and intensity. This is done by running NIC180 program described in Appendix C. The result of this data transformation is shown in TEST.KIN in the next section.

E.2 TEST.KIN

```
      -7.320, 0.100E-05, 10588.000, 0.100E+01,    -9.760, 0.100E-05, 11022.000, 0.
100E+01,
   -12.200, 0.100E-05, 11388.000, 0.100E+01,   -14.640, 0.100E-05, 11613.000, 0.
100E+01,
   -17.080, 0.100E-05, 11738.000, 0.100E+01,   -19.520, 0.100E-05, 11933.000, 0.
100E+01,
   -21.960, 0.100E-05, 12367.000, 0.100E+01,   -24.400, 0.100E-05, 13071.000, 0.
100E+01,
   -26.840, 0.100E-05, 13914.000, 0.100E+01,   -29.280, 0.100E-05, 14789.000, 0.
100E+01,
   -31.720, 0.100E-05, 15650.000, 0.100E+01,   -34.160, 0.100E-05, 16469.000, 0.
100E+01,
   -36.600, 0.100E-05, 17248.000, 0.100E+01,   -39.040, 0.100E-05, 18072.000, 0.
100E+01,
   -41.480, 0.100E-05, 19079.000, 0.100E+01,   -43.920, 0.100E-05, 20322.000, 0.
100E+01,
   -46.360, 0.100E-05, 21752.000, 0.100E+01,   -48.800, 0.100E-05, 23296.000, 0.
100E+01,
   -51.240, 0.100E-05, 24888.000, 0.100E+01,   -53.680, 0.100E-05, 26431.000, 0.
100E+01,
   -56.120, 0.100E-05, 27906.000, 0.100E+01,   -58.560, 0.100E-05, 29511.000, 0.
100E+01,
   -61.000, 0.100E-05, 31528.000, 0.100E+01,   -63.440, 0.100E-05, 34054.000, 0.
100E+01,
   -65.880, 0.100E-05, 36991.000, 0.100E+01,   -68.320, 0.100E-05, 40311.000, 0.
100E+01,
   -70.760, 0.100E-05, 44152.000, 0.100E+01,   -73.200, 0.100E-05, 48584.000, 0.
100E+01,
   -75.640, 0.100E-05, 53553.000, 0.100E+01,   -78.080, 0.100E-05, 59044.000, 0.
100E+01,
   -80.520, 0.100E-05, 65161.000, 0.100E+01,   -82.960, 0.100E-05, 71950.000, 0.
100E+01,
   -85.400, 0.100E-05, 79385.000, 0.100E+01,   -87.840, 0.100E-05, 87556.000, 0.
100E+01,
   -90.280, 0.100E-05, 96737.000, 0.100E+01,   -92.720, 0.100E-05,107105.000, 0.
100E+01,
   -95.160, 0.100E-05,118731.000, 0.100E+01,   -97.600, 0.100E-05,131830.000, 0.
100E+01,
  -100.040, 0.100E-05,146742.000, 0.100E+01,  -102.480, 0.100E-05,163635.000, 0.
```

```
100E+01,
  -104.920, 0.100E-05,182572.000, 0.100E+01,  -107.360, 0.100E-05,203707.000, 0.
100E+01,
  -109.800, 0.100E-05,226285.000, 0.100E+01,  -112.240, 0.100E-05,246743.000, 0.
100E+01,
  -114.680, 0.100E-05,258716.000, 0.100E+01,  -117.120, 0.100E-05,256744.000, 0.
100E+01,
  -119.560, 0.100E-05,240785.000, 0.100E+01,  -122.000, 0.100E-05,216394.000, 0.
100E+01,
  -124.440, 0.100E-05,190559.000, 0.100E+01,  -126.880, 0.100E-05,167451.000, 0.
100E+01,
  -129.320, 0.100E-05,147892.000, 0.100E+01,  -131.760, 0.100E-05,131437.000, 0.
100E+01,
  -134.200, 0.100E-05,117685.000, 0.100E+01,  -136.640, 0.100E-05,106130.000, 0.
100E+01,
  -139.080, 0.100E-05, 96050.000, 0.100E+01,  -141.520, 0.100E-05, 86965.000, 0.
100E+01,
  -143.960, 0.100E-05, 78831.000, 0.100E+01,  -146.400, 0.100E-05, 71677.000, 0.
100E+01,
  -148.840, 0.100E-05, 65350.000, 0.100E+01,  -151.280, 0.100E-05, 59705.000, 0.
100E+01,
  -153.720, 0.100E-05, 54735.000, 0.100E+01,  -156.160, 0.100E-05, 50395.000, 0.
100E+01,
  -158.600, 0.100E-05, 46571.000, 0.100E+01,  -161.040, 0.100E-05, 43188.000, 0.
100E+01,
  -163.480, 0.100E-05, 40214.000, 0.100E+01,  -165.920, 0.100E-05, 37566.000, 0.
100E+01,
  -168.360, 0.100E-05, 35105.000, 0.100E+01,  -170.800, 0.100E-05, 32803.000, 0.
100E+01,
  -173.240, 0.100E-05, 30722.000, 0.100E+01,  -175.680, 0.100E-05, 28848.000, 0.
100E+01,
  -178.120, 0.100E-05, 27111.000, 0.100E+01,  -180.560, 0.100E-05, 25555.000, 0.
100E+01,
  -183.000, 0.100E-05, 24282.000, 0.100E+01,  -185.440, 0.100E-05, 23247.000, 0.
100E+01,
  -187.880, 0.100E-05, 22200.000, 0.100E+01,  -190.320, 0.100E-05, 20983.000, 0.
100E+01,
  -192.760, 0.100E-05, 19602.000, 0.100E+01,  -195.200, 0.100E-05, 18133.000, 0.
100E+01,
  -197.640, 0.100E-05, 16677.000, 0.100E+01,  -200.080, 0.100E-05, 15470.000, 0.
100E+01,
  -202.520, 0.100E-05, 14780.000, 0.100E+01,  -204.960, 0.100E-05, 14559.000, 0.
100E+01,
```

```
  -207.400, 0.100E-05, 14399.000, 0.100E+01,  -209.840, 0.100E-05, 13918.000, 0.
100E+01,
  -212.280, 0.100E-05, 13100.000, 0.100E+01,  -214.720, 0.100E-05, 12190.000, 0.
100E+01,
  -217.160, 0.100E-05, 11397.000, 0.100E+01,  -219.600, 0.100E-05, 10815.000, 0.
100E+01,
```

For the full-line-shape-analysis by KINFIT, additional information needs to be supplied, and the name of the data file has to be changed to TESTK.DAT. See the next section.

E.3 TESTK.DAT

```
88, ,20,  ,  ,  ,  , 8, .00001
LISN231N.DAT. 0.0262M LITPB/0.0064M 15C5/AN AT 299K.
.7574, .0215, -791.248, .2426,.0149, -456.344, 250.0E-6, 47.1239
0.308939E+08, 0.397078E+04, -0.434963E-01, -0.806E+02, 0.116403E-02
    -7.320, 0.100E-05, 10588.000, 0.100E+01,    -9.760, 0.100E-05, 11022.000, 0.
100E+01,
   -12.200, 0.100E-05, 11388.000, 0.100E+01,   -14.640, 0.100E-05, 11613.000, 0.
100E+01,
   -17.080, 0.100E-05, 11738.000, 0.100E+01,   -19.520, 0.100E-05, 11933.000, 0.
100E+01,
   -21.960, 0.100E-05, 12367.000, 0.100E+01,   -24.400, 0.100E-05, 13071.000, 0.
100E+01,
   -26.840, 0.100E-05, 13914.000, 0.100E+01,   -29.280, 0.100E-05, 14789.000, 0.
100E+01,
   -31.720, 0.100E-05, 15650.000, 0.100E+01,   -34.160, 0.100E-05, 16469.000, 0.
100E+01,
   -36.600, 0.100E-05, 17248.000, 0.100E+01,   -39.040, 0.100E-05, 18072.000, 0.
100E+01,
   -41.480, 0.100E-05, 19079.000, 0.100E+01,   -43.920, 0.100E-05, 20322.000, 0.
100E+01,
   -46.360, 0.100E-05, 21752.000, 0.100E+01,   -48.800, 0.100E-05, 23296.000, 0.
100E+01,
   -51.240, 0.100E-05, 24888.000, 0.100E+01,   -53.680, 0.100E-05, 26431.000, 0.
100E+01,
   -56.120, 0.100E-05, 27906.000, 0.100E+01,   -58.560, 0.100E-05, 29511.000, 0.
100E+01,
   -61.000, 0.100E-05, 31528.000, 0.100E+01,   -63.440, 0.100E-05, 34054.000, 0.
100E+01,
   -65.880, 0.100E-05, 36991.000, 0.100E+01,   -68.320, 0.100E-05, 40311.000, 0.
100E+01,
   -70.760, 0.100E-05, 44152.000, 0.100E+01,   -73.200, 0.100E-05, 48584.000, 0.
100E+01,
   -75.640, 0.100E-05, 53553.000, 0.100E+01,   -78.080, 0.100E-05, 59044.000, 0.
100E+01,
   -80.520, 0.100E-05, 65161.000, 0.100E+01,   -82.960, 0.100E-05, 71950.000, 0.
100E+01,
   -85.400, 0.100E-05, 79385.000, 0.100E+01,   -87.840, 0.100E-05, 87556.000, 0.
```

```
100E+01,
   -90.280, 0.100E-05, 96737.000, 0.100E+01,   -92.720, 0.100E-05,107105.000, 0.
100E+01,
   -95.160, 0.100E-05,118731.000, 0.100E+01,   -97.600, 0.100E-05,131830.000, 0.
100E+01,
  -100.040, 0.100E-05,146742.000, 0.100E+01,  -102.480, 0.100E-05,163635.000, 0.
100E+01,
  -104.920, 0.100E-05,182572.000, 0.100E+01,  -107.360, 0.100E-05,203707.000, 0.
100E+01,
  -109.800, 0.100E-05,226285.000, 0.100E+01,  -112.240, 0.100E-05,246743.000, 0.
100E+01,
  -114.680, 0.100E-05,258716.000, 0.100E+01,  -117.120, 0.100E-05,256744.000, 0.
100E+01,
  -119.560, 0.100E-05,240785.000, 0.100E+01,  -122.000, 0.100E-05,216394.000, 0.
100E+01,
  -124.440, 0.100E-05,190559.000, 0.100E+01,  -126.880, 0.100E-05,167451.000, 0.
100E+01,
  -129.320, 0.100E-05,147892.000, 0.100E+01,  -131.760, 0.100E-05,131437.000, 0.
100E+01,
  -134.200, 0.100E-05,117685.000, 0.100E+01,  -136.640, 0.100E-05,106130.000, 0.
100E+01,
  -139.080, 0.100E-05, 96050.000, 0.100E+01,  -141.520, 0.100E-05, 86965.000, 0.
100E+01,
  -143.960, 0.100E-05, 78831.000, 0.100E+01,  -146.400, 0.100E-05, 71677.000, 0.
100E+01,
  -148.840, 0.100E-05, 65350.000, 0.100E+01,  -151.280, 0.100E-05, 59705.000, 0.
100E+01,
  -153.720, 0.100E-05, 54735.000, 0.100E+01,  -156.160, 0.100E-05, 50395.000, 0.
100E+01,
  -158.600, 0.100E-05, 46571.000, 0.100E+01,  -161.040, 0.100E-05, 43188.000, 0.
100E+01,
  -163.480, 0.100E-05, 40214.000, 0.100E+01,  -165.920, 0.100E-05, 37566.000, 0.
100E+01,
  -168.360, 0.100E-05, 35105.000, 0.100E+01,  -170.800, 0.100E-05, 32803.000, 0.
100E+01,
  -173.240, 0.100E-05, 30722.000, 0.100E+01,  -175.680, 0.100E-05, 28848.000, 0.
100E+01,
  -178.120, 0.100E-05, 27111.000, 0.100E+01,  -180.560, 0.100E-05, 25555.000, 0.
100E+01,
  -183.000, 0.100E-05, 24282.000, 0.100E+01,  -185.440, 0.100E-05, 23247.000, 0.
100E+01,
  -187.880, 0.100E-05, 22200.000, 0.100E+01,  -190.320, 0.100E-05, 20983.000, 0.
100E+01,
```

```
 -192.760, 0.100E-05, 19602.000, 0.100E+01,  -195.200, 0.100E-05, 18133.000, 0.
100E+01,
 -197.640, 0.100E-05, 16677.000, 0.100E+01,  -200.080, 0.100E-05, 15470.000, 0.
100E+01,
 -202.520, 0.100E-05, 14780.000, 0.100E+01,  -204.960, 0.100E-05, 14559.000, 0.
100E+01,
 -207.400, 0.100E-05, 14399.000, 0.100E+01,  -209.840, 0.100E-05, 13918.000, 0.
100E+01,
 -212.280, 0.100E-05, 13100.000, 0.100E+01,  -214.720, 0.100E-05, 12190.000, 0.
100E+01,
 -217.160, 0.100E-05, 11397.000, 0.100E+01,  -219.600, 0.100E-05, 10815.000, 0.
100E+01,
```

This is the final complete version of the data file that is to be fitted to a two-site exchange equation by running KINFIT program to derive the best estimate of τ along with some other parameters. The top line is equivalent to the control card given in the older version of KINFIT. It contains information such as the number of points(88), the maximum number of iterations allowed before convergence(20), the number of constants that are to be read for the equation to fit the data(8), the maximum value of Δparameter/parameter for convergence(0.00001), Δparameter is the change in the parameter from one iteration to the next). The second line is the title of the file, which can be any information desired by users. The third and the last line are the constants and the estimates of the parameters to be fitted, the orders of which are in accordance with that given in NMR2siteb subroutine(see Appendix H).

Appendix F

KINBLD.COM

```
$ !=========================================================================
$ !
$ !     KINFIT:KINBLD.COM  -  Submit a batch job to build a KINFIT prog.
$ !
$ !     T V Atkinson
$ !     Department of Chemistry
$ !     Michigan State University
$ !     East Lansing, MI 48824
$ !
$ !     Date: 08-MAY-1987
$ !
$ !=========================================================================
$ !
$ HERE  := 'F$LOGICAL("SYS$DISK")''F$DIRECTORY()'
$ SET DEF 'HERE'
$ JNAME ="KIN_"+F$EXTRACT(0,5,P1)
$ LENFN = F$LOCATE(".",P1)
$ FILNAME = F$EXTRACT(0,LENFN,P1)
$ FN      = FILNAME
$ SET MESSAGE/NOID/NOFACILITY/NOSEV/NOTEXT
$ DELETE 'FILNAME'.LOG;*,'FILNAME'.JOB;*
$ SET MESSAGE/ID/FACILITY/SEV/TEXT
$ OPEN/WRITE TEMPFILE 'FILNAME'.JOB
$ WRITE TEMPFILE "$ ! Temporary file for building  KINFIT"
$ WRITE TEMPFILE "$ SET DEF ",HERE
$ WRITE TEMPFILE "$ SET MESSAGE/NOID/NOFACILITY/NOSEV/NOTEXT"
$ WRITE TEMPFILE "$ DELETE ",FN,".OBJ;*,",FN,".EXE;*,",FN,".LIS;*"
$ WRITE TEMPFILE "$ SET MESSAGE/ID/FACILITY/SEV/TEXT
$ WRITE TEMPFILE "$ FORTRAN/LIST ",P1
$ WRITE TEMPFILE "$ LINK/MAP=",FN,"/EXE=",FN," KINFIT:VAXKINFIT,",HERE,FN
$ CLOSE TEMPFILE
$ SUBMIT/QUEUE=KINFITQ/LOG='HERE''FILNAME'.LOG/NOPRINTER/NOTIFY/NAME='JNAME'-
  'FILNAME'.JOB
```

Appendix G

KINRUN.COM

```
$ !=================================================================
$ !
$ !     KINFIT:KINRUN.COM  -  Submit a batch job to run a KINFIT prog.
$ !
$ !     T V Atkinson
$ !     Department of Chemistry
$ !     Michigan State University
$ !     East Lansing, MI 48824
$ !
$ !     Date: 31-SEP-86
$ !
$ !-----------------------------------------------------------------
$ !
$ !     Usage:
$ !
$ !             $ KINRUN eqn dataset
$ !
$ !     where "eqn" is the name of the EQN to be used, and "dataset" is
$ !     the name of the file containing the data set.
$ !
$ !=================================================================
$ !
$ HERE  := 'F$LOGICAL("SYS$DISK")''F$DIRECTORY()'
$ SET DEF 'HERE'
$ JNAME ="KIN_"+F$EXTRACT(0,5,P1)
$ LENFN = F$LOCATE(".",P1)
$ LENFN1 = F$LOCATE(".",P3)
$ EQNNAME = F$EXTRACT(0,LENFN,P1)
$ DATNAME = F$EXTRACT(0,LENFN,P2)
$ SET MESSAGE/NOID/NOFACILITY/NOSEV/NOTEXT
$ DELETE 'DATNAME'.JOB;*
$ SET MESSAGE/ID/FACILITY/SEV/TEXT
$ OPEN/WRITE TEMPFILE 'DATNAME'.JOB
$ WRITE TEMPFILE "$ ! Temporary file for doing a KINFIT run"
```

```
$ WRITE TEMPFILE "$ SET DEF ",HERE
$ WRITE TEMPFILE "$ ASSIGN ",P2,".DAT FOR001"
$ WRITE TEMPFILE "$ ASSIGN ",P2,".REP FOR002"
$ IF LENFN1 .NE. 0 THEN  $ WRITE TEMPFILE "$ ASSIGN ",P3,".DAT FOR060"
$ WRITE TEMPFILE "$ RUN ",P1
$ CLOSE TEMPFILE
$ SUBMIT/QUEUE=KINFITQ/LOG='HERE''DATNAME'.LOG/NOPRINTER/NOTIFY/NAME='JNAME'-
  'DATNAME'.JOB
```

Appendix H

SUBROUTINE EQN-NMR2SITE.FOR

```
      SUBROUTINE EQN
C=====================================================================
C
C     NMR2SITE.FOR  -
C
C      NMR TWO-SITE EXCHANGE WITH CORRECTION FOR LINE
C
C      BROADENING, DELAY TIME AND ZERO-ORDER DEPHASING.
C
C
C
C
C
C      PARAMETERS     U(1) = K      (INTENSITY . UNITLESS)
C
C                     U(2) = B      (BASELINE INTENSITY . UNITLESS)
C
C                     U(3) = THETA  (ZERO ORDER PHASE CORRECTION . RAD
C
C                     U(4) = DELTAW (FREQ. CORR.=2(PI)(DELTANU) . RAD.
C
C                     U(5) = TAU    (EXCHANGE RATE . SEC.)
C
C      CONSTANTS      CONST(1) = PA   (POP. OF FREE SITE . UNITLESS)
C
C                     CONST(2) = T2A  (RELAXATION TIME . SEC./RAD.)
C
C                     CONST(3) = WA   (WA=2(PI)(NUA) . RAD./SEC.)
C
C                     CONST(4) = PB   (POP. OF COMPLEXED SITE . UNITLE
C
C                     CONST(5) = T2B  (RELAXATION TIME . SEC./RAD.)
C
C                     CONST(6) = WB   (WB=2(PI)(NUB) . RAD./SEC.)
```

```
C
C                     CONST(7) = DE   (DELAY TIME . SEC.)
C
C                     CONST(8) = LB   (LINE BROAD.=(PI)(LB(HZ)) . RAD.
C
C=====================================================================
C
        IMPLICIT REAL*8(A-H,O-Z)
        IMPLICIT INTEGER*4(I-N)
C
        INCLUDE 'KINFIT:KINFITCOM.FOR/LIST'
        INCLUDE 'KINFIT:KINEQNCOM.FOR/LIST'
C
      COMPLEX*16 ALPHA,ALPHB,XLAMA,XLAMB,C1,C2,XS,BRUCE,ALEX,AL,FRED
C
C---------------------------------------------------------------------
C
C       Entry/Control Point
C
C---------------------------------------------------------------------
C
        GOTO (2,3,4,5,1,7,8,9,10,11,12,13) ITYPE
C
C-----------------------------
C
C       ITYPE = 5: Initial call.  No input has taken place
C
C-----------------------------
C
 1      CONTINUE
        WRITE (LUNOUT,8500)     ! Log the ID of this routine
 8500   FORMAT ('  ***EQN:  CEM 471 Method 2  (06-SEP-85)***')
        RETURN
C
C-----------------------------
C
C       ITYPE = 6:  Control card #1 and CONST have been input
C
C-----------------------------
C
 7      CONTINUE
      NOUNK=5
      NOVAR=2
```

```
      RETURN
C
C-----------------------------
C
C     ITYPE = 3:              ! Experimental data has been read
C
C-----------------------------
C
 8    CONTINUE
      RETURN
C
C-----------------------------
C
C     ITYPE = 1:  Evaluate algebraic equation and residual
C
C-----------------------------
C
 2    CONTINUE
      IF(U(1).GT.0.)GO TO 1002
      U(1)=1.E+09
 1002 CONTINUE
      IF(U(5).LT.1.)GO TO 1001
      U(5)=.0001
 1001 CONTINUE
      IF(U(5).GT.0.)GO TO 1000
      U(5)= .0001
 1000 CONTINUE
      PI=2*3.14159
      ALPHA=1./CONST(2)+CMPLX(0.,1.)*(CONST(3)-XX(1)*PI+U(4))
      ALPHB=1./CONST(5)+CMPLX(0.,1.)*(CONST(6)-XX(1)*PI+U(4))
      BRUCE=-(ALPHA+ALPHB+1./U(5))
      FRED=(ALPHA-ALPHB+CONST(4)/U(5)-CONST(1)/U(5))**2
      BOB=4*CONST(1)*CONST(4)/(U(5)*U(5))
      ALEX=FRED+BOB
      AL=CDEXP(CDLOG(ALEX)/2.)
      XLAMA=(BRUCE+AL)/2.
      XLAMB=(BRUCE-AL)/2.
      C1=CMPLX(0.,1.)*(XLAMB+CONST(1)*ALPHA+CONST(4)*ALPHB)/(-XLAMA+
     1XLAMB)
      C2=CMPLX(0.,1.)*(XLAMA+CONST(1)*ALPHA+CONST(4)*ALPHB)/(XLAMA-
     1XLAMB)
      XS=-C1*(CDEXP((XLAMA-CONST(8))*CONST(7)))/(XLAMA-CONST(8))+
     1(-C2)*(CDEXP((XLAMB-CONST(8))*CONST(7)))/(XLAMB-CONST(8))
```

```
      REAP=REAL(XS)
      AMAG=DIMAG(XS)
      CALC=U(1)*(-REAP*SIN(U(3)-(CONST(3)-XX(1)*PI+U(4))*CONST(7))+
     1AMAG*COS(U(3)-(CONST(3)-XX(1)*PI+U(4))*CONST(7)))+U(2)
        IF (IMETH .NE. -1) GOTO 35
C
C       Simulations only
C
        RETURN
C
C       Fits
C
 35     CONTINUE
       RESID=CALC-XX(2)
        RETURN
C
C-----------------------------
C
C       ITYPE = 2:  Set the initial conditions for differential eqn's
C
C-----------------------------
C
 3      CONTINUE
        Y(1) = 1.0E-20
        NOEQN = 1               ! Set the number of equations
        RETURN
C
C-----------------------------
C
C       ITYPE = 3:  Evaluate the differential eqn's
C
C-----------------------------
C
 4      CONTINUE
        IF (U(1) .LE. 0.0) U(1) = ABS(U(1))
        IF (U(2) .LE. 0.0) U(2) = ABS(U(2))
        CONC1 = CONST(1)
        CONC2 = CONST(2)
        DY(1) = U(1) * (CONC1 - Y(1))*(CONC2-Y(1))-(U(2)*Y(1))
        RETURN
C
C-----------------------------
C
```

```
C       ITYPE = 4:  Calculate the residual for differential eqn's
C
C-----------------------------
C
 5      CONTINUE
        IF (IMETH .NE. -1) GOTO 20
C
C       Simulations only
C
        RETURN
C
C       Fits
C
 20     CONTINUE
C
C       CONST(6) is the molar absorptivity -- substitute exp val if known.
C
        CONST(6) = 5000.0
        RESID = Y(1)+DLOG10(XX(2)/CONST(4))/(CONST(6)*0.2)
        RETURN
C
C-----------------------------
C
C       ITYPE = 8:  Calculate X(KVAR,I) the IPLT = 2 plotting mode
C
C-----------------------------
C
 9      CONTINUE
        RETURN
C
C-----------------------------
C
C       ITYPE = 9:  FOP(I) = X(KVAR+1,I) for the IPLT = 3 mode
C
C-----------------------------
C
 10     CONTINUE
        RETURN
C
C-----------------------------
C
C       ITYPE = 10:  FOP(I) = X(KVAR+2,I) for the IPLT = 4 mode
C
```

```
C-----------------------------
C
 11     CONTINUE
        RETURN
C
C-----------------------------
C
C       ITYPE = 11:  FU(I) <<<< x-axis;  FO(I) <<<< yaxis (IPLT = 5)
C
C-----------------------------
C
 12     CONTINUE
        RETURN
C
C-----------------------------
C
C       ITYPE = 12:  Called after simulation
C
C-----------------------------
C
 13     CONTINUE
        RETURN
        END
```

This is the subroutine of the equation for a two-site exchange NMR signals. To initialize the curve fitting process for this data file, which is a digitized format of an NMR signal of the nuclei under a chemical exchange between the two sites, type on the VAX system: KINRUN NMR2SITEB TESTK(or a file name in general).

Appendix I

SUBROUTINE EQN-NMR1SITE.FOR

```
            SUBROUTINE EQN
C=====================================================================
C
C
C       LORENTZIAN LINESHAPE CORRECTED FOR  LINE
C
C       BROADENING, DELAY TIME AND ZERO-ORDER DEPHASING.
C
C
C        PARAMETERS     U(1) = K      (INTENSITY . UNITLESS)
C
C                       U(2) = T2     (RELAXATION TIME. SEC./RAD.)
C
C                       U(3) = NU     (FREQENCY. HERTZ.)
C
C                       U(4) = THETA  (ZERO ORDER PHASE CORRECTION. RAD.)
C
C                       U(5) = B      (BASELINE INTENSITY.UNITLESS.)
C
C        CONSTANTS      CONST(1) = DE (DELAY TIME. SEC.)
C
C                       CONST(2) = LB (LINE BROADENING. HERTZ.)
C
C
C=====================================================================
C
        IMPLICIT REAL*8(A-H,O-Z)
        IMPLICIT INTEGER*4(I-N)
C
        INCLUDE 'KINFIT:KINFITCOM.FOR/LIST'
        INCLUDE 'KINFIT:KINEQNCOM.FOR/LIST'
C
      COMPLEX*16 ALPHA,ALPHB,XLAMA,XLAMB,C1,C2,XS,BRUCE,ALEX,AL,FRED
C
```

```
C-----------------------------------------------------------------
C
C       Entry/Control Point
C
C-----------------------------------------------------------------
C
        GOTO (2,3,4,5,1,7,8,9,10,11,12,13) ITYPE
C
C-----------------------------
C
C       ITYPE = 5: Initial call.  No input has taken place
C
C-----------------------------
C
 1      CONTINUE
        WRITE (LUNOUT,8500)     ! Log the ID of this routine
 8500   FORMAT ('  ***EQN:  CEM 471 Method 2  (06-SEP-85)***')
        RETURN
C
C-----------------------------
C
C       ITYPE = 6:  Control card #1 and CONST have been input
C
C-----------------------------
C
 7      CONTINUE
      NOUNK=5
      NOVAR=2
        RETURN
C
C-----------------------------
C
C       ITYPE = 3:              ! Experimental data has been read
C
C-----------------------------
C
 8      CONTINUE
        RETURN
C
C-----------------------------
C
C       ITYPE = 1:  Evaluate algebraic equation and residual
C
```

```
C-----------------------------
C
 2      CONTINUE
       BROAD=3.14159*U(2)*CONST(2)+1
       PHASE=2.*3.14159*CONST(1)*(XX(1)-U(3))+U(4)
       TOP=EXP(-CONST(1)*BROAD/U(2))*(COS(PHASE)-2.*3.14159*(U(2)/BROAD)*
      1(XX(1)-U(3))*SIN(PHASE))
       BOT=1.+(U(2)/BROAD)**2*(2.*3.14159*(XX(1)-U(3)))**2
       CALC=U(1)*(U(2)/BROAD)*TOP/BOT+U(5)
         IF (IMETH .NE. -1) GOTO 35
C
C       Simulations only
C
         RETURN
C
C       Fits
C
 35      CONTINUE
       RESID=CALC-XX(2)
         RETURN
C
C-----------------------------
C
C       ITYPE = 2:  Set the initial conditions for differential eqn's
C-----------------------------
C
 3      CONTINUE
         Y(1) = 1.0E-20
         NOEQN = 1               ! Set the number of equations
         RETURN
C
C-----------------------------
C
C       ITYPE = 3:  Evaluate the differential eqn's
C
C-----------------------------
C
 4      CONTINUE
         IF (U(1) .LE. 0.0) U(1) = ABS(U(1))
         IF (U(2) .LE. 0.0) U(2) = ABS(U(2))
         CONC1 = CONST(1)
         CONC2 = CONST(2)
         DY(1) = U(1) * (CONC1 - Y(1))*(CONC2-Y(1))-(U(2)*Y(1))
```

```
      RETURN
C
C-----------------------------
C
C     ITYPE = 4:  Calculate the residual for differential eqn's
C
C-----------------------------
C
 5    CONTINUE
      IF (IMETH .NE. -1) GOTO 20
C
C     Simulations only
C
      RETURN
C
C     Fits
C
 20   CONTINUE
C
C     CONST(6) is the molar absorptivity -- substitute exp val if known.
C
      CONST(6) = 5000.0
      RESID = Y(1)+DLOG10(XX(2)/CONST(4))/(CONST(6)*0.2)
      RETURN
C-----------------------------
C
C     ITYPE = 8:  Calculate X(KVAR,I) the IPLT = 2 plotting mode
C
C-----------------------------
C
 9    CONTINUE
      RETURN
C
C-----------------------------
C
C     ITYPE = 9:  FOP(I) = X(KVAR+1,I) for the IPLT = 3 mode
C
C-----------------------------
C
 10   CONTINUE
      RETURN
C
C-----------------------------
```

```
C
C       ITYPE = 10:  FOP(I) = X(KVAR+2,I) for the IPLT = 4 mode
C
C-----------------------------
C
 11     CONTINUE
        RETURN
C
C-----------------------------
C
C       ITYPE = 11:  FU(I) <<<< x-axis;  FO(I) <<<< yaxis (IPLT = 5)
C
C-----------------------------
C
 12     CONTINUE
        RETURN
C-----------------------------
C       ITYPE = 12:  Called after simulation
C
C-----------------------------
C
 13     CONTINUE
        RETURN
        END
```

This is a subroutine KINFIT program for the fitting of the NMR signals not undergoing the exchange reactions. Relaxation times(T_2) and frequencies(v) can also be obtained by running this program, in alternative to the method by running the built-programs on Bruker-180 spectrometer. Here, the same procedures as running NMR2SITEB are performed in order to obtain T_2 and v.

REFERENCES

1. Pedersen, C.J. J. Am. Chem. Soc., 1967, 89, 7017
2. Pedersen, C.J. Fed.Proc., Fed. Am. Soc. Exp. Biol., 1968, 27, 1305
3. Pedersen, C.J. J. Am. Chem. Soc., 1970, 92, 386
4. Lehn, J.M. Structure Bonding, 1973, 16, 1
5. Dietrich, B.; Lehn, J.M. and Sauvage, J.P. Tetrahedron Lett., 1972, 2885-2889
6. Burgermeister, W. and Winkler-Oswatitsch, R. Top. Curr. Chem., 1977, 69, 91
7. Chock, P.B.; Eggers, F.; Eigen, M. and Winkler, R. Biophys. Chem., 1977, 6, 239
8. Frensdorff, H.K. J. Am. Chem. Soc., 1971, 93, 600
9. Christensen, J.J.; Eatough, D.J. and Izatt, R.M. Chem. Rev., 1974, 74, 351
10. Lardy, H. Fed. Proc., Fed. Am. Soc. Exp. Biol., 1968, 27, 1278
11. Eiseman, G.; Ciani, S.M. and Szabo, G. Fed. Proc., Fed. Am. Soc. Exp. Biol., 1968, 27, 1289
12. Tostesen, D.C. Fed. Proc., Fed. Am. Soc. Exp. Biol., 1968, 27, 1269
13. Eiseman, G. Fed. Proc., Fed. Am. Soc. Exp. Biol., 1968, 27, 1249
14. Pressman, B.C. Fed. Proc., Fed. Am. Soc. Exp. Biol., 1968, 27, 1283

15. Izatt, R.M.; Rytting, J.H.; Nelson, D.O.; Haymore, B.L. and Christensen, J. Science, 1968, 64, 444

16. Chem. Eng. News, 1970, 48(9), 26

17. Kolthoff, I.M. Anal. Chem., 1979, 51(5), 1R

18. Liesegang, G.W. and Eyring, E.M. in "Synthetic Multidentate Macrocyclic Compounds", edited by Reed, R.M. and Christensen, J.J. Academic Press, New York, 1978, pp245-287

19. Eigen, M.; Winkler, R. in "The Neurosciences, 2nd Study Program". Schmitt, F.O., Ed. Rockefeller University Press, New York, N.Y., 1970, p 685

20. Liesegang, G.W.; Farrow, M.M.; Purdie, N. and Eyring, E.M. J. Am. Chem. Soc., 1976, 98, 6905-6909

21. Chock, P.B. Proc. Natl. Acad. Sci. U.S.A., 1972, 69, 1939

22. Petrucci, S.; Adamic, R.J. and Eyring, E.M. J. Chem. Phys., 1986, 90, 1677-1683

23. Maynard, K.J.; Irish, D.E.; Eyring, E.M. and Petrucci, S. J. Chem. Phys., 1984, 88, 729-736

24. Rodriguez, L.J.; Liesegang, G.W.; White, R.D.; Farrow, M.M.; Purdie, N. and Eyring, E.M. J. Chem. Phys., 1977, 81, 2118-2122

25. Chen, C.C.; Petrucci, S. J. Chem. Phys., 1982, 88, 2601-2605

26. Wallace, W.; Chen, C.; Eyring, E.M. and Petrucci, S. J. Chem. Phys., 1985, 89, 1357-1366

27. Lehn, J.M., and coworkers, J. Am. Chem. Soc., 1970, 92, 2916

28. Loyola, V.M.; Wilkins, R. and Pizer R. J. Am. Chem. Soc., 1975, 97, 7382

29. Henco, K.; Tümmler, B. and Maass, G. Angew. Chem., Int. Ed. Engl. 1977, 16, 538

30. Cox, B.G. and Schneider, H. J. Am. Chem. Soc., 1977, 99, 2809

31. Gresser, R.; Albrecht-Gary, A.M.; Lagrange, P. and Schwing, J.P. Nouv. J. Chim., 1978, 7, 239

32. Cox, B.G.; Schneider, H.; Stroka, J. J. Am. Chem. Soc. 1978, 100, 4746-4749

33. Cox, B.G.; Schneider, H. Inorganic Chimica Acta, 1982, 64, L263-L265

34. Cox, B.G.; Garcia-Rosas, J. Ber. Bunsenges Phys. Chem., 1982, 86, 293-297

35. Kodama, M.; Kimura, E. J.C.S.Chem.Comm., 1975, 326

36. Kodama, M.; Kimura, E. J.C.S. Dalton, 1976, 116-119

37. Kodama, M.; Kimura, E. J.C.S. Dalton, 1977, 2269-2276

38. Hinz, F.P and Margerum, D.W. J. Am. Chem. Soc., 1974, 96, 4993; Inorg. Chem. 1974, 13, 2941

39. Busch, D.H.; Farmery, K.; Goedken, V.; Katovic, V.; Melnyk, A.C.; Sperati, C.R. and Tokel, N. Adv. Chem. Ser., 1971, No.100, 44

40. Degani, H. Biophys. Chem, 1977, 6, 345-349

41. Funck, F.; Eggers, F. and Grell, E. Chimica, 1972, 26, 637

42. Liesegang, G.W.; Farrow, M.M.; Vazquez, F.A.; Purdie, N. and Eyring, E.M. J. Am. Chem. Soc., 1977, 99, 3240

43. Dibler, H.; Eigen, M.; Ilgenfrita, G.; Maass, G.; Winkler, R. Pure Appl. Chem., 1969, 20, 93

44. Cox, B.G.; van Trugon, NG; Rzeszotarska, J.; Schneider, H. J. Am. Chem. Soc., 1984, 106, 5965

45. Pointud, Y.; Tissier, C.; Juillard, J. J. Solution Chem., 1983, 7, 473

46. Hoogerheide, J.G.; Popov, A.I. J. Solution Chem., 1979, 8, 83

47. Eyring, E.M.; et al. J. Phys. Chem., 1986, 90, 6571-6576

48. Eyring, E.M.; et al. J. Phys. Chem., 1986, 90, 1659-1663

49. Cox, B.G.; Truong, N.V.; Garcia-Rosas, J.; Schneider, H. J. Phys. Chem. 1984, 88, 996-1001

50. Strasser, B.O.; Shamsipur, M.; Popov, A.I. J. Phys. Chem., 1985, 89, 4822

51. Shchori, E.; Jagur-Grodzinski, J.; Luz, Z. and Shporer, M. J. Am. Chem. Soc., 1971, 93, 7133

52. Lin, J.D., and Popov, A.I. J. Am. Chem. Soc., 1981, 103, 3773

53. Strasser, B.O.; Hallenga, K.; Popov, A.I. J. Am. Chem. Soc., 1985, 107, 789-792

54. Carvajal, C.; Tölle, K.J.; Smid, J.; Szwarc, M. J. Am. Chem. Soc. 1965, 87, 5548

55. Smid, J.; Grotens, A.M. J. Phys. Chem., 1973, 77, 2377

56. Bhattacharyya, D.N.; Lee, C.L.; Smid, J.; Szwarc, M. J. Phys. Chem., 1965, 69, 612

57. Gutmann, V. "Coordination Chemistry in Nonaqueous Solutions", New York, Springer-Verley (1968)

58. Cox, B.G.; Garcia-Rosas, J. and Schneider, H. J. Am. Chem. Soc., 1981, 103, 1054-1059

59. Mei, E.; Popov, A.I. J. Phys. Chem., 1977, 81, 1677

60. Cox, B.G.; Guminsky, C.; Firman, P. and Schneider, H. J. Phys. Chem., 1983, 87, 1357-1361

61. Chen, C.; Wallace, W.; Eyring, E. and Petrucci, S. J. Phys. Chem., 1984, 88, 2541-2547

62. Grell, E. and Oberbäumer, in "Chemical Relaxation in Molecular Biology", Pecht, I.; Rigler, R. ED., Springer-Verlag, Berlin, 1977

63. Cox, B.G.; Truong, N.G. and Schneider, H. J. Am. Chem. Soc., 1984, 106, 1273-1280

64. Shamsipur, M.; Popov, A.I. J. Phys. Chem., 1988, 92, 147

65. Schmidt, E.; Popov, A.I. J. Am. Chem. Soc., 1983, 105, 1873-1878

66. Cahen, Y.M.; Dye, J.L.; Popov, A.L. J. Phys. Chem., 1975, 79, 1292-1295

67. Shamsipur, M.; Popov, A.I. J. Phys. Chem., 1987, 91, 447-451

68. Ceraso, J.M.; Smith, P.B.; Landers, J.S.; Dye, J.L. J. Phys. Chem., 1977, 81, 760-766

69. Shchori, E.; Jagur-Grodzinski, J.; Shporer, M. J. Am. Chem. Soc., 1973, 95, 3842

70. Laidler, K.J. "Chemical Kinetics", McGraw-Hill: New York, 1965, p251

71. Schmidt, E. Ph.D. Thesis, 1981, Department of Chemistry, Michigan State University, East Lansing, Michigan 48824

72. Strasser, B. Ph.D. Thesis, 1984, Department of Chemistry, Michigan State University, East Lansing, Michigan 48824; a.p81 and p160.

73. Szczygiel, P.F. Master Degree Thesis, 1984, Department of Chemistry, Michigan State University, East Lansing, Michigan 48824; a. p.52; b.8; c.54

74. Sirlin, C. Bull. Soc. Chim. Fr., 1984, II-5

75. Szczygiel, P.; Shamsipur, M.; Hallenga, K.; Popov, A.I. J. Phys. Chem., 1987, 91, 1252-1255

76. Delville, A.; Stover, H.D.; Detellier, C. J. Am. Chem. Soc., 1985, 107, 4172

77. Buschmann, H.J. Inorg. Chim. Acta., 1985, 98, 43

78. Okoroafor, N.; Popov, A.I. in press

79. Riddick, J.A.; Bunger, W.B. "Techniques of Chemistry-Volume II: Organic Solvents", 3rd Edition,

Weissberger, A. ed., Wiley-Interscience, New York, (1970), p.353

80. Okoroafor, N.O. Ph.D Thesis, 1987, Department of Chemistry, Michigan State University, East Lansing, Michigan 48824

81. Shaw, D. "Fourier Transform NMR Spectroscopy", second edition, IGE Medical Systems Ltd., Slough, Berkshire, United Kindom

82. Abragam, A. "The Principles of Nuclear Magnetism", Oxford University Press, London, 1961

83. Deverell, C. Prog. Nucl. Magn. Reson. Spectrosc., 1969, 4, 278

84. Lincoln, S.F. Progress in Reaction Kinetics, 1977, vol.9, No.1., pp. 1-91

85. Gupta, R.K.; Pitna, T.P.; Wasylishen, R. J. Magn. Res., 1974, 13, 383

86. Live, D.H.; Chan, S.I. Anal. Chem., Vol. 42, No. 7, 791

87. Van Geet,A.L. Anal. Chem., 1968, 40, 227

88. Van Geet,A.L. Anal. Chem., 1970, 42, 679

89. Kaplan, M.L.; Bobey, F.A.; Chang, H.N. Anal. Chem., 1975, 47, 1703

90. Nicely, V.A.; Dye, J.L. J. Chem. Educ., 1971, 48, 443

91. Petrucci and coworkers, personal communications.

92. Lin, J.D. Ph.D Thesis, 1980, Department of Chemistry, Michigan State University, East Lansing, Michigan 48824

93. Burkhard Tuemmler; Gueter Maass; Fritz Vogtle; Heenz Sieger; Ulrich Heimann; Edwin Weber a. J. Am. Chem. Soc. 1977, 99, 4683 - 4690; J. Am. Chem. Soc., 1979, 101, 2588 - 2598

94. Erlich, R.H.; Popov, A.I. J. Am. Chem. Soc., 1971, 93, 5620

95. Burden, I.J.; Coxon, A.C.; Stoddart, J.F.; Wheatley, C.M. J. Chem. Soc., Perkin Trans. I, 1977, 220-226

96. Takeda, Y. Bull. Chem. Soc. Jpn., 1983, 56, 866-868

97. Kolthoff, I.M.; Chantooni, M.K.; J. Anal. Chem., 1980,52, 1039-1044

98. Smetana, A.J.; Popov, A.I. J. Solution Chem., 1980, 9, 183-196

99. Perelygin, I.S. et al., a. Russ. J. Phys. Chem. 1986, 60, 1474; b. Russ. J. Phys. Chem. 1973, 47, 1138,

100. Mosier-Boss, P.A. Ph.D Thesis, 1985, Department of Chemistry, Michigan State University, East Lansing, Michigan 48824